AWARD NUMBER: W81XWH-18-1-0005

TITLE: Novel Noninvasive Methods of Intracranial Pressure and Cerebrovascular Autoregulation Assessment: Seeing the Brain through the Eyes

PRINCIPAL INVESTIGATOR: Mohamad Hakam Tiba, MD, MS

CONTRACTING ORGANIZATION: University of Michigan

REPORT DATE: January 2020

TYPE OF REPORT: **Annual**

PREPARED FOR: U.S. Army Medical Research and Materiel Command
Fort Detrick, Maryland 21702-5012

REPORT DOCUMENTATION PAGE

Form Approved
OMB No. 0704-0188

1. REPORT DATE	2. REPORT TYPE	3. DATES COVERED
January 2020	Annual	01/01/2019 - 12/31/2019

4. TITLE AND SUBTITLE

Novel Noninvasive Methods of Intracranial Pressure and Cerebrovascular Autoregulation Assessment: Seeing the Brain Through the Eyes

5a. CONTRACT NUMBER

5b. GRANT NUMBER

W81XWH-18-1-0005

5c. PROGRAM ELEMENT NUMBER

6. AUTHOR(S)

Mohamad H. Tiba, MD
Kevin Ward, MD
Abdelrahman Awad, MD
Brendan McCracken, BS
Brandon Cummings, BS

E-Mail: tibam@med.umich.edu

5d. PROJECT NUMBER

5e. TASK NUMBER

5f. WORK UNIT NUMBER

7. PERFORMING ORGANIZATION NAME(S) AND ADDRESS(ES)

University of Michigan
Michigan Center for Integrative Research in Critical Care
2800 Plymouth Road, NCRC Building
10, Room A107
Ann Arbor, Michigan 48109-2800

8. PERFORMING ORGANIZATION REPORT NUMBER

9. SPONSORING / MONITORING AGENCY NAME(S) AND ADDRESS(ES)

U.S. Army Medical Research and Materiel Command

Fort Detrick, Maryland 21702-5012

10. SPONSOR/MONITOR'S ACRONYM(S)

11. SPONSOR/MONITOR'S REPORT NUMBER(S)

12. DISTRIBUTION / AVAILABILITY STATEMENT

Approved for Public Release; Distribution Unlimited

13. SUPPLEMENTARY NOTES

14. ABSTRACT

Traumatic brain injury (TBI) plays a major role in approximately 30% of injury related civilian deaths in the U.S. The Defense and Veterans Brain Injury Center (DVBIC) has reported over 34,000 moderate to severe combat-related TBI (CRTBI) since 2000, making it a major source of mortality and morbidity for the U.S. military between 2000 and 2016. The significance of such numbers becomes apparent with the military's increased focus on Prolonged Field Care (PFC) and prolonged damage control resuscitation (pDCR). PFC is field medical care, applied beyond doctrinal planning time-lines by a SOCM (Special Operations Combat Medic) or higher, in order to decrease patient mortality and morbidity, utilize limited resources, and provide sustained care until the patient arrives at an appropriate level of care.

One of the significant management strategies in the treatment of TBI is aimed at preventing secondary brain damage, which mainly manifests itself as brain ischemia and inflammation. Monitoring of intracranial pressure (ICP) and cerebral autoregulation (CAR) to optimize cerebral perfusion pressure (CPP) to a target and maintain cerebral blood flow (CBF) are the primary methods to prevent secondary injury and are the mainstays of current practice. In a recent study, Juul et al. has concluded that acute neurological deterioration is a powerful predictor of poor outcomes following TBI. The study showed that 29% of patients with acute neurological decline having an unfavorable outcome and the most powerful predictor of such neurological deterioration was the patient's measured ICP. Therefore, it is critical to be able to monitor and manage ICP as early as possible following TBI. Current guidelines of the Brain Trauma Foundation recommend the use of invasive ICP monitoring in patients who meet specific criteria, with the aim of achieving significant reduction in mortality in civilian centers.

Recently, physicians and healthcare providers began utilizing a more dynamic, patient-oriented optimization of CPP based on CAR. Autoregulation is considered one of the most important central nervous system auto-protective mechanisms. It is described as the ability of vessels to modulate their tone in response to changes in CAR is a complex process (critical in preventing secondary brain injury) often impaired after injury and has been shown to be a significant predictor of outcomes in patients with various acute neurological diseases, including severe TBI-related and ischemic injuries. Therefore, continuous monitoring of autoregulation may be beneficial as a means to enable optimization of CPP on a patient-by-patient basis. This represents a more precise and personalized approach to managing the CPP components (ICP and mean arterial pressure) as there is likely great variation in autoregulation ability among individuals and across injuries. Assessment methods such as Transcranial-Doppler (TCD), brain tissue oxygenation (ORx), hemoglobin saturation measured by near-infrared spectroscopy (NIRS), and Laser-Doppler flowmetry of CBF have been used in the past to assess cerebral autoregulation, but with mixed results. Such methods are problematic in PFC settings for a number of reasons, including the intermittent or invasive nature of the measure, the need for a high level of operator experience, and the lack of technology available in far-forward echelons of care.
Newer approaches to autoregulation monitoring, such as pressure reactivity monitoring (PRx, a correlation between mean arterial pressure and ICP), have proven to be independent predictors of outcome. PRx is calculated as the moving Pearson correlation coefficient between certain count of consecutive 5-10 second averages of mean arterial blood pressure (MAP) and ICP. Since PRx is calculated as a correlation, its values would range between -1 and 1, with positive values indicating impaired autoregulation (pressure-passive behavior of the arterial walls) and negative values indicating intact autoregulation (vascular bed with active vasomotor responses). However, PRx is frequently difficult to interpret due to noise in the signal, and would be difficult to apply in early echelons of care due to the requirement for invasive ICP and arterial blood pressure monitoring. In addition, because of the complexity of PRx calculation and the requirement for additional software, PRx monitoring has been limited to research-oriented academic centers.
Therefore, there exists an unmet need for non-invasive, portable diagnostic tools for the early detection impairment of autoregulation and elevated ICP, prior to a potentially catastrophic clinical decline, in patients or injured warfighters who may require initiation of medical therapy and priority evacuation for neurosurgical intervention.

15. SUBJECT TERMS

TBI, Bioimpedance, ICP, Cerebrovascular Autoregulation, Ultrasound, cerebral blood flow, Optic Nerve Sheath, PRX, Non-invasive

16. SECURITY CLASSIFICATION OF:			**17. LIMITATION OF ABSTRACT**	**18. NUMBER OF PAGES**	**19a. NAME OF RESPONSIBLE PERSON**
					USAMRMC
a. REPORT	**b. ABSTRACT**	**c. THIS PAGE**		103	**19b. TELEPHONE NUMBER** *(include area code)*
Unclassified	Unclassified	Unclassified	Unclassified		

Table of Contents

INTRODUCTION:

Traumatic brain injury (TBI) is a major public health problem both in the U.S. and around the world. One of the significant management strategies in the treatment of TBI is aimed at preventing secondary brain injury, which mainly manifests itself as brain ischemia and inflammation. Monitoring of intracranial pressure (ICP) and cerebrovascular autoregulation (CA) to optimize cerebral perfusion pressure (CPP) and maintain cerebral blood flow (CBF) are the primary methods to prevent secondary injury and are the mainstays of current practice. Care of moderate to severe combat-related traumatic brain injury (TBI) continues to pose enormous challenges sometimes compounded by the need to provide prolonged field care (PFC). TBI in the presence of other injuries requiring prolonged damage control resuscitation (pDCR) provides additional challenges. The austere, resource-constrained combat environment and lack of readily available diagnostic capabilities often lead to delayed recognition of the severity of TBIs, resulting in exacerbated damage and increased TBI-related disabilities. CA and ICP monitoring has been used in cases of civilian TBI-related injuries to optimize cerebral perfusion pressure and blood flow to prevent secondary injury. However, technologies currently available to monitor CA and ICP require invasive techniques and a high level of experience, while providing intermittent readings, making them impractical and unavailable in PFC and pDCR settings. Robust methods of noninvasive monitoring of CA and ICP would allow for early application by combat medics, first responders, emergency departments, surgeons, and critical care staff. The proposed project aims to utilize trans-ocular brain bioimpedance and optic nerve ultrasound in a novel manner to assess CA and ICP, utilizing the eye as a window to the brain.

KEYWORDS:
TBI, Bioimpedance, ICP, Cerebrovascular Autoregulation, Ultrasound, cerebral blood flow, Optic Nerve Sheath, PRx, Non-invasive

ACCOMPLISHMENTS:

- **What were the major goals of the project?**
  - **Major Task 1: Evaluation of trans-ocular brain impedance (TOBI) in two swine TBI models. Months 0-36**
    1. A swine model of blunt trauma. Months 3-36
    2. A swine TBI model with provocative maneuvers to manipulate cerebral blood flow (elevated blood pressure, systemic hemorrhage, elevations in ICP and changes in ventilation. Months 3-36

  - **Major Task 2**: **Evaluation of trans-ocular brain impedance (TOBI) as an indicator of cerebral autoregulation in humans who are undergoing both invasive arterial blood pressure and ICP monitoring for brain injury. Months 0-36**

  - **Major Task 3: Collection of ONS ultrasound videos for assessment of ICP in humans who are undergoing both invasive arterial blood pressure and ICP monitoring for brain injury. Months 0-36**

  - **Major Task 4: Development of an ultrasound video analytic system to evaluate ONSD. Months 6-36**

What was accomplished under these goals?

1. **Major Task 1:** Evaluation of trans-ocular brain impedance (TOBI) in two swine TBI models. *Months 0-36*

1) Overall target: 5 animals (either model)/quarter
2) Specific objectives:
    a. IACUC approval: June 12, 2017
    b. ACURO approval: August 11, 2017
3) Animals use Data:
    a. Species: Sus Scrofa Domestica
    b. Total animal number used: 44
    c. USDA pain category for all animals used: D
4) Significant Results:

    a. Data collection using cortical impact and provocative maneuvers models:

Thirty six animals have been used to date for this study using Model 1: Provocative maneuvers to manipulate cerebral blood flow (CBF) systemic blood pressure (MAP) and ICP, and eight animals have been used to date for this study using Model 2: Blunt Trauma. A combination of maneuvers and injuries were performed including slow infusion of vasopressors (Norepinephrine) to increase MAP to ~ 140-160 mmHg, epidural hematoma by insertion of a Foley catheter into the epidural region and inflating the balloon, and lastly a slow systematic hemorrhage and crystalloid resuscitation.

All animals were intubated, anesthetized, and received the same surgical Instrumentation for monitoring and evaluation of:

- Invasive arterial blood pressure (MAP)
- Intracranial pressure (ICP)
- Cerebral blood flow (CBF)
- End tidal CO_2 ($PetCO_2$)
- Cerebral perfusion pressure (CPP)
- Pressure reactivity index (PRx)
- Ocular bioimpedance
- Laser Doppler flow (LDF)
- Transcranial Doppler flow (TAMEAN)

Injury and maneuvers:

a. Vasopressor (norepinephrine) administration: Norepinephrine will be administered and titrated upward to increase MAP to ~ 140-160 mmHg. MAP will be maintained for 2-30 minutes while data is recorded. Afterward, norepinephrine solution infusion will be stopped and the animal's MAP will be allowed to return to near baseline level. The norepinephrine infusion procedure may be repeated up to three times.
b. Epidural Hematoma: Simulation of an epidural hematoma was created using a 8F Foley catheter placed under the skull above the parietal cortex of the brain. Catheter's balloon will be inflated using a syringe pump and ICP was monitored with a target maximum pressure of 20-40mmHg. When the target ICP was reached, the pressure will be maintained for a period of 1-15 minutes. After the monitoring period, balloon will be deflated till ICP reaches baseline level.
c. Systemic Hemorrhage: Approximate 40% of the animal's estimated blood volume will be removed to reach a mean blood pressure of 35-40 mmHg. Low pressure will be maintained for

up to 60min then animal will be resuscitated with a combination of shed blood and normal saline to return blood pressure to baseline value.

d. Combination of A-D above will be performed to simulate intracranial pathology and various concomitant injuries (systemic hemorrhage) and treatments (transfusion, vasopressor use).

Measurements of all physiological data and hemodynamics (MAP, ICP, CBF, CPP, as well as ocular impedance) will be recorded at baseline then at different intervals during maneuvers.
At the end of all maneuvers and monitoring, animals will be euthanized under anesthesia and not allowed to recover. All non-invasive data was time stamped and matched with invasive data collected by the monitors described above. This allowed for temporal comparison of invasive and non-invasive data.

b. Data analysis:

Using the data collected during the course of the provocative maneuvers model, we have developed several novel analytic tools for the assessment of the trans-ocular bioimpedance waveform as it relates to cerebrovascular autoregulatory parameters such as MAP, ICP, CPP, and CBF. Our initial analysis pipeline involved the hand-measurement of peak-to-peak respiratory amplitude (Figure 1), however, we have made progress in two major areas. One, we have been able to fully automate the quantification of the respiratory amplitude in an effort to move to a continuous real-time analytic. Secondly, we have begun to assess the potential information available in the cardiac component of the bioimpedance signal in conjunction to the respiratory component. We have also investigated how the bioimpedance signal interacts with arterial blood pressure in an effort to create an analytic similar to the pressure-reactivity index (PRx).

we have attempted create a surrogate of the pressure reactivity index (PRx). PRx is calculated as the moving Pearson correlation between MAP and ICP, and positive PRx values may be indicative of impaired CA function. Similarly, we sought to create a bioimpedance index (termed DZx) using *dz* and MAP in a similar calculation. We are still investigating the relationship between DZx, PRx, and CA, however, it is notable that DZx and PRx often move opposite one another due to the inverse relationship between *dz* and ICP.

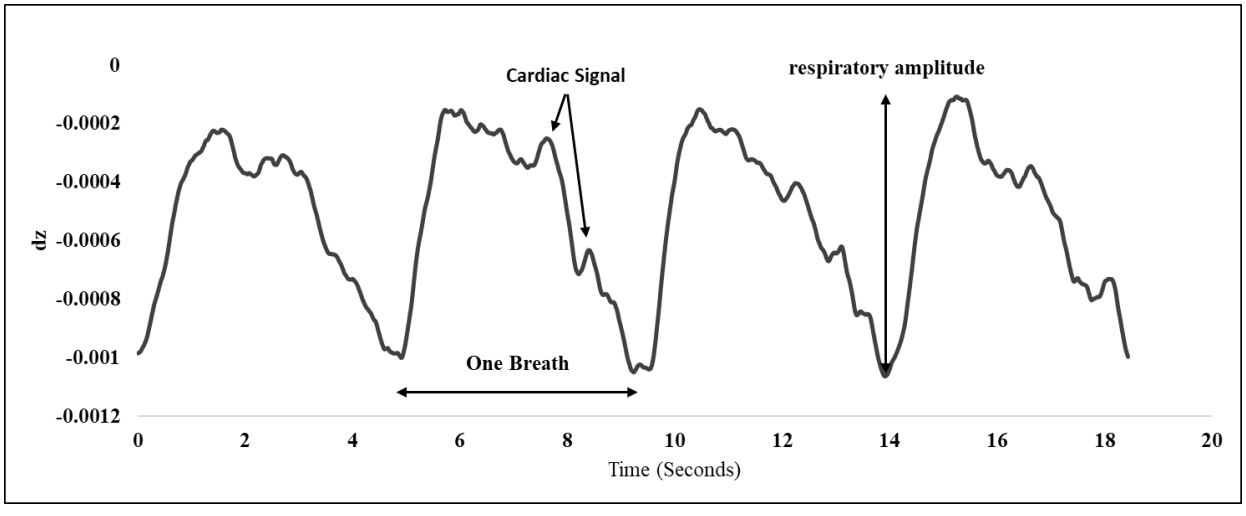

Figure 1: Respiratory-induced changes in trans-ocular brain bioimpedance. The figure shows four breaths. dz is calculated as peak to peak difference in the impedance signal.

C. Data Presentation

Introduction: Cerebrovascular autoregulation is an auto-protective mechanism that is often impaired post traumatic brain injury leading to exacerbation of the injury by ischemia or edema. Current technologies and metrics used to assess autoregulation are often invasive and hard to obtain in a meaningful and timely manner. We developed a trans-ocular bioimpedance method that may provide a non-invasive and effective measure to assess autoregulation. In this study, we utilized respiratory-induced brain impedance changes to evaluate autoregulation and its major constituents such as cerebral perfusion pressure. We compared this to pressure reactivity index (PRx), another measure of autoregulation. **Methods:** Twelve Yorkshire swine were anesthetized, mechanically ventilated, and instrumented to continuously record intracranial pressure (ICP), mean arterial pressure (MAP), and cerebral blood flow (CBF). Transocular brain impedance was measured and recoded by placement of Standard ECG electrodes on the closed eyelids and connected to a data acquisition system. Pressures and cerebral blood flow were manipulated utilizing an intravenous vasopressor challenge (Norepinephrine). Brain bioimpedance indices (*dz* and DZx) were compared to PRx as well as hemodynamic indicators before and during the vasopressor challenge. **Results:** During the vasopressor challenge, brain impedance metric (*dz*) was highly correlated with ICP, CPP, and CBF ($p<0.0001$). ICP, CPP, and CBF had an average percent increase (SD) from baseline at 29(23.2)%, 70(25)%, and 37(72.6)% respectively. While *dz* decrease by -31(15.6)%. Receiver Operator Curve test showed high predictive performance of the relationship between *dz* and arterial blood pressure (DZx) when compared to PRx with area under the curve above 0.86, high sensitivity and specificity. **Conclusion:** In this study, the impedance indices appear to track changes in PRx and hemodynamics that affect autoregulation. Transocular brain bioimpedance may be a suitable non-invasive surrogate to pressure reactivity index.

DZx	PRx Threshold > 0.3	PRx Threshold > 0.2	PRx Threshold > 0.1	PRx Threshold > 0
Sample size	177	177	177	177
Positive group	103 (58.19%)	107 (60.45%)	112 (63.28%)	114 (64.41%)
Negative group	74 (41.81%)	70 (39.55%)	65 (36.72%)	63 (35.59%)
Area under the ROC curve (AUC)	0.88	0.89	0.87	0.89
Standard Error	0.0251	0.0246	0.0276	0.0247
95% Confidence interval	0.835 to 0.933	0.845 to 0.942	0.817 to 0.925	0.842 to 0.939
Significance level P (Area=0.5)	<0.0001	<0.0001	<0.0001	<0.0001
Associated criterion	≤-0.16	≤-0.08	≤-0.08	≤-0.08
Sensitivity	0.82	0.81	0.78	0.79
Specificity	0.81	0.82	0.83	0.82
Positive Predictive Value	0.69	0.68	0.65	0.62
Negative Predictive Value	0.90	0.90	0.90	0.91
Positive Likelihood Ratio	4.3	4.4	4.5	4.4
Negative Likelihood Ratio	0.23	0.23	0.22	0.22

Table 1: A) Area under the Curve for DZx and its associated test performance metrics and criterion at different thresholds of PRx. DZx: Impedance Index. PRx: Pressure Reactivity Index

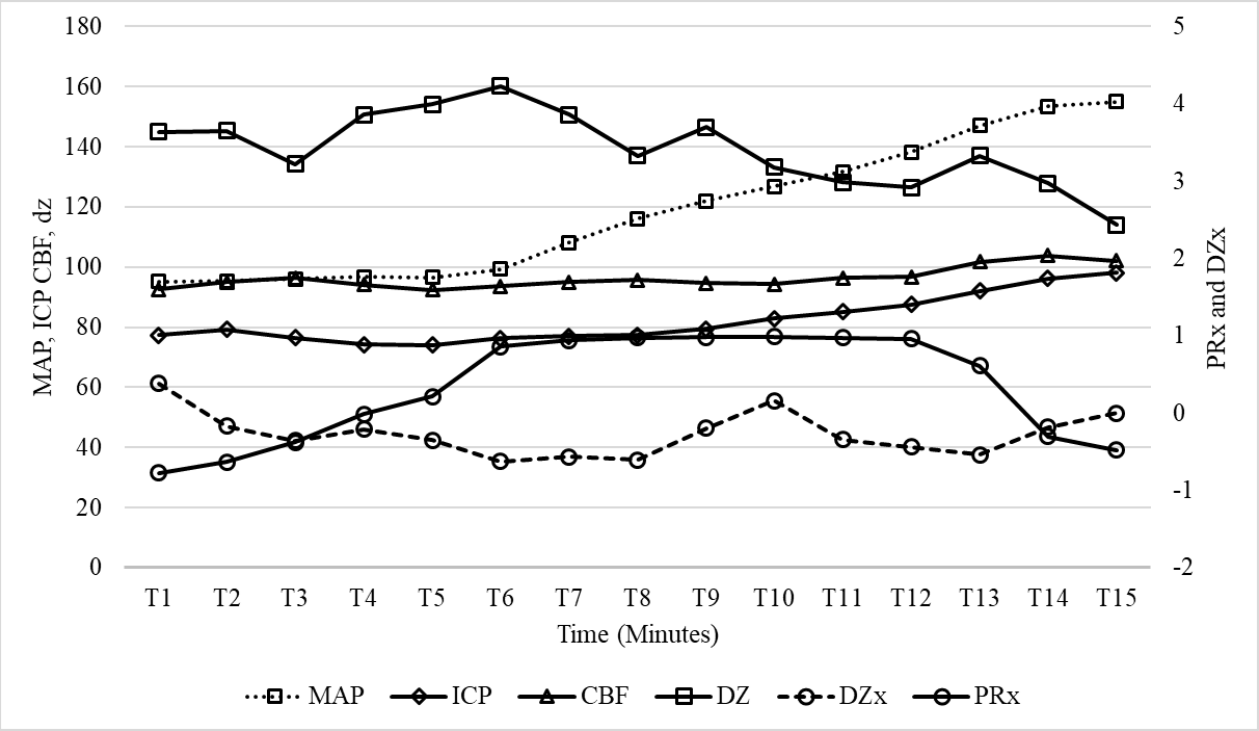

Figure 2: A sample longitudinal view of hemodynamics, PRx, dz, and DZx changes during vasopressor challenge. MAP: Mean arterial pressure. ICP: Intracranial pressure. CPP: Cerebral perfusion pressure, CBF: Cerebral blood flow. dz: Impedance peak to peak difference. PRx: Pressure reactivity index. DZx: Impedance index. Data is presented as means and standard errors

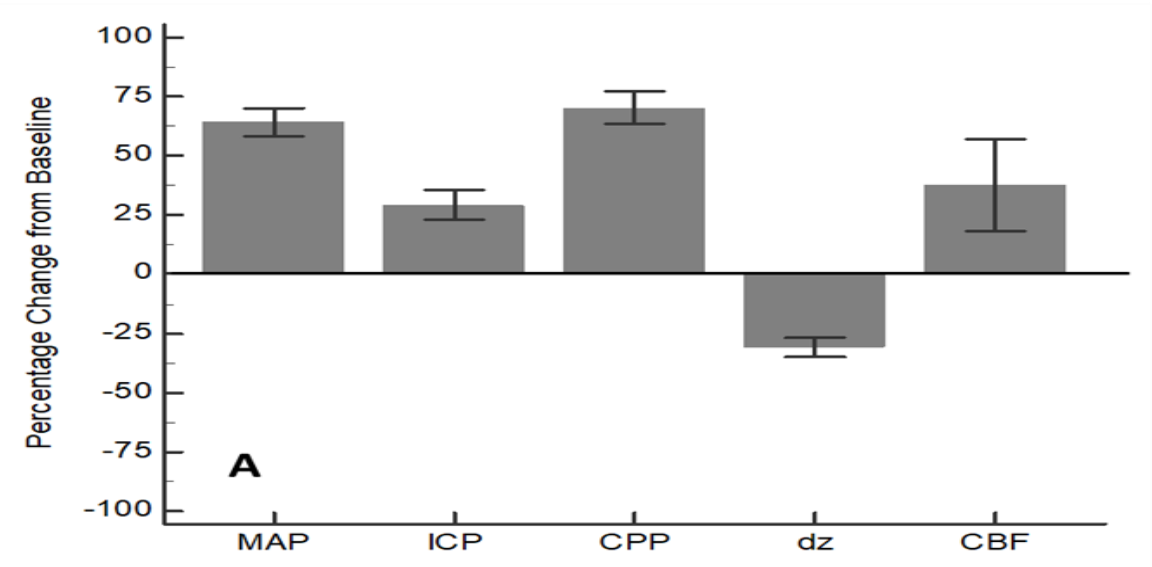

Figure 3: Percentage change from baseline of MAP, ICP, CPP, dz, and CBF during vasopressors challenge.

5) Other achievements:
Established a state of the art large animal model of TBI to be utilized as testing bed for this and other technologies

- **Major Task 2:** *Evaluation of ocular impedance as an indicator of cerebral autoregulation in humans who are undergoing both invasive arterial blood pressure and ICP monitoring for brain injury. Months 0-36*

1. Specific objectives:
    a) IRB approval May 11, 2017
    b) HRPO approval September 22, 2017
    c) Total patient recruitment: 66 patients
    d) Annual patient recruitment: 35 patients

Patients who were admitted to the University of Michigan neurosurgery ICU or the trauma ICU with a ventriculostomy or an ICP monitor and arterial blood pressure monitoring were consented and enrolled into the study. In cases where the patient was unable to consent, the legally authorized representative consented on their behalf. A signed copy of the informed consent document was provided. Patients were admitted to the ICUs most commonly for subarachnoid hemorrhage (31 patients) but also for brain tumors (10), hematoma (4), hydrocephalus (4), trauma (2), meningioma (2), intracranial hemorrhage (2), cortical hemorrhage (2), dermoid cyst (1), compression of the brain stem (1),intraventricular hemorrhage (2), moyamoya (1), artery aneurysm(1), hypoxic ischemic brain injury (1) and idiopathic Intracranial Hypertension (2). 33 females and 33 males were enrolled with an average age of 49.3 (15.5).

At a time when the physicians clamped the ventriculostomy as part of routine care, standard electrode patches (ConMed) were placed over the closed eyes of the patient and anchored at the nasal bridge, superior orbital rim, and the inferior orbital rim. Bioimpedance data was collected (Biopac Data Acquisition System) for 20-45 minutes while arterial blood pressures and ICPs were collected simultaneously. Starting January 4, 2019, the electrodes were changed from the standard electrodes to proprietary electrodes manufactured by In2Being Inc. and fitted onto a device resembling ocular glass wear only contacting the patient's eyelids. This setup has so far been tested on 29 patients with positive feedback for comfort, skill required for use, as well as signal integrity. This allows us to test on patients with orbital fractures and other facial traumas.

2. Significant results:
    a) Data analysis
    b) development of analytics for bioimpedance to current standard predictors of autoregulation

As with animals, the trans-ocular bioimpedance signal is largely composed of two frequencies of interest, relating to the respiratory and cardiac cycles. As expressed in the Q3 Quarterly Technical Progress Report, we have continued to investigate and refine our analysis of the cardiac component of the signal in conjunction with the respiratory oscillations to glean additional information from the signal. Figure 4 depicts a sample of the trans-ocular bioimpedance signal before and after 30 minutes of ventriculostomy clamping, during which ICP rose several points. Note the difference in wave morphology - the amplitude of the respiratory signal decreases slightly, and the higher-frequency cardiac component is significantly lessened. We've refined our analytic technique to quantify this change, using a root-mean-square envelope as it is more resistant to changes in respiratory rate, hard rate, and movement artifact.

Secondly, we have continued to analyze pressure-reactivity index (PRx) and our bioimpedance-driven analogue (DZx) in human subjects. Arterial blood pressure and ICP waveforms were extracted from the patient monitors through MCIRCC's data warehouse platform and aligned in time with the impedance data collected through our portable acquisition system. A new artifact detection and removal process was developed, which uses an adaptive threshold to excise sections of noise due to movement and other sources of motion artifact which often occur in a clinical setting. This process allowed for the recovery of data that would otherwise be considered too noisy for PRx calculation.

As discussed above, PRx is the moving Pearson correlation between MAP and ICP, which may provide latent information about a patient's autoregulatory status. In the calculation of DZx, MAP is instead correlated against respiratory variability in the bioimpedance signal over a five-minute window. An example PRx and DZx calculation for one subject is reported in Figure 5 below. Note the inverse relationship between PRx and DZx, which occurs because the bioimpedance measure is inversely correlated with ICP.

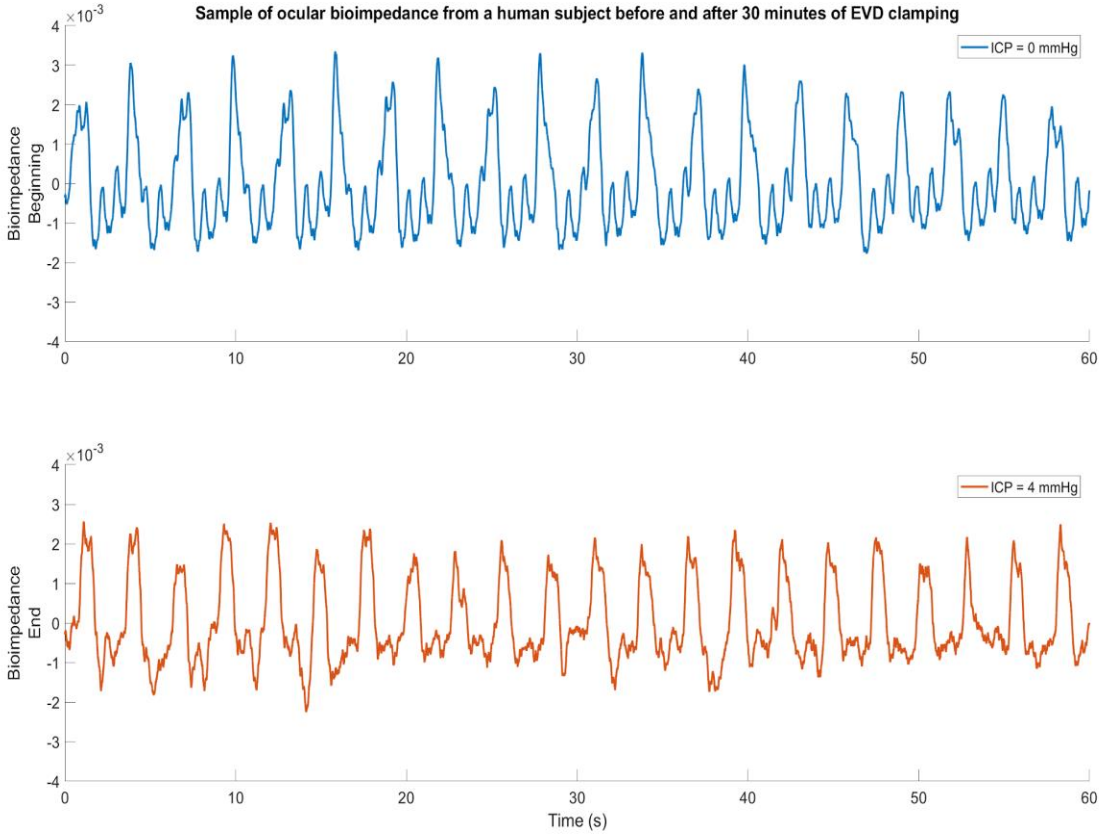

Figure 4: Sample of transocular bioimpedance waveform before (blue) and 30 minutes after EVD clamping (red). Note the differences in wave morphology - while the respiratory amplitude decreases slightly, the cardiac component is significantly lessened.

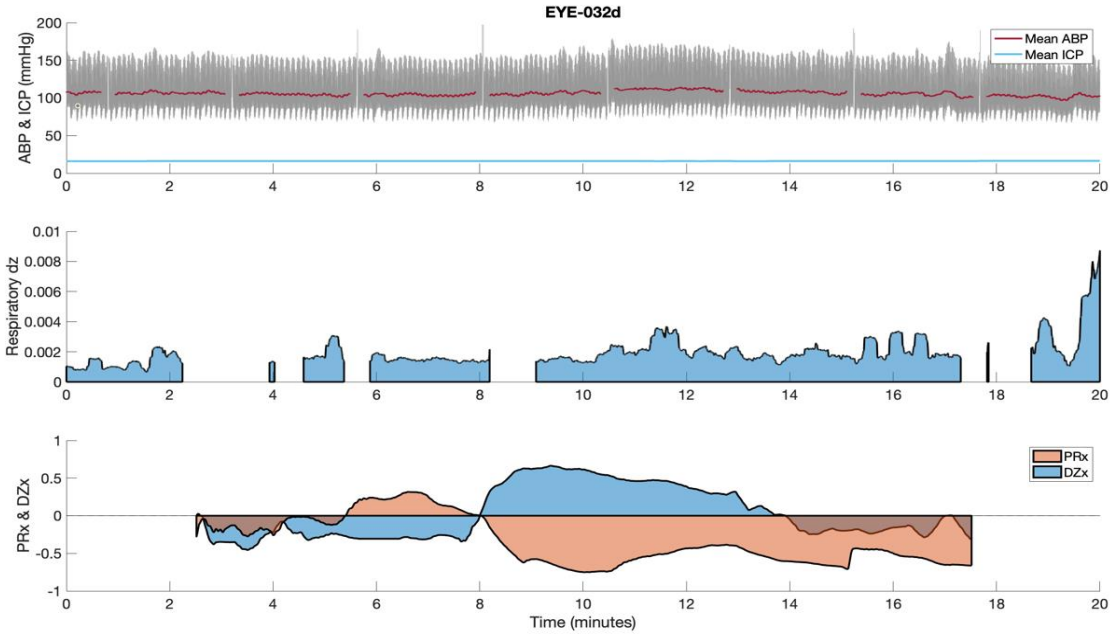

Figure 5: Sample calculation of mean ABP and ICP, respiratory dz, and PRx and DZx. Mean ABP and ICP are calculated by moving average. Respiratory dz is calculated via root-mean-square envelope, then sections of movement artifact are removed from the signal via an adaptive thresholding mechanism. PRx and DZx are calculated through a moving Pearson correlation spanning a 5-minute center-adjusted window. PRx and DZx were moderately anit-correlated ($R = -0.58$, $p < 0.001$).

1. **Other achievements**

Development of novel electrodes in collaboration with In2Being, LLC. The electrodes are fitted onto a 3D printed glasses with only the electrodes contacting patient's eyelids. This electrodes/goggles combination prototype has received positive feedback from patients for comfort and ease of application. This prototype will be used during patients testing in conjunction with Biopac system (Figure 6).

Figure 6. Goggles with new electrodes.

- **Major tasks 3 and 4:** *Collection of Optic Nerve Sheath (ONS) ultrasound videos for assessment of optic nerve sheath diameter (ONSD) in humans who are undergoing both invasive arterial blood pressure and ICP monitoring for brain injury (Months 0-36) and Development of an ultrasound video analytic system to evaluate ONSD. Months 6-36*

1. Specific Objectives:
    a. IRB approval May 11, 2017
    b. HRPO approval September 22, 2017
    c. Total patient recruitment: **47** patients

d. Annual patient recruitment: **21** patients
e. Development of ultrasound analytic system
f. Compare reading of automated ONSD with manual reading by clinicians

The optic nerve is part of the central nervous system surrounded by cerebrospinal fluid (CSF) and encased in a sheath (Figure 8). The sheath is continuous with the dura mater and diameter of this sheath changes rapidly with changing CSF pressure. It has been shown that ventriculostomy measurements of intracranial pressure (ICP) are correlated with Ultrasound (US) optic nerve sheath diameter (ONSD) measurements. Therefore, ONSD can be used as a non-invasive test for elevated ICP. However, manual ONSD measurement is cumbersome and prone to human error. An automated ONSD measurement can help physicians diagnose TBI patients faster and more accurately.

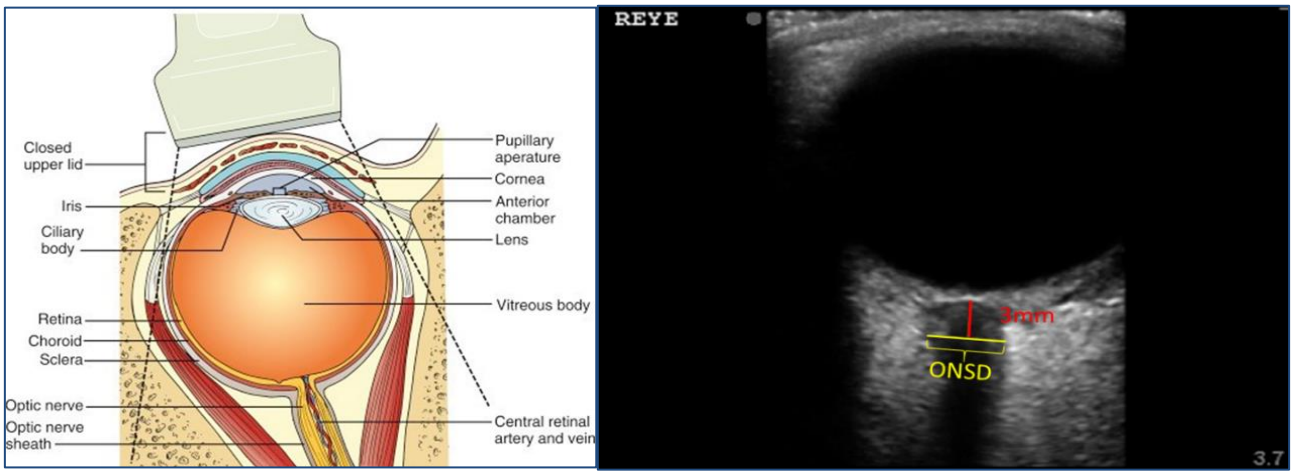

Figure 8: Gross anatomy and ultrasound image with the optic nerve sheath diameter (ONSD)

Method:

Here, we develop an automated algorithm using image processing techniques to analyze US images and calculate the ONSD in 3 mm posterior to the orbit/globe as shown in Figure 7. The schematic diagram of the proposed method is shown in Figure 9. Briefly, the steps are as follows:

1. Determine lowest point in the eye
2. Look for the ONS
3. Go ~3 mm down the globe
4. Determine outer sheath boundary within a region
5. Determine the inner sheath boundary within a region
6. Track the inner and outer boundaries over time

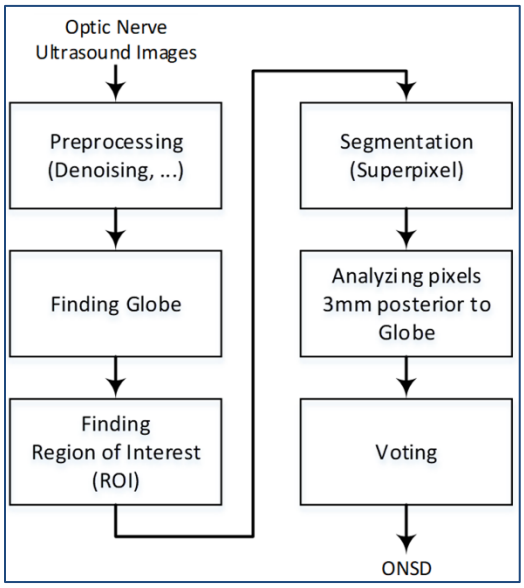

Figure 9: Algorithm development steps

Data Collection and Management: The following parameters were monitored for each patient throughout the experiment.

- ONSD using ultrasound (non-invasive); and
- Invasive ICP (invasive)

2. Significant results
   a. Data analysis

      I. Pearson correlation between manual and algorithm assessment of ONSD
      II. Tukey mean-difference plot (Bland-Altman plot) (Manual and Algorithm)
      III. Intra-class correlation coefficient (ICC)
      IV. Student's t-test

b. Data Presentation

Introduction: Using ultrasound to measure optic nerve sheath diameter (ONSD) has been shown to be a useful modality to detect elevated intracranial pressure. However, manual assessment of ONSD by a human operator is cumbersome and prone to human error. We aimed to develop and test an automated algorithm for ONSD measurement using ultrasound images and compare it to measurements performed by physicians. **Materials and Methods**: Patients were recruited from the Neurological ICU. Ultrasound images of the optic nerve sheath from both eyes were obtained using an ultrasound unit with an ocular preset. Images were processed by two attending physicians to calculate ONSD manually. The images were processed as well using a novel computerized algorithm that automatically analyzes ultrasound images and calculates ONSD. Algorithm-measured ONSD was compared to manually-measured ONSD using multiple statistical measures. **Results**: Forty-Four patients with an Average/Standard Deviation (SD) ICP of 14(9.7) mmHg were recruited and tested (with a range between 1 and 57 mmHg). A t-test showed no statistical difference between the ONSD from left and right eyes ($p>0.05$). Furthermore, a paired t-test showed no significant difference between the manual and algorithm measure ONSD with a mean difference(SD) of 0.012(0.046) cm ($p>0.05$) and percentage error of difference of 6.43% ($p=0.15$). Agreement between the two operators was highly correlated (ICC = 0.8, p=0.26). Bland-Altman analysis revealed Mean difference (SD) of 0.012 (0.046) ($p = 0.303$) and limits of agreement between -0.1 to 0.08. Receiver Operator Curve analysis yielded an AUC of 0.965 ($p<0.0001$) with high sensitivity and specificity. **Conclusions**: The automated image-analysis algorithm calculates ONSD reliably and with high precision when compared to measurements obtained by expert physicians. The algorithm may have a role in computer-aided decision support systems in acute brain injury.

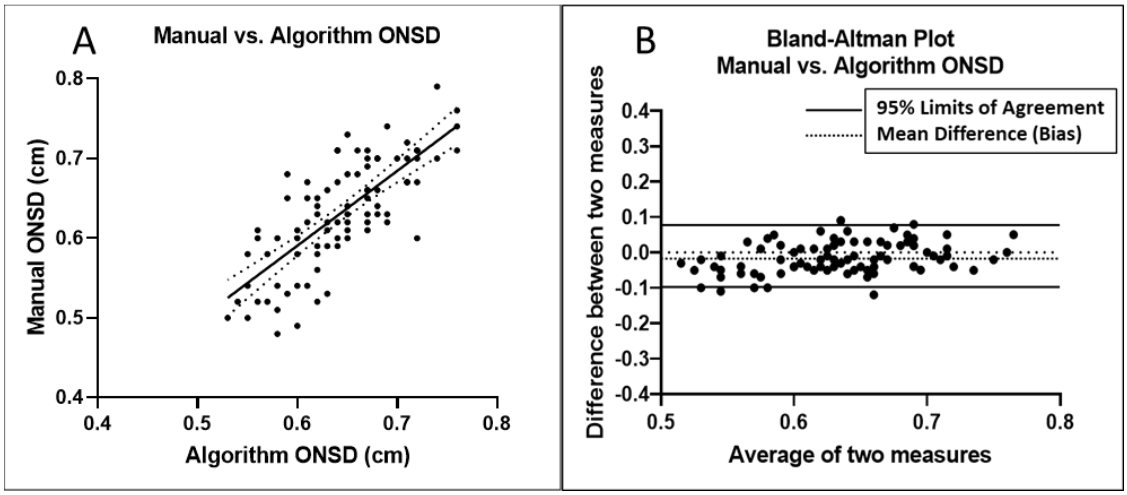

Figure 10: A) Regression of algorithm vs. manual ONSD measurements. B) Bland-Altman plot of algorithm vs. manual ONSD measurements. ONSD: Optic nerve sheath diameter.

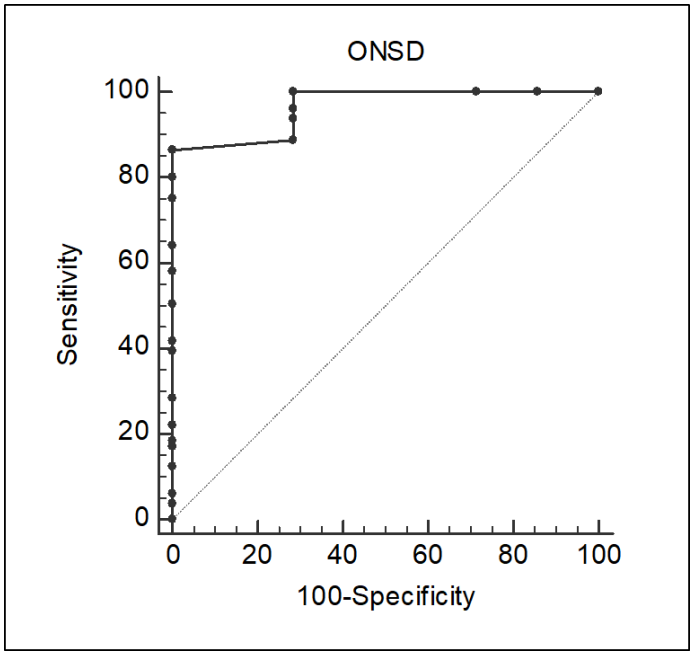

Figure 11: Receiver Operator Curve for the algorithm-measured optic nerve sheath diameter.

In order to find out if there is any correlation between ICP and ONSD we performed several calculations. In each one we computed the correlation between ICP and different ONSD measures such as maximum of left and right ONSD, average of left ONSD (L) and right ONSD (R), shown in the following table.

		Manual				Algorithm			
		ONSD Right Eye	ONSD Left Eye	Average	Difference	ONSD Right Eye	ONSD Left Eye	Average	Difference
Pearson Correlation (All)	r	-0.093	-0.104	-0.107	0.006	-0.257	-0.031	-0.166	-0.246
	95% CI	-0.379 to 0.209	-0.389 to 0.198	-0.391 to 0.196	-0.291 to 0.302	-0.514 to 0.0428	-0.324 to 0.268	-0.440 to 0.138	-0.505 to 0.055
	p	0.549	0.500	0.488	0.967	0.091	0.841	0.283	0.107
Spearman Correlation (All)	r	0.057	-0.013	0.005	0.107	-0.208	0.062	-0.090	-0.303
	95% CI	-0.252 to 0.355	-0.316 to 0.293	-0.300 to 0.309	-0.204 to 0.399	-0.482 to 0.103	-0.248 to 0.359	-0.384 to 0.221	-0.556 to 0.002
	p	0.713	0.933	0.976	0.490	0.175	0.692	0.560	0.046
Pearson Correlation Average above 0.56	r	0.056	-0.021	0.022	0.076	-0.306	-0.009	-0.186	-0.253
	95% CI	-0.268 to 0.369	-0.338 to 0.301	-0.299 to 0.339	-0.249 to 0.386	-0.569 to 0.0154	-0.327 to 0.311	-0.477 to 0.141	-0.529 to 0.072
	p	0.739	0.902	0.894	0.649	0.062	0.957	0.263	0.126
	r	0.052	-0.065	-0.033	0.214	-0.265	0.053	-0.125	-0.280

Spearman Correlation Average above 0.56	95% CI	-0.280 to 0.374	-0.385 to 0.268	-0.357 to 0.298	-0.123 to 0.506	-0.549 to 0.0746	-0.285 to 0.378	-0.440 to 0.216	-0.560 to 0.058
	p	0.755	0.697	0.843	0.197	0.113	0.757	0.459	0.094

Table2: This table shows that the most correlation is between the ICP and the absolute difference of right and left ONSD. However, this correlation is not statistically significant. Of note is that the algorithm assessment correlated better with ICP than the manual calculation

What opportunities for training and professional development has the project provided?

Opportunity was provided for Dr. Reza Soroushmehr, a Research Fellow to present a conference paper at the 2019 *41st Annual International Conference of the IEEE Engineering in Medicine and Biology Society (EMBC)* in Berlin Germany. Dr. Soroushmehr works with the PI and Co-I on development of automated algorithm to measure ONSD.

The conference paper was published online and can be found at

https://ieeexplore.ieee.org/abstract/document/8856449

Soroushmehr, R., Rajajee, K., Williamson, C., Gryak, J., Najarian, K., Ward, K. and Tiba, M.H., 2019, July. Automated Optic Nerve Sheath Diameter Measurement Using Super-pixel Analysis. In *2019 41st Annual International Conference of the IEEE Engineering in Medicine and Biology Society (EMBC)* (pp. 2793-2796). IEEE.

How were the results disseminated to communities of interest?

- Two posters have been presented at the 2019 Military Health Science Research Symposium (MHSRS).
    - Mohamad Hakam Tiba, MD, MS, Venkatakrishna Rajajee, MD, Craig A. Williamson, MD, Brandon C. Cummings, BS, Brendan M. McCracken, BS, Carmen I. Colmenero, BS, Danielle C. Leander, BS, Anne Marie Weitzel, BS, Abdelrahman Awad, MD, Amanda J. Pennington, MS, Kevin R. Ward, MD. Novel Monitoring Modality of Traumatic Brain Injury Patients Using Transocular Brain Impedance (TOBI).

    - Reza Soroushmehr, PhD, Krishna Rajajee, MD, Craig Williamson, MD, Jonathan Gryak, PhD, Kayvan Najarian, PhD, Kevin Ward, MD, Mohamad H. Tiba, MD, MS. Automated Optic Nerve Sheath Diameter Measurement

- A poster has been presented at the
    - 2019 41st Annual International Conference of the IEEE Engineering in Medicine and Biology Society (EMBC)

Posters will be included with this report

- Successful submission of the annuals TBI data upload to The Federal Interagency Traumatic Brain Injury Research (FITBIR)

- A manuscript has been submitted for publication consideration in Military Medicine 2019 MHSRS Supplement.
  "Rajajee, V, Soroushmehr, R, Williamson, C, Najarian, K, Gryak, J, Awad, A, Ward, K, and Tiba, M. H. Novel Algorithm for Automated Optic Nerve Sheath Diameter Measurement Using a Clustering Approach"

A copy of the manuscript draft will be provided with this report

What do you plan to do during the next reporting period to accomplish the goals?

The activities in all major task areas will be continued for the duration of the next reporting period. We plan to continue animal testing using the provocative maneuvers and the blunt trauma TBI models. Human subjects' recruitment and testing will continue for the remainder of the project. Human subjects' data collection will be collected using the latest iteration of the Trans-Ocular Bioimpedance prototype (TOBI), and compared to preliminary data for signal quality device validation. In tandem with collection, data analysis and signal processing will continue for the duration of the next reporting period. (Signal processing a validation of bioimpedance signal against autoregulation parameters such as MAP, ICP, or cerebral blood flow). Further development of ultrasound technique and algorithm for assessment of ONSD will continue for the duration of the project (Patients recruitment and algorithm validation). Data and project progress will continue to be divulged via presentations at scientific meetings both locally at the University of Michigan and nationally at the MHSRS and the Shock Society Meeting during the next reporting period. Lastly, scientific manuscript writing will begin this reporting period with a target of 2-4 publications in major scientific and clinical journals covering all major tasks outlined in the report.

i. Continue testing animals both models 1 & 2
ii. Continue patient recruitment
iii. Continue patients testing using prototype
iv. Further algorithm development for ONSD ultrasound
v. Data analysis and signal processing
vi. Data presentation (national and local
vii. Manuscript submission

IMPACT:

a. **What was the impact on the development of the principal discipline(s) of the project?**

Nothing to report at this time as we are still in testing phase. However, we are expecting a high level of impact by the end of the project on the understanding of cerebrovascular autoregulation and its relationship to cerebral blood flow with the ability to monitor and track these events using transocular impedance that can be commercialized. We will also continue to assess ICP non-invasively using ONSD via ultrasound and an automated algorithm.

b. What was the impact on other disciplines?

Nothing to report.

c. What was the impact on technology transfer?

1. **A provisional patent application "Automated Optic Nerve Sheath Diameter Measurement" was filed on July 23, 2019, and assigned Serial No. 62/877,539.**
2. Prototype developed by In2Being, LLC.
3. TOBI technology now exclusively licensed to New Vital Signs, Inc.

d. What was the impact on society beyond science and technology?

The proposed work is envisioned to lead to development of technologies for noninvasive evaluation of CA and ICP. Such technologies are envisioned to be suitable for in-hospital and out-of-hospital setting in both the civilian and military setting and will allow for:

1) Early application by first responders and military medics for precision management of the severe TBI patient including providing optimal and personalized cerebral perfusion pressure as opposed to a range.
2) Rapid point of care diagnostic indicators of severity of TBI allowing for earlier intervention in more far forward echelons of care.
3) Improved outcomes by earlier detection of injury and prevention of secondary damage.
4) Greater uninterrupted continuum of care as casualties moves from lower to higher levels of care.
5) Reduction in the need for experienced personnel to perform the time consuming procedures necessary for invasive monitoring as well as elimination of associated complications.
6) Improved resource allocation by providing indications for invasive monitoring as well as earlier termination of such invasive monitoring (when they are indicated) by transitioning into noninvasive monitoring.

CHANGES/PROBLEMS:

e. Changes in approach and reasons for change
Nothing to report

f. Actual or anticipated problems or delays and actions or plans to resolve them
We have encountered a lower than anticipated enrollment during the last quarter due to the Holiday time off and personnel travel. Recruitment will continue as planned and as many patients as possible will be enrolled during the next quarters to resolve the enrolment deficit.

g. Changes that had a significant impact on expenditures
Nothing to report

h. **Significant changes in use or care of human subjects, vertebrate animals, biohazards, and/or select agents**

1. **Significant changes in use or care of human subjects:** None to report
2. **Significant changes in use or care of vertebrate animals:** None to report
3. **Significant changes in use of biohazards and/or select agents:** None to report

PRODUCTS:

i. Publications, conference papers, and presentations

1. **Journal publications.** Nothing to report
2. **Books or other non-periodical, one-time publications.** Nothing to report

3. **Other publications, conference papers, and presentations.**

i. Two abstracts have been submitted to the 2019 Military Health System Research Symposium (MHSRS) and have been accepted for poster presentations.

MHSRS-19-01121: Reza Soroushmehr, Krishna Rajajee, Craig Williamson, Jonathan Gryak, Kayvan Najarian, Kevin Ward, Mohamad H. Tiba. Automated Optic Nerve Sheath Diameter Measurement

MHSRS-19-01526: Mohamad Hakam Tiba, Venkatakrishna Rajajee, Craig A. Williamson, Brandon C. Cummings, Brendan M. McCracken, Carmen I. Colmenero, Danielle C. Leander, Anne Marie Weitzel, Abdelrahman Awad, Amanda J. Pennington, Kevin R. Ward. Novel Monitoring Modality of Traumatic Brain Injury Patients Using Transocular Brain Impedance (TOBI).

b. A conference paper has been submitted for the 2019 41st Annual International Conference of the IEEE Engineering in Medicine and Biology Society (EMBC)

Soroushmehr, R., Rajajee, K., Williamson, C., Gryak, J., Najarian, K., Ward, K. and Tiba, M.H., 2019, July. Automated Optic Nerve Sheath Diameter Measurement Using Super-pixel Analysis.

A copy of the abstracts and paper will be included with this submission

j. **Website(s) or other Internet site(s)**

1. https://mcircc.umich.edu/tobi
2. http://newvitalsigns.bio/#technology

k. **Technologies or techniques**

Nothing to report

l. **Inventions, patent applications, and/or licenses**

1. A provisional patent application "Automated Optic Nerve Sheath Diameter Measurement" was filed on July 23, 2019, and assigned Serial No. 62/877,539.

A copy of the patent application will be provided with this report

m. **Other Products**

Web based information

1. https://mcircc.umich.edu/tobi
2. http://newvitalsigns.bio/#technology

n. Research material (e.g., Germplasm; cell lines, DNA probes, animal models);
Animal TBI model developed for this project is now being utilized for testing beyond bioimpedance

Describe the Regulatory Protocols and Activity Status (if applicable).

1- Human Use Regulatory Protocols

TOTAL PROTOCOLS:
One human use protocol will be required to complete the Statement of Work

PROTOCOL(S):

TOTAL PROTOCOLS: 1

PROTOCOL (1 of 1 total):
Protocol [HRPO Assigned Number]: DM160225
Title: Novel Noninvasive Methods of Intracranial Pressure and Cerebrovascular Autoregulation Assessment: Seeing the Brain Through the Eyes
Target required for clinical significance:150
Target approved for clinical significance: 150

SUBMITTED TO AND APPROVED BY:

- IRBMED Initial Approval 7/2/15
- IRBMED Amendment to add retrospective enrollment 1/11/16
- IRBMED Amendment to add bioimpedance 8/12/16
- HRPO Initial Approval 5/11/17
- IRBMED Amendment to add DoD and edits to comply with DoD regulations 7/10/17
- IRBMED Amendment to add TCD 4/26/18
- IRBMED Amendment to add wearable 3/4/19
- IRBMED Amendment to add/ remove staff, consent changes for FITBIR wording 8/13/19
- IRBMED Amendment to add PZT 11/19/19
- IRBMED Amendment to add staff 1/20/20
- IRBMED continuing review report 10/21/19

STATUS:

(i) Number of subjects recruited/original planned target: 66/150
Number of subjects screened/original planned target: 66/150
Number of patients enrolled/original planned target: 66/150
Number of patients completed/original planned target: 55/150

(ii) Report amendments submitted to the IRB and USAMRMC HRPO for review:
None

(iii) Adverse event/unanticipated problems involving risks to subjects or others and actions or plans for mitigation:
None

2. Use of Human Cadavers for Research Development Test & Evaluation (RDT&E), Education or Training

No RDT&E, education or training activities involving human cadavers will be performed to complete the Statement of Work (SOW).

3. Animal Use Regulatory Protocols

TOTAL PROTOCOL(S):

One large animal protocol will be required to complete the Statement of Work

PROTOCOL(S):

TOTAL PROTOCOL(S): 1

PROTOCOL (1 of 1 total):
Protocol [ACURO Assigned Number]: DM160225
Title: *Noninvasive Methods of Intracranial Pressure and Cerebrovascular Autoregulation Assessment*

Target required for statistical significance: 66
Target approved for statistical significance: 66

SUBMITTED TO AND APPROVED BY:

- Protocol submitted to University of Michigan (UofM) IACUC on 5/2/2017
- Protocol approved by University of Michigan IACAC on 6/12/2017
- Protocol submitted to ACURO on 8/2/2017
- Protocol approved by ACURO on 8/11/2017

Amendments

- Scientific amendment AME000035590 was submitted to U of M IACUC on 5/28/2019
- Scientific amendment AME000035590 was approved by U of M IACUC on 6/04/2019
- Scientific amendment AME000035590 was submitted to ACURO on 6/06/2019
- Scientific amendment AME000035590 was approved by ACURO on 6/10/2019

STATUS:

- We have used 18 animals this year to test the performance of bioimpedance during TBI and Provocative maneuvers. 8 animals were used in the blunt impact model and 10 were used in the provocative maneuvers model. Total use for years 1-2 in the project is 44 animals.
- Data from these experiments were specifically collected to assist with the characterization of new indices of autoregulation assessment (DZx) compared to PRx. Additionally, they will be used to further correlate ocular bioimpedance with cerebral blood flow, intracranial pressure, and transcranial Doppler.
- Fully automated data quantification methods and indices for assessment of cerebrovascular auto-regulatory function are continually being explored and developed.
- We have not encountered any administrative, technical, or logistical issues that may impact the performance or progress of our study.

PARTICIPANTS & OTHER COLLABORATING ORGANIZATIONS

o. **What individuals have worked on the project?**

A. Name:	*Mohamad Hakam Tiba, MD, MS*
Project Role:	*PI*
Researcher Identifier (e.g. ORCID ID):	
Nearest person month worked:	*3*
Contribution to Project:	*Oversight of data collection and analysis*
Funding Support:	

Name:	*Kevin Ward, MD*
Project Role:	*Co-I*
Researcher Identifier (e.g. ORCID ID):	
Nearest person month worked:	*1*
Contribution to Project:	*Oversight of data collection and analysis*
Funding Support:	

Name:	*Venkatakrishna Rajajee, MD*
Project Role:	*Co-I*
Researcher Identifier (e.g. ORCID ID):	
Nearest person month worked:	*1*
Contribution to Project:	*Perform ultrasounds, medical consultation*
Funding Support:	

Name:	*Craig Williamson, MD*
Project Role:	*Co-I*
Researcher Identifier (e.g. ORCID ID):	
Nearest person month worked:	*1*
Contribution to Project:	*Perform ultrasounds, medical consultation*
Funding Support:	

Name:	*Hasan Alam, MD PhD*
Project Role:	*Co-I*
Researcher Identifier (e.g. ORCID ID):	
Nearest person month worked:	*1*
Contribution to Project:	*Oversight of data collection and analysis*
Funding Support:	

Name:	*Kayvan Najarian, PhD*
Project Role:	*Co-I*
Researcher Identifier (e.g. ORCID ID):	
Nearest person month worked:	*1*
Contribution to Project:	Development of a computer image analysis algorithm
Funding Support:	

Name:	*Reza Soroushmehr, PhD*
Project Role:	*Research Staff*
Researcher Identifier (e.g. ORCID ID):	
Nearest person month worked:	*3*
Contribution to Project:	Development of a computer image analysis algorithm
Funding Support:	

Name:	*Brendan McCracken, BS*
Project Role:	*Laboratory Assistant Director*
Researcher Identifier (e.g. ORCID ID):	
Nearest person month worked:	*2*
Contribution to Project:	*Oversight and lab management, data collection, data analysis*
Funding Support:	

Name:	*Abdelrahman Awad, MD*
Project Role:	Clinical Research Coordinator
Researcher Identifier (e.g. ORCID ID):	
Nearest person month worked:	*1*
Contribution to Project:	*Patients' recruitment, data collection, data analysis*
Funding Support:	

Name:	*Amanda Pennington, MS*
Project Role:	Clinical Research Coordinator
Researcher Identifier (e.g. ORCID ID):	
Nearest person month worked:	*4*
Contribution to Project:	*Patients' recruitment, data collection, data analysis*
Funding Support:	

Name:	*Brandon Cummings, BS*
Project Role:	*Research Staff*
Researcher Identifier (e.g. ORCID ID):	
Nearest person month worked:	*1*
Contribution to Project:	*Data collection, signal processing and data analysis*
Funding Support:	

Name:	*Carmen Colmenero, BS*
Project Role:	*Research Staff*
Researcher Identifier (e.g. ORCID ID):	
Nearest person month worked:	*5*
Contribution to Project:	*Animal lab duties, data collection, data analysis*
Funding Support:	

Name:	*Danielle Leander, BS*
Project Role:	*Research Staff*
Researcher Identifier (e.g. ORCID ID):	
Nearest person month worked:	*4*
Contribution to Project:	*Animal lab duties, data collection, data analysis*
Funding Support:	

Name:	*Nicholas Greer, BS*
Project Role:	*Research Staff*
Researcher Identifier (e.g. ORCID ID):	
Nearest person month worked:	*3*
Contribution to Project:	*Animal lab duties, data collection, data analysis*
Funding Support:	

Name:	*Daniel Taylor, MA*
Project Role:	*Data Engineer*
Researcher Identifier (e.g. ORCID ID):	
Nearest person month worked:	*4*
Contribution to Project:	*Signal processing, data storage and analysis*
Funding Support:	

Name:	*Jonathan Motyka*
Project Role:	*Data Engineer*
Researcher Identifier (e.g. ORCID ID):	
Nearest person month worked:	*2*
Contribution to Project:	*Signal processing, data storage and analysis*
Funding Support:	

a. **Has there been a change in the active other support of the PD/PI(s) or senior/key personnel since the last reporting period?**
Nothing to report

b. **What other organizations were involved as partners?**
None

c. **Other.**
Nothing to report

SPECIAL REPORTING REQUIREMENTS

d. COLLABORATIVE AWARDS:
None

e. **QUAD CHARTS:** Included with this report before the appendices

PPENDICES:

a. **Abstract MHSRS-19-01121 and poster:** *"Reza Soroushmehr, Krishna Rajajee, Craig Williamson, Jonathan Gryak, Kayvan Najarian, Kevin Ward, Mohamad H. Tiba. Automated Optic Nerve Sheath Diameter Measurement"*

b. **Abstract MHSRS-19-01526 and poster:** *"Mohamad Hakam Tiba, Venkatakrishna Rajajee, Craig A. Williamson, Brandon C. Cummings, Brendan M. McCracken, Carmen I. Colmenero, Danielle C. Leander, Anne Marie Weitzel, Abdelrahman Awad, Amanda J. Pennington, Kevin R. Ward. Novel Monitoring Modality of Traumatic Brain Injury Patients Using Transocular Brain Impedance (TOBI)."*

c. **Conference paper and poster:** *"Soroushmehr, R., Rajajee, K., Williamson, C., Gryak, J., Najarian, K., Ward, K. and Tiba, M.H., 2019, July. Automated Optic Nerve Sheath Diameter Measurement Using Super-Pixel Analysis."*

d. **Draft manuscript:** Submitted for publication consideration in Military Medicine 2019 MHSRS Supplement. *"Rajajee, V, Soroushmehr, R, Williamson, C, Najarian, K, Gryak, J, Awad, A, Ward, K, and Tiba, M. H. Novel Algorithm for Automated Optic Nerve Sheath Diameter Measurement Using a Clustering Approach"*

e. **A provisional patent application**: *"Automated Optic Nerve Sheath Diameter Measurement" was filed on July 23, 2019, and assigned Serial No. 62/877,539.*

f. PI Curriculum Vitae

Novel Noninvasive Methods of Intracranial Pressure and Cerebrovascular Autoregulation Assessment: Seeing the Brain through the Eyes

DM160225 Prolonged Field Care Research Award

Co-PIs: Mohamad Hakam Tiba and Kevin R. Ward **Org:** University of Michigan **Award Amount:** $1,480,171

Study/Product Aim(s)

- Use non-invasive ocular electrical bioimpedance methodologies to track dynamic changes in cerebral blood flow (CBF) and associated changes in cerebrovascular autoregulation (CAR).
- Develop a computer image analysis algorithm and program capable of automating the analysis of images of the optic nerve sheath (ONS) obtained by ultrasound to evaluate intracranial pressure (ICP).

Approach

We will utilize two animal models concomitant with a clinical study. The animal models will include a swine TBI model of blunt trauma as well as a model designed to examine cerebral and systemic hemodynamics in response to various modulators of CBF. We will test ocular impedance as an indicator of cerebral autoregulation and ocular ultrasound videos for assessment of ICP in humans who are undergoing invasive arterial blood pressure and ICP monitoring for brain injury.

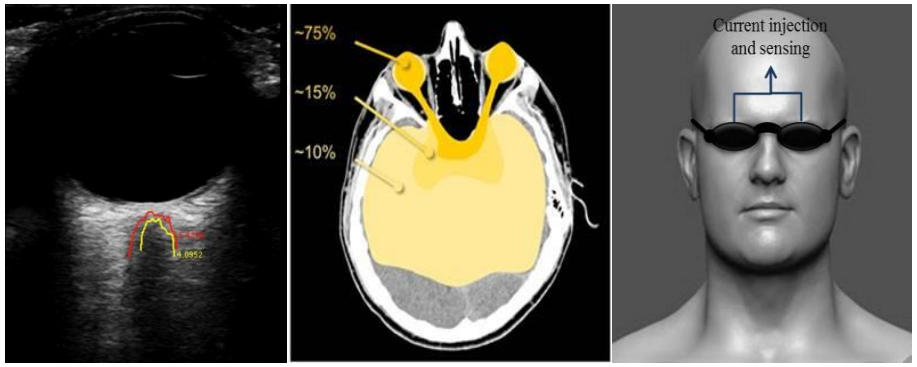

Ocular impedance and ocular nerve sheath ultrasound will be studied in both animals and humans with TBI

Timeline and Cost

Activities / CY	18	19	20	
Ultrasound video analytic and algorithm development				
Animal testing and recruitment of human subjects				
Development of big data platform				
Data analysis and report				
Estimated Budget ($K)	**$507,353**	**$482,327**	**$490,491**	

Updated: (07.22.2019)

Goals/Milestones

CY18 Goal – Validation and system development

- Start validation of ocular impedance in both animals human subjects
- Collection of ONS ultrasound videos for assessment of ICP in humans
- Development of Ultrasound video analytic and algorithm
- Data Analysis and development of big data platform

CY19 Goals – Validation

- Continue animal testing, patients recruitment for both ocular impedance and ultrasound. As well as development of Ultrasound video analytic and algorithm
- Big data platform, data Analysis, reports and presentations

CY20 Goal – Validation, Final reports and presentations

- Continue animal testing, patients recruitment for both ocular impedance and ultrasound. As well as development of Ultrasound video analytic and algorithm
- Big data platform, data Analysis, final reports and presentations
- Development of a transition plan for future trials

Comments/Challenges/Issues/Concerns: None

- **Budget Expenditure to Date: $1,019,812.98**

Appendix A:

Abstract MHSRS-19-01121 and poster: *"Reza Soroushmehr, Krishna Rajajee, Craig Williamson, Jonathan Gryak, Kayvan Najarian, Kevin Ward, Mohamad H. Tiba. Automated Optic Nerve Sheath Diameter Measurement"*

Automated Optic Nerve Sheath Diameter Measurement

Reza Soroushmehr, Krishna Rajajee, Craig Williamson, Jonathan Gryak, Kayvan Najarian, Kevin Ward, Mohamad H. Tiba

Background: The optic nerve is part of the central nervous system surrounded by cerebrospinal fluid (CSF) and encased in a sheath. The sheath is continuous with the dura mater and diameter of this sheath changes rapidly with changing CSF pressure. Using ultrasound to measure optic nerve sheath diameter (ONSD) has been shown to be a useful modality to track changes intracranial pressure (ICP) with high precision. However, manual assessment of ONSD by a human operator is cumbersome and prone to human error. We aim to develop and test an automated algorithm for ONSD measurement and compare it to measurement that are performed by physicians.

Methods: The algorithm uses image processing techniques to analyze ultrasound images and calculate the ONSD in 3 mm posterior to the orbit/globe. We first de-noise images using guided filtering that preserves image edges and then find the region of interest (ROI) where the sheath is located. We use simple image line integral calculation for finding the ROI. After that we analyze images through a super-pixel approach that clusters pixels according to their intensities and then measure the diameter in each image. To find the diameter, we analyze the image row which is 3mm below the globe and calculate the derivative of its pixels. By voting, using median, among the diameters measured from all the images in an ultrasound video, we find the diameter.

Results: 25 patients who were admitted to the University of Michigan health system were recruited and tested. Ultrasound was used to image the ocular nerve sheath on both left and right eyes. ONSD from both sides was assessed using our novel automated algorism and compared to manual assessment by two blinded clinicians. In addition, correlation between two experts' measurements was calculated using intra class correlation (ICC). The average percentage of error between the results of the algorithm and the average manual measurements for the left and right eyes are 6.2% and 4.9% respectively. These values between two manual measurements are 5.2% and 4.4% respectively for left and right eyes. We also performed t-test using the confidence interval of 95% and calculated the p-value. The p-values of the t-test between the algorithm results and the average manual measurements for the left and right eyes are 0.37 and 0.7 respectively while p-values of the t-test between the two manual measurements are 0.32 and 0.85 respectively for the left and right eyes. ICC coefficient between the algorithm results and the average of two experts' measurements was 0.7. Moreover, this coefficient between two experts' measurements was 0.8.

Conclusions: We developed a fully automated method to calculate the optic nerve sheath diameter from ultrasound images and showed the performance of the method through experimental results. Intraclass correlation coefficients, t-test and percentage of error indicated strong correlation between the proposed method' s results and the ground truth and also between two manual measurements. In future studies we will run the method on more videos and also calculate the correlation between the ONSD and the elevated ICP.

This abstract is supported by DoD award W81XWH-18-1-0005.

Automated Optic Nerve Sheath Diameter Measurement Using Super-pixel Analysis

Reza Soroushmehr[1,4], Krishna Rajajee[2,4], Craig Williamson[2,4], Brandon Cummings[3,4], Jonathan Gryak[1,4], Kayvan Najarian[1,3,4], Kevin Ward[3,4], Mohamad Hakam Tiba[3,4]

[1]Department of Computational Medicine and Bioinformatics, [2]Department of Neurosurgery, [3]Department of Emergency Medicine
[4]Michigan Center for Integrative Research in Critical Care (MCIRCC), University of Michigan, Ann Arbor, U.S.A

Introduction

Traumatic Brain Injury (TBI)

- Silent epidemic" because of associated complications
- 2.5 million people sustained TBI in 2010
- Accounts for 30% of all injury related deaths

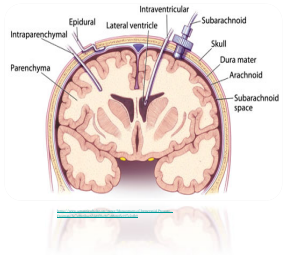

Management & Monitoring Strategies

- Preventing secondary brain damage
  - Inflammation
  - Ischemia
- Monitoring of intracranial pressure (ICP)
  - Gold standard for detection of intracranial hypertension
  - *Invasive, increased risk of infection and further damage to the brain*

Optic Nerve Sheath (ONS)

- Continuation of dura that contains the subarachnoid space
- Elevated ICP results in swelling of the optic disk (papilledema)
  - Can take hours to days
  - Unsuitable as a guide for management of acute TBI
- Increase in ICP results in distension of the retrobulbar ONS within seconds.

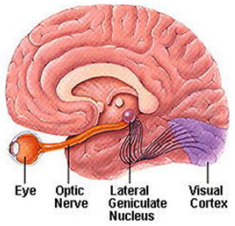

Optic Nerve Sheath Diameter ONSD

- Measurement of ONSD at a standardized 3mm distance behind the globe
- Same principle as papilledema, except more rapidly responsive to ICP
- Identify distension using point-of-care ultrasound devices
- Threshold value suggests intracranial hypertension
- Potential surrogate to invasive ICP monitoring and useful approach for assessing intracranial hypertension

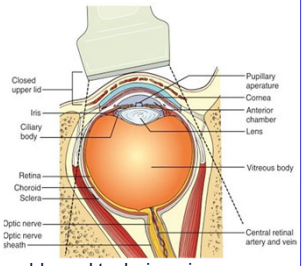

- This non-invasive and portable-ultrasound-based technique is a promising technology for the early, non-invasive detection of elevated ICP and may have significant potential and advantage for use in the PFC setting.

Aim

Develop a computer image analysis algorithm and software program capable of automating the analysis of images of the optic nerve sheath diameter (ONSD) obtained by ultrasound to evaluate ICP.

Methods

- 33 TBI patients were consented and tested
- ONUS were performed with the patient's eye closed, using a linear array transducer placed on the upper margin of the orbit to obtain a sonographic image of the eye.
- Imaging was performed on both eyes for each patient.
- Images were processed and ONSD analyzed by two subject matter expert neurosurgeons (Manual)
- Operators were blinded
- ONSD was analyzed by our novel algorithm as well

Ultrasound algorithm

1. Determine lowest point in the eye
2. Look for the ONS
3. Go ~3 mm down the globe
4. Determine outer sheath boundary within a region
5. Determine the inner sheath boundary within a region
6. Track the inner and outer boundaries over time

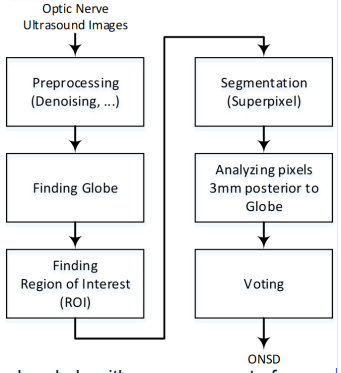

Statistical Analysis

- Pearson correlation between manual and algorithm assessment of ONSD
- Tukey mean-difference plot (Bland-Altman plot) (Manual and Algorithm)
- Intra-class correlation coefficient (ICC)
- Student's *t*-test

Results

- 66 images were recorded and analyzed (33 from left eye and 33 from right eye)
- t-test showed no difference between left and right eye ONSD
- t-test showed no significant difference between manual and algorithm ONSD
  - Mean difference (SD) 0.012 (0.046) (p = 0.303)
- Correlation between manual and algorithm ONSD

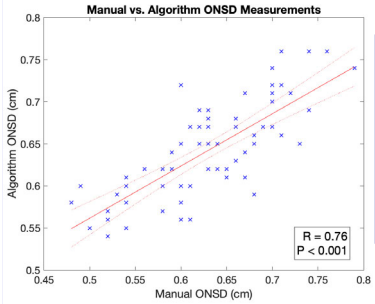

	ONSD Manual	ONSD Algorithm
Minimum	0.48	0.54
Maximum	0.79	0.76
Range	0.31	0.22
Mean	0.63	0.64
Std. Deviation	0.070	0.057
Std. Error of Mean	0.0086	0.0070
Lower 95% CI of mean	0.62	0.63
Upper 95% CI of mean	0.65	0.66

- Bland-Altman and ICC analysis

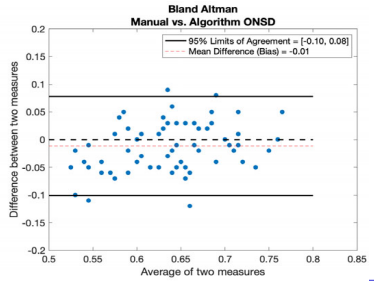

	Algorithm vs Manual	Operator 1 vs. Operator 2
Error (e)	6.33%	4.74%
MSE	0.0022	0.0016
ICC	..	0.80
p-value	0.15	0.26

Conclusion

- Our fully automated method to calculate ONSD performed with high precision.
- Intra-class correlation coefficients, t-test and percentage of error indicated strong correlation between the proposed and manual method
- The automated algorithm seems to be an appropriate alternative to manual measurements

Acknowledgement

- This work has been supported by a Department of Defense – Combat Casualty Care grant award W81XWH-18-1-0005
- The authors would like to thank the Michigan Center for Integrative Research in Critical Care

Appendix B:

Abstract MHSRS-19-01526 and poster: *"Mohamad Hakam Tiba, Venkatakrishna Rajajee, Craig A. Williamson, Brandon C. Cummings, Brendan M. McCracken, Carmen I. Colmenero, Danielle C. Leander, Anne Marie Weitzel, Abdelrahman Awad, Amanda J. Pennington, Kevin R. Ward. Novel Monitoring Modality of Traumatic Brain Injury Patients Using Transocular Brain Impedance (TOBI)."*

Novel Monitoring Modality of Traumatic Brain Injury Patients using Transocular Brain Impedance (TOBI).

Mohamad Hakam Tiba, MD, MS[1,2], Venkatakrishna Rajajee, MD[2,3], Craig A. Williamson, MD[2,3], Brandon C. Cummings, BS[1,2], Brendan M. McCracken, BS[1,2], Carmen I. Colmenero, BS[1,2], Danielle C. Leander, BS[1,2], Anne Marie Weitzel, BS[1,2], Abdelrahman Awad, MD[1,2], Amanda J. Pennington, MS[1,2], Kevin R. Ward, MD[1,2,4]

[1] Department of Emergency Medicine, University of Michigan, Ann Arbor, MI.
[2] Michigan Center of Integrative Research in Critical Care (MCIRCC), University of Michigan, Ann Arbor, MI.
[3] Departments of Neurosurgery and Neurology, University of Michigan, Ann Arbor, MI.
[4] Department of Biomedical Engineering, University of Michigan, Ann Arbor, MI.

Introduction: Management and monitoring of severe traumatic brain injury (TBI) patients remains a challenging task. In addition to management of the initial injury, one of the primary objectives when dealing with TBI is to prevent secondary brain injury due to ischemia, inflammation or edema. Cerebrovascular autoregulation (CAR) is an auto-protective mechanism where consistent levels of cerebral blood flow (CBF) are maintained in the face of changing intracranial or systemic pressure, by modulating vascular tone. Impairment of CAR after TBI often leads to exacerbation of the injury by the ensuing ischemia or edema. Monitoring and assessment of CAR is envisioned to be valuable during the management of TBI patients as a means to optimizing cerebral perfusion pressure (CPP), delay or prevent secondary injury and ultimately, improve outcome. Direct assessment of CAR is difficult and has proven to be elusive. Current modalities assessing CAR are often invasive and hard to obtain in a meaningful and timely manner. Impedance may be a novel, non-invasive and effective measure to assess CAR. Impedance is a measure of the passive electrical properties of tissues and is affected directly by the volume of blood in the interrogated area, and indirectly by respiration's quality and quantity. In this study, we aim to test a novel real time, portable and non-invasive monitoring modality to assess CAR utilizing brain impedance as measured through a transocular pathway.

Hypothesis: We hypothesize that using transocular brain impedance will provide a real time and non-invasive assessment of CAR. Development of monitoring devices to assess CAR will be of utmost benefit in the management of TBI.

Methods: We utilized both a porcine animal model of TBI as well as monitoring and testing of severe TBI patients in the ICU. In the animal model, male Yorkshire swine with a mean(SD) weight of 44(2.2) kg were anesthetized, mechanically ventilated, and instrumented to continuously record intracranial pressure (ICP), mean arterial pressure (MAP), CPP and CBF. Transocular brain impedance was measured and recoded by placement of ECG electrodes on the eyelids and connected to data acquisition system. Cerebral blood volume and blood pressure were manipulated with maneuvers such as intravenous norepinephrine challenge,

epidural hematoma and systemic hemorrhage. Brain impedance was also continuously monitored in human TBI patients without any provocative maneuvers, provided that their ICP and MAP were already being monitored as part of their clinical management. Using the data collected during the course of human testing as well as the provocative maneuvers during animal testing, we have developed several novel analytic tools and indices for the assessment of the trans-ocular bioimpedance waveform as it relates to CAR parameters such as MAP, ICP, CPP, and CBF. First, we investigated how the bioimpedance signal interacts with arterial blood pressure (*DZx*) in an effort to create an analytic impedance *index* similar to the pressure-reactivity index (*PRx*). Second, we investigated the role of the cardiac frequency of the impedance signal by calculating the ratio of cardiac to respiratory amplitude (*DZr*). Both *DZx* and *DZr* were compared to CAR surrogates such PRx, CPP, ICP and CBF.

Results: 26 animals were tested in the porcine model. The impedance cardiac to respiratory ratio (*DZr*) index tracked changed in CAR parameters such as ICP, CPP, and CBF with moderate to high precision. When considering the various provocative maneuvers, *DZr* demonstrated significant correlation with changes in ICP, CPP and CBF with *median p*-value 0f 0.08, 0.06 and 0.07 respectively. In addition, *DZx* demonstrated the presence of a dynamic relationship between the ocular-brain impedance signal and MAP similar to *PRx*. *DZx* seems to mirror changes in *PRx* and it is notable that *DZx* and *PRx* often move opposite one another due to the inverse relationship between impedance and ICP. The same indices, *DZx* and *DZr* exhibited similar behavior when tested in patients with severe TBI. Both impedance *indices* were able to track changes in CAR parameters with high precision ($p<0.0001$).

Conclusion: In this study, the impedance indices appear to track changes in parameters that affect CAR (ICP, CPP, CBF) and PRx as an indicator of CAR impairment. Development of indices (*DZx & DZr*) that can be extracted from the impedance signal may prove to be useful as part of a portable, easily-applied device, and will be a significantly less-invasive alternative for the early assessment of TBI and detection of CAR impairment. Further studies in animals and humans are currently underway to further validate this promising technology.

Describe Dynamic relationship between cerebrovascular autoregulation, cerebral perfusion pressure and cerebral blood volume.

Describe ocular brain impedance changes during Interventions that manipulate levels of ICP, CPP, and CBF.

Describe a novel measures and indices to assess cerebrovascular autoregulation.

Novel Monitoring Modality of Traumatic Brain Injury Patients using Transocular Brain Impedance (TOBI)

Mohamad Hakam Tiba[1,2], Brendan M. McCracken[1,2], Venkatakrishna Rajajee[2,3], Craig A. Williamson[2,3], Brandon C. Cummings[1,2], Carmen I. Colmenero,1,2, Danielle C. Leander[1,2], Anne Marie Weitzel[1,2], Abdelrahman Awad[1,2], Amanda J. Pennington[1,2], Kevin R. Ward[1,2,4]

[1] Department of Emergency Medicine, [2] Michigan Center of Integrative Research in Critical Care (MCIRCC), [3] Department of Neurosurgery,

[4] Department of Biomedical Engineering, University of Michigan, Ann Arbor, MI.

CENTER FOR INTEGRATIVE RESEARCH IN CRITICAL CARE
UNIVERSITY OF MICHIGAN

INTRODUCTION

Traumatic Brain Injury (TBI)

- "Silent epidemic" because of associated complications
- 2.5 million people sustained a TBI in 2010
- Accounts for 30% of all injury related deaths

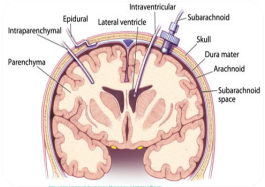

Management & Monitoring Strategies

- Monitoring of intracranial pressure (ICP)
  - *Invasive, increased risk of infection and further damage to the brain*
- Optimization of cerebral perfusion pressure (CPP) to a target level
- Preventing secondary brain damage (ischemia, edema)

Cerebrovascular Autoregulation

- Vessels modulate their tone in response to changes in pressure
- Maintains constant levels of cerebral blood flow (CBF)
- Auto-protective mechanism
- Prevention of secondary brain injury
- Impaired in severe head injury or acute ischemic stroke
- Predictor of poor outcomes in acute neurological disease
- Continuous monitoring is beneficial to optimize CPP

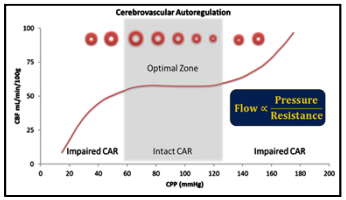

- Precision or personalized approach in managing the components of CPP

Measuring autoregulation remains a challenge

- Current monitoring modalities include:
  - *Transcranial Doppler (TCD)*
  - *Hemoglobin saturation by near-infrared spectroscopy (NIRS)*
  - *Laser Doppler flowmetry of CBF*
- Many of these methods are:
  - *Invasive and non-specific*
  - *Intermittent spot-checks*
  - *Require high levels of expertise*
  - *Unavailable at earlier echelons of care*
  - *Produce mixed results*

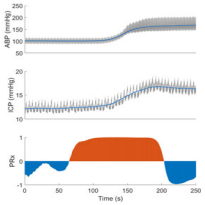

Pressure reactivity index (PRx)

- Moving Pearson correlation between MAP and ICP
- Requires invasive ICP measurement
- Calculation is complex and produces a noisy signal
- Often unavailable outside of research-minded academic settings

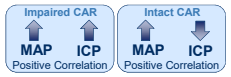

BIOIMPEDANCE

Opposition to an electrical current flow through tissues

- Passive bioelectricity. Tissues' response to external electrical excitation.
- Cumulative effect of individual impedances

Blood has a distinct effect on bioimpedance:

- Good conductor of electricity
- More blood present → lower bioimpedance

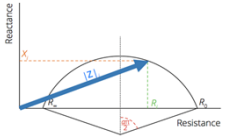

RESPIRATION affects bioimpedance indirectly

- Thoracic pressure gradient
- Changes in venous return

Transocular Brain Impedance (TOBI)

- Bipolar impedance measured from noninvasive electrodes placed over the eyelids
- Brain encounters a significant portion of the electrical current sent through the globes
- Magnitude of respiratory variation reflects brain blood volume

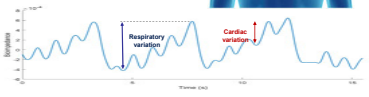

AIM

To use Trans-ocular Brain Impedance in conjunction with arterial blood pressure to create a novel index of cerebrovascular autoregulation.

METHODS

Large Animal Model

- Anesthetized animals 39(1.2) kg
- Challenges: hyper/hypotension and epidural hematoma (1)
- Trans-Ocular Brain Impedance (dz)
- Arterial Blood Pressure (MAP)
- Intracranial Pressure (ICP) (2)
- Laser Doppler Flow (LDF) (3)
- Transcranial Doppler Flow (MCA: TA_{MEAN})

Clinical Testing

University of Michigan Hospital System, Neurosurgery ICU or Trauma ICU with 44 severe TBI patients 49(16.9) y/o. Invasive MAP and ICP
ICP: 11(6.4)mmHg. Range 1 -24mmHg. **MAP**:104(16.5)mmHg. Range: 70-142mmHg

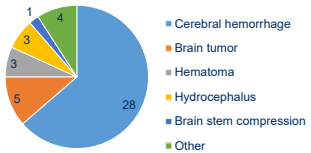

RESULTS

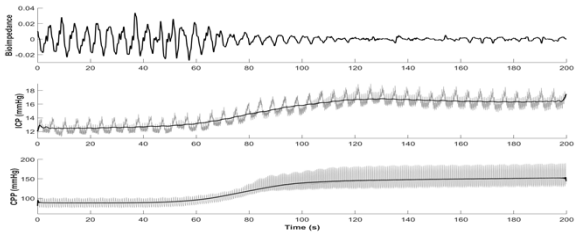

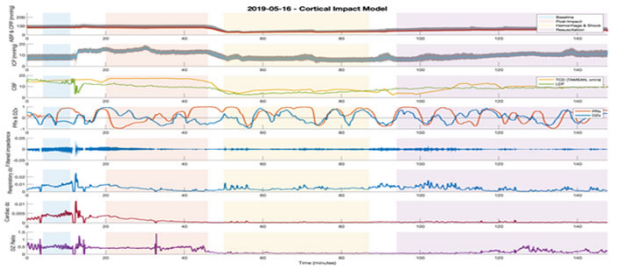

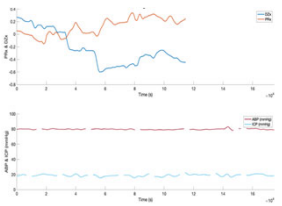

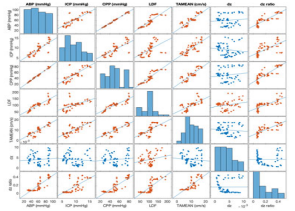

CONCLUSION

- Impedance indices appear to track changes in parameters that affect CAR (ICP, CPP, CBF) and PRx as an indicator of CAR impairment.
- Development of indices (*DZx & DZr*) that can be extracted from the impedance signal may prove to be useful as part of a portable, easily-applied device, and will be a significantly less-invasive alternative for the early assessment of TBI and detection of CAR impairment.
- Further studies in animals and humans are currently underway to further validate this promising technology.

ACKNOWLEDGEMENT

- Supported by the Department of Defense – Combat Casualty Care grant award W81XWH-18-1-0005
- The authors would like to thank the Michigan Center for Integrative Research in Critical Care (MCIRCC), New Vital Sign Inc., and In2Being LLC.
- KRW and MHT have submitted an invention disclosure. Office of Tech Transfer. University of Michigan

Appendix C:

Conference paper and poster: *"Soroushmehr, R., Rajajee, K., Williamson, C., Gryak, J., Najarian, K., Ward, K. and Tiba, M.H., 2019, July. Automated Optic Nerve Sheath Diameter Measurement Using Super-Pixel Analysis."*

Automated Optic Nerve Sheath Diameter Measurement Using Super-pixel Analysis*

Reza Soroushmehr, Krishna Rajajee, Craig Williamson, Jonathan Gryak,
Kayvan Najarian, Kevin Ward, Mohamad H. Tiba

***Abstract*— The optic nerve is a part of the central nervous system surrounded by cerebrospinal fluid and is encased in a sheath. Changes to the cerebrospinal fluid due to injury, tumor rupture and so on can increase intracranial pressure (ICP) and can result in changes in the sheath diameter. Measuring the changes in the sheath can be done through ultrasound imaging with which the optic nerve sheath diameter can be measured. Since this approach is non-invasive, it would reduce the cost for patients and healthcare if sheath diameter could be used as a predictor of increase in ICP. However, the manual measurement of the nerve sheath diameter is very time consuming and could be affected by human errors. In this paper we propose an image processing approach in which the optic nerve sheath diameter is measured automatically. In our proposed method, we first denoise images and then detect the region of interest using a simple line integral method. After that by analyzing super-pixels we measure the diameter. We compared the results of the proposed method with manual measurements from two experts and achieved the average percentage of error of 5.48%.**

I. Introduction

The optic nerve sheath is an anatomical extension of the duramater, the outermost and most substantial meningeal layer of central nervous system, and the subarachnoid space around the optic nerve is continuous with the intracranial subarachnoid space and is surrounded by cerebrospinal fluid (CSF) [1-3]. The diameter of this sheath changes rapidly with changes in CSF pressure that can result from or result in brain injury [1]. The CSF pressure can increase the intracranial pressure (ICP) whose elevation degree and duration are correlated with patients' outcomes [4]. Therefore, ICP monitoring can provide important information for patients' management and treatment and hence can improve the mortality and morbidity rates of patients with brain injuries. This is also a standard tool for management of brain injured patients. However, as an invasive monitoring device, ICP monitoring can cause complications such as intracranial haemorrhage, dislocation, breakage of the fiberoptic cable and monitor-related infection [5]. Moreover, direct measurement of ICP, especially for patients with minor brain injury, is an unrealistic and aggressive requirement [6]. Therefore, the objective of some clinical trials and research studies is to replace the ICP monitoring with a non-invasive measurement [7-9]. Since it has been shown that ventriculostomy measurements of intracranial pressure are correlated with ultrasound (US) optic nerve sheath diameter (ONSD) measurements, ONSD can be used as a non-invasive test for elevated ICP [6]. However, manual measurement of ONSD is tedious, time-consuming, and subject to human errors. Therefore, an automated measurement method not only can avoid many possible errors, but it can also make a large clinical study that requires the measurement, feasible. In order to measure the diameter automatically, we first need to segment the ultrasound images. A number of methods have been proposed for ultrasound image segmentation [10-.12]. Nobel and Boukerroui [10] review ultrasound image segmentation methods developed for applications such as left ventricle segmentation, breast cancer, prostate cancer, obstetrics and gynecology and vascular disease. They also review state-of-the-art ultrasound segmentation techniques in terms of methodology. They refer to the techniques used for segmentation where they use different information such as image features (e.g. gray level distribution, intensity gradient, phase and texture), shape and temporal prior for those containing image sequences. In our proposed method we also use the temporal information and calculate the diameter in all the images in the video sequence and then we vote among all the measurements to reduce the measurement's error. Liu *et al.* [11] refer to some challenges facing the ultrasound image segmentation such as low signal to noise ratio (SNR), low contrast and blurry boundaries and propose an active contour model based on the level set method to segment breast ultrasound images. They propose an energy function based on level set approach using differences between the estimated and the actual probability densities of different regions' intensities. The minimum of the function is calculated using partial differential equation and is used for segmenting the images. In our method we use a denoising method to increase the SNR. In a recent research study, Xu *et al.*[12] propose an ultrasound image processing method for breast tumor segmentation. They used images from 21 subjects where they have 250 slices for each subject to train and test a convolutional neural network (CNN). They use an 8-layer CNN which has 3 convolutional layers, 3 pooling layers, one fully connected (FC) layer, and a softmax layer and achieve accuracy, precision and recall above 80%. In our research study, the consecutive images in a sequence are very correlated/similar to each other and the number of subjects is small. Therefore, we use traditional image processing techniques to calculate the diameter instead

*Research supported by DOD (W81XWH-18-1-0005)

R. Soroushmehr and J. Gryak and K. Najarian are with the Department of Computational Medicine and Bioinformatics and also the Michigan Center for Integrative Research in Critical Care (MCIRCC), University of Michigan, Ann Arbor, MI, 48109, U.S.A.

M.H. Tiba and K. Ward are with the Emergency Medicine Department and also the Michigan Center for Integrative Research in Critical Care (MCIRCC), University of Michigan, Ann Arbor, MI, 48109, U.S.A.

K. Rajajee, C. Williamson are with the Department of Neurological surgery and Neurology and also the Michigan Center for Integrative Research in Critical Care (MCIRCC), University of Michigan, Ann Arbor, MI, 48109, U.S.A.

of using convolutional neural networks. The rest of the paper is organized as follows. In Section II, we describe the details of the method which includes preprocessing (denoising the images and finding the region of interest), segmenting images using a super-pixel approach, calculating the diameter in each image and voting among all the measurements. In Section III, we show the experimental setup and present the results of the proposed method and compare the results with ground truth. Finally, in Section IV we conclude the paper.

II. Proposed Method

The goal of this study is to develop an automated method using image processing techniques to measure the optic nerve sheath diameter from ultrasound images. This diameter is measured 3mm behind the globe as shown in Figure 1.

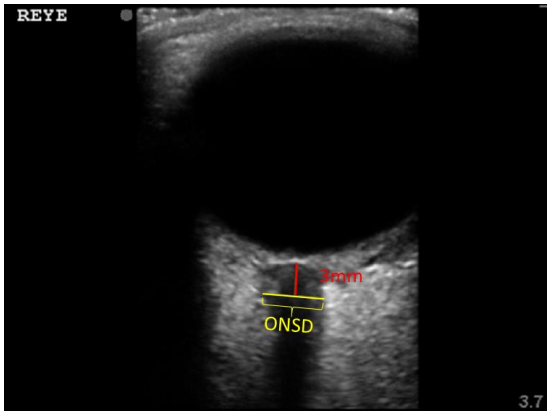

Figure 1: An ultrasound image with the optic nerve sheath diameter (ONSD)

The schematic diagram of the proposed method is shown in Figure 2.

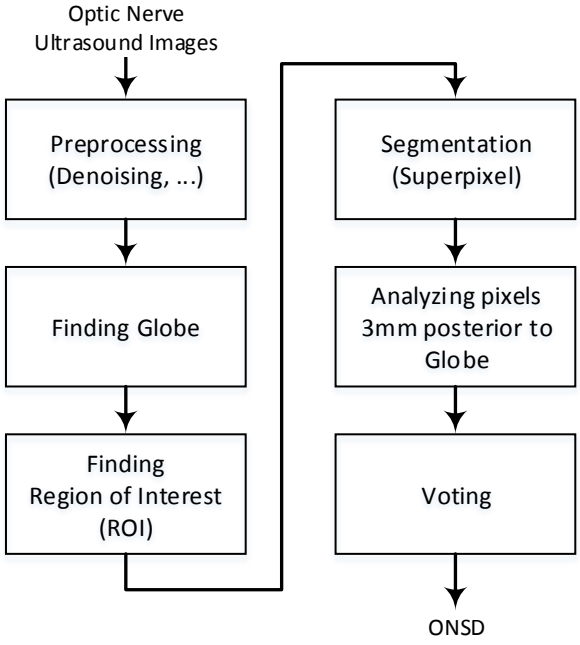

Fig.2: Schematic diagram of the proposed method

In the first stage of the proposed method, we perform preprocessing in which we crop images using Digital Imaging and Communications in Medicine (DICOM) attributes that specify the location of the entire scan containing the nerve sheath and the retinal detachment. We also denoise images using a technique called image guided filtering [13] which is an edge-preserving method. In the following we briefly describe this method.

Suppose that the filtering input image and guidance image are shown as P and I respectively. The images are divided to overlapped windows with radius of r and following coefficients are computed in each window:

$$a_k = \frac{cov_k(I,P)}{var_k(I)+\varepsilon} \qquad b_k = \bar{p}_k - a_k\bar{I}_k \tag{1}$$

where k is the window index, $\bar{I}_k$ and $\bar{p}_k$ are average of intensities in k^{th} window in noisy and guidance images respectively. Also ε is called regularization parameter that determines the edge-preserving property of the filter. The filtered pixel q_i is the average of $a_k I_i + b_k$ in all the windows that cover q_i. cov and var functions compute the covariance and variance respectively

After denoising images, we find the region of interest (ROI) which only contains the nerve sheath by analyzing the image integral. This is done through calculating the summation of pixel values in each column and each row separately. Suppose that the denoised image is an $N \times M$ image shown as I_d. We analyze the following one dimensional signals.

$$v(n) = \sum_{m=1}^{M} I_d(n,m) \quad for\ n = 1, \dots, N \tag{2}$$

$$h(m) = \sum_{n=1}^{N} I_d(n,m) \quad for\ m = 1, \dots, M \tag{3}$$

The v signal (i.e. the yellow curve in Fig. 3 which is a result of vertical line/column integral) has two main peaks, Max_1 and Max_2 , corresponding to the brighter regions and a local minimum between these peaks corresponding to the dark region inside the sheaths.

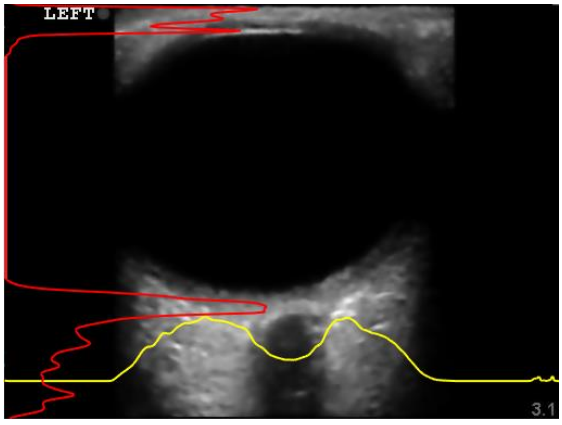

Figure 3: Vertical line and horizontal line integrals for finding the globe point and the region of interest (ROI)

The h signal (i.e. the red curve in Fig.3 resulting from horizontal line/row integral) is used to identify the globe point. In this figure, the v and h signals are superimposed on the image. We use the peaks of v to identify the borders of the ROI.

Suppose that the minimum of the v signal is gth element of the signal. This value corresponds to the column where we can find the globe.

$$g = \underset{Max_1 \le i \le Max_2}{argmin} \; v(i) \tag{4}$$

After finding the globe point and the ROI, we use a super-pixel segmentation technique called simple linear iterative clustering (SLIC) [14] to segment each image to super-pixels. This method partitions an image to homogenous regions based on spatially localized k-means clustering technique. The image is first partitioned to non-overlapped blocks/tiles and the center of each tile is used as an initial parameter for clustering. After that the center of each tile is refined and also its shape is modified in an iterative process using Lloyd algorithm [15]. The modified shape is called super-pixel. Finally, in a post processing stage super-pixels are analyzed in terms of their areas and small ones are excluded from the results.

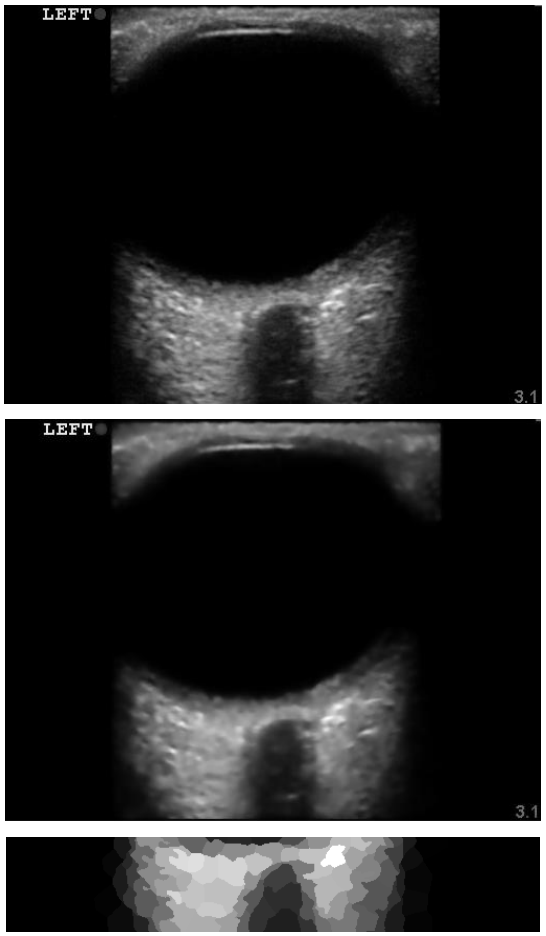

Fig. 4: The top image is the raw image, the middle image is the denoised image and the bottom image is the result of the SLIC algorithm on ROI.

Suppose that the output of this method is called I_s and the row which is $3mm$ below the globe is $r_{3\text{mm}}$th row of I_s. It should be mentioned that as the size of each pixel can be extracted from DICOM metadata, we can easily find the row which is 3mm below the globe. We analyze the peaks and also derivatives of this row to calculate the ONSD. As can be seen in figure 5, the minimum super-pixel value is at the globe point. As the derivative is calculated by subtracting each value from the previous one, we find the positive peaks after the globe point and negative peaks before the globe point from the derivate curve to find the border of nerve sheath and hence to calculate the diameter (i.e. ONSD).

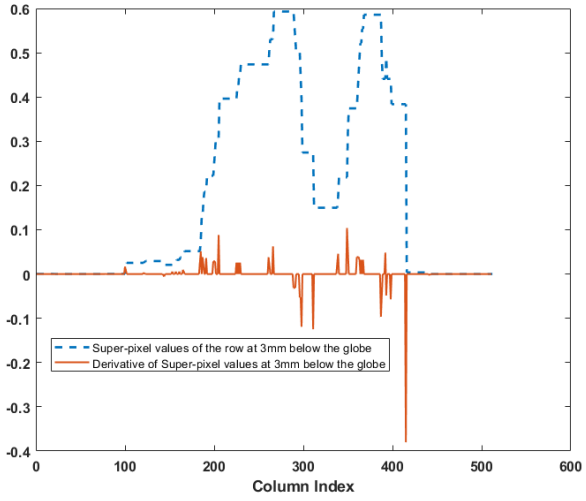

Fig. 5: Superpixel values of the r_{3mm}th row below the globe and also the derivatives of that row in one of the ultrasound images.

We repeat this process for all the images in the ultrasound video and then we vote among all the values by calculating their median.

III. Experimental Results

We implemented our proposed method in MATLAB 2018b and applied it on 50 de-identified videos of 25 traumatic injured patients. These patients were admitted to the University of Michigan health system and for each patient we have ultrasound images of both eyes. We compared the results of the proposed method with ground truth measurements which are measurements from two experts. We also calculated the correlation between two experts' measurements. It should be noted that the individuals performing the manual measurements were blinded to each other's measurements as well as the algorithm measurement. We calculated the average error between the proposed method and the ground truth using Eq. (5).

$$e = \frac{1}{n_u} \sum_{k=1}^{n_u} \left| 1 - \frac{ONSD_1(k)}{ONSD_2(k)} \right| \times 100 \tag{5}$$

In (5), n_u is the number of ultrasound images. Also, $ONSD_1$ and $ONSD_2$ are the ONSD measurements from two sources. For instance, for comparing the results of the proposed method with the ground truth, $ONSD_1$ and $ONSD_2$ are the algorithm results and the average of two experts' measurements respectively. Moreover, for comparing two experts' measurement, $ONSD_1$ and $ONSD_2$ are the

measurements from each expert. The average percentage of error between the results of the algorithm and the average manual measurements is 5.49%. This error is 4.8% for two experts' measurements. The difference between these two errors show that the proposed algorithm can calculate the ONSD accurately. We also calculated the mean square error using Eq (6) where $\|.\|_2$ is the norm-2.

$$MSE = \frac{1}{n_u}\|ONSD_1 - ONSD_2\|_2 \qquad (6)$$

The MSE between the algorithm results and the average of two experts' measurements is 0.0018 while the MSE between two experts' measurement is 0.0016. Moreover, we calculated intraclass correlation coefficient (ICC) which shows the similarity between two quantitative measurements [16]. The ICC between the algorithm results and the average between two experts' measurements is 0.70 while the ICC between two experts' measurement is 0.87. These comparisons indicate strong correlation between the proposed method' s results and the ground truth.

IV. Conclusion

Even though intracranial-pressure monitoring is a standard care for severe traumatic injured patients, using such invasive devices might be associated with worsening of survival and there might be complications following the placement of ICP sensors. Therefore, a non-invasive monitoring can prevent secondary complications. It has been shown that there is a correlation between the ICP elevation and the optic nerve sheath diameter. In this paper, we proposed an automated method to calculate this diameter using image processing techniques. We first denoised images and identified the region of interest using a simple method and then applied a super-pixel segmentation method. After that we analyzed the row which is 3mm below the globe to measure the diameter of the nerve sheath. This was done by performing derivative of that row and finding its peaks. We compared the results of the proposed method with the average of two experts' measurements and achieved the percentage error of 5.49%, mean square error of 0.0018 and ICC of 0.70 while these values between two experts' measurements were 4.6% and 0.0016 and 0.87 respectively. In our future studies we will run the method on more videos and also calculate the correlation between the ONSD and the elevated ICP.

References

[1] P. Williams, "Optic nerve sheath diameter as a bedside assessment for elevated intracranial pressure," *Case reports in critical care*, vol. 2017, pp.1-2, 2017.

[2] J. Chacko, "Optic nerve sheath diameter: An ultrasonographic window to view raised intracranial pressure? *Indian journal of critical care medicine*, vol. 18, no. 11, pp. 707-708, 2014

[3] J.T. Maikos, R.A. Elias, and D.I. Shreiber, "Mechanical properties of dura mater from the rat brain and spinal cord," *Journal of neurotrauma*, vol. 25, no. 1, pp.38-51, 2008.

[4] M. Smith, "Monitoring intracranial pressure in traumatic brain injury," *Anesthesia & Analgesia*. vol. 106, no. 1, pp. 240-8. 2008.

[5] A. Bekar, S. Doğan, F. Abaş, B. Caner, G. Korfalı, H. Kocaeli, S. Yılmazlar, and E. Korfalı, "Risk factors and complications of intracranial pressure monitoring with a fiberoptic device," *Journal of Clinical Neuroscience*, vol. 16, no. 2, pp.236-240, 2009.

[6] V.S. Tayal, M. Neulander, H.J. Norton, T. Foster, T. Saunders, and M. Blaivas, "Emergency department sonographic measurement of optic nerve sheath diameter to detect findings of increased intracranial pressure in adult head injury patients," *Annals of emergency medicine*, vol. 49, no. 4, pp.508-514, 2007.

[7] H.H. Kimberly, S. Shah, K. Marill, and V. Noble, "Correlation of optic nerve sheath diameter with direct measurement of intracranial pressure," *Academic Emergency Medicine*, vol. 15, no. 2, pp.201-204, 2008.

[8] A. Ragauskas, L. Bartusis, I. Piper, R. Zakelis, V. Matijosaitis, K. Petrikonis, and D. Rastenyte, "Improved diagnostic value of a TCD-based non-invasive ICP measurement method compared with the sonographic ONSD method for detecting elevated intracranial pressure," *Neurological research*, vol. 36, no. 7, pp.607-614, 2014.

[9] J. Dubourg, E. Javouhey, T. Geeraerts, M. Messerer, and B. Kassai, "Ultrasonography of optic nerve sheath diameter for detection of raised intracranial pressure: a systematic review and meta-analysis," *Intensive care medicine*, vol. 37, no. 7, pp.1059-1068, 2011.

[10] A. Noble, D. Boukerroui, "Ultrasound image segmentation: a survey," *IEEE Transactions on medical imaging*, vol. 25, no. 8, pp.987-1010, 2006.

[11] B. Liu, H.D. Cheng, J. Huang, J. Tian, K. Tang, and J. Liu, "Probability density difference-based active contour for ultrasound image segmentation,". *Pattern Recognition*, vol. 43, no. 6, pp.2028-2042, 2010.

[12] Y. Xu, Y. Wang, J. Yuan, Q. Cheng, X. Wang. and P.L. Carson, "Medical breast ultrasound image segmentation by machine learning,". *Ultrasonics*, vol. 91, pp.1-9, 2019.

[13] K. He, J. Sun, X. Tang, "Guided image filtering," *IEEE transactions on pattern analysis and machine intelligence*, vol. 35, no. 6, pp.1397-1409, 2013.

[14] R. Achanta, A. Shaji, K. Smith, A. Lucchi, P. Fua, S. Süsstrunk S. "SLIC superpixels compared to state-of-the-art superpixel methods," *IEEE transactions on pattern analysis and machine intelligence*, vol. 34, no. 11, pp. 2274-2282, 2012.

[15] S. Lloyd, "Least squares quantization in PCM," *IEEE transactions on information theory*, vol. 28, no. 2, pp.129-137, 1982.

[16] T.K. Koo, and M.Y Li, "A guideline of selecting and reporting intraclass correlation coefficients for reliability research," *Journal of chiropractic medicine*, vol. 15, no. 2, pp.155-163, 2016.

Automated Optic Nerve Sheath Diameter Measurement Using Super-pixel Analysis

Reza Soroushmehr[1,2], Krishna Rajajee[2,3], Craig Williamson[2,3], Jonathan Gryak[1,2], Kayvan Najarian[1,2,4], Kevin Ward[2,4], Mohamad Tiba[2,4]

[1]Department of Computational Medicine and Bioinformatics, University of Michigan, Ann Arbor, MI, U.S.A

[2]Michigan Center for Integrative Research in Critical Care (MCIRCC), University of Michigan, Ann Arbor, MI, U.S.A

[3]Department of Neurosurgery, University of Michigan, Ann Arbor, MI, USA

[4]Department of Emergency Medicine, University of Michigan, Ann Arbor, U.S.A

Research supported by DOD (W81XWH-18-1-0005)

ssoroush@med.umich.edu

Introduction

- Traumatic Brain Injury (TBI): a major cause of morbidity and mortality
- Vital role of its proper diagnosis in treatment

Introduction

- ICP monitoring:
  - ✓ Providing important information for patient management and treatment
  - ✓ Widely used in the management of severe TBI patients.
  - Invasive
    - ONSD may be used as a non-invasive test for elevated ICP.
- ***Optic nerve sheath***:
  Anatomical extension of the dura mater, the outermost and most substantial meningeal layer of the central nervous system

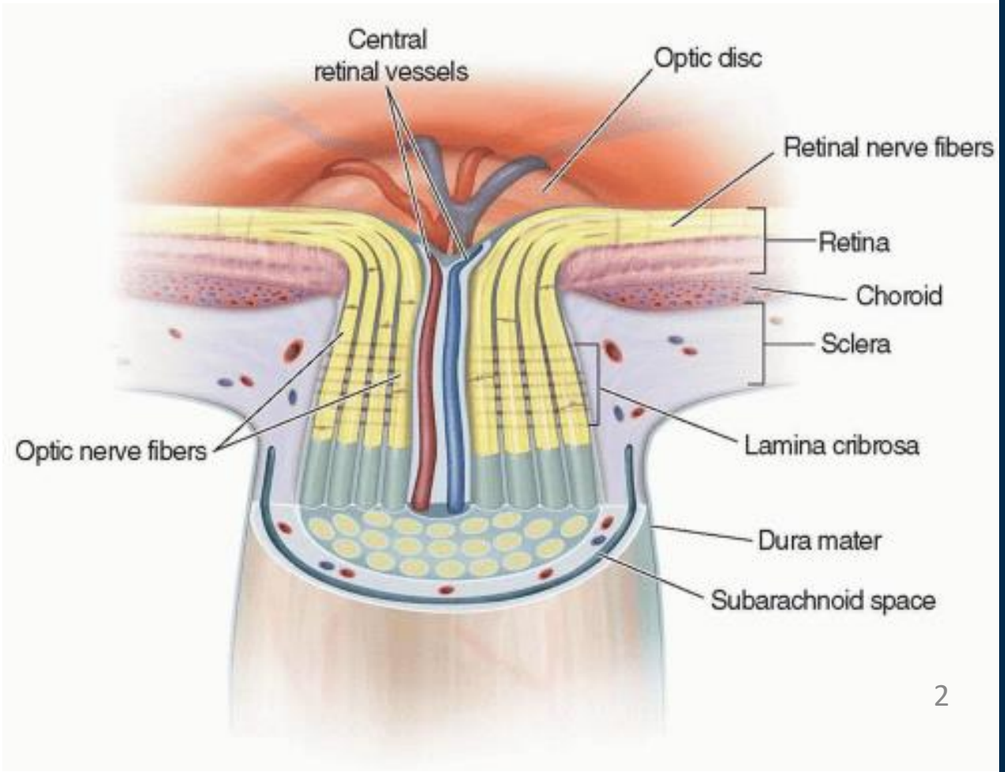

Method

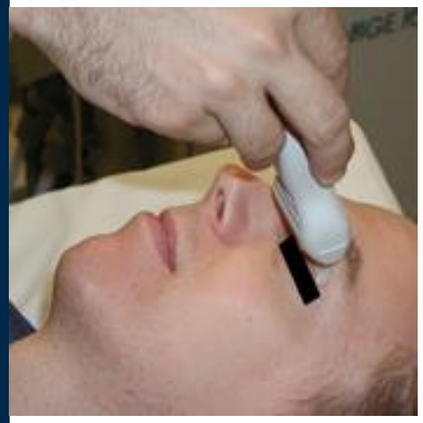

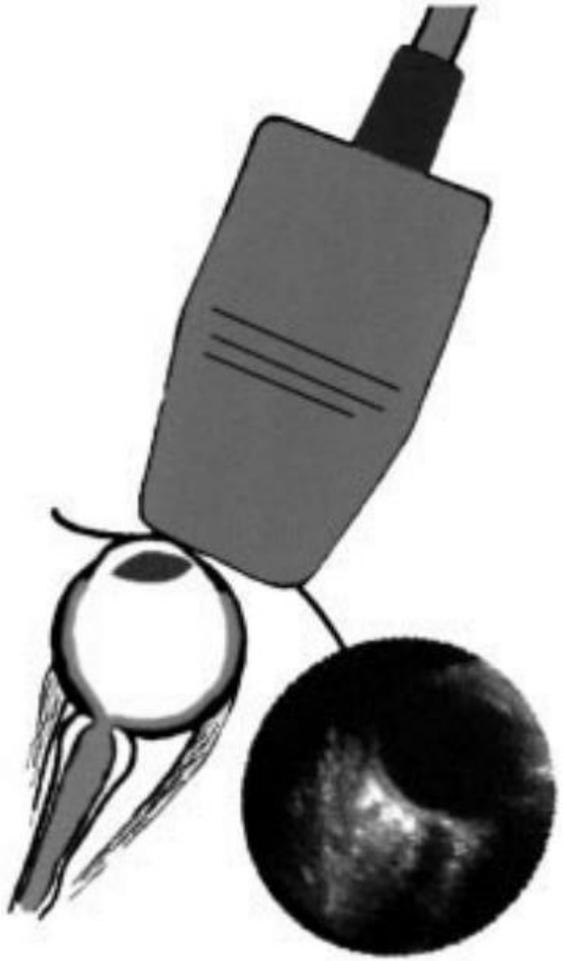

The diameter is measured 3mm behind the globe.

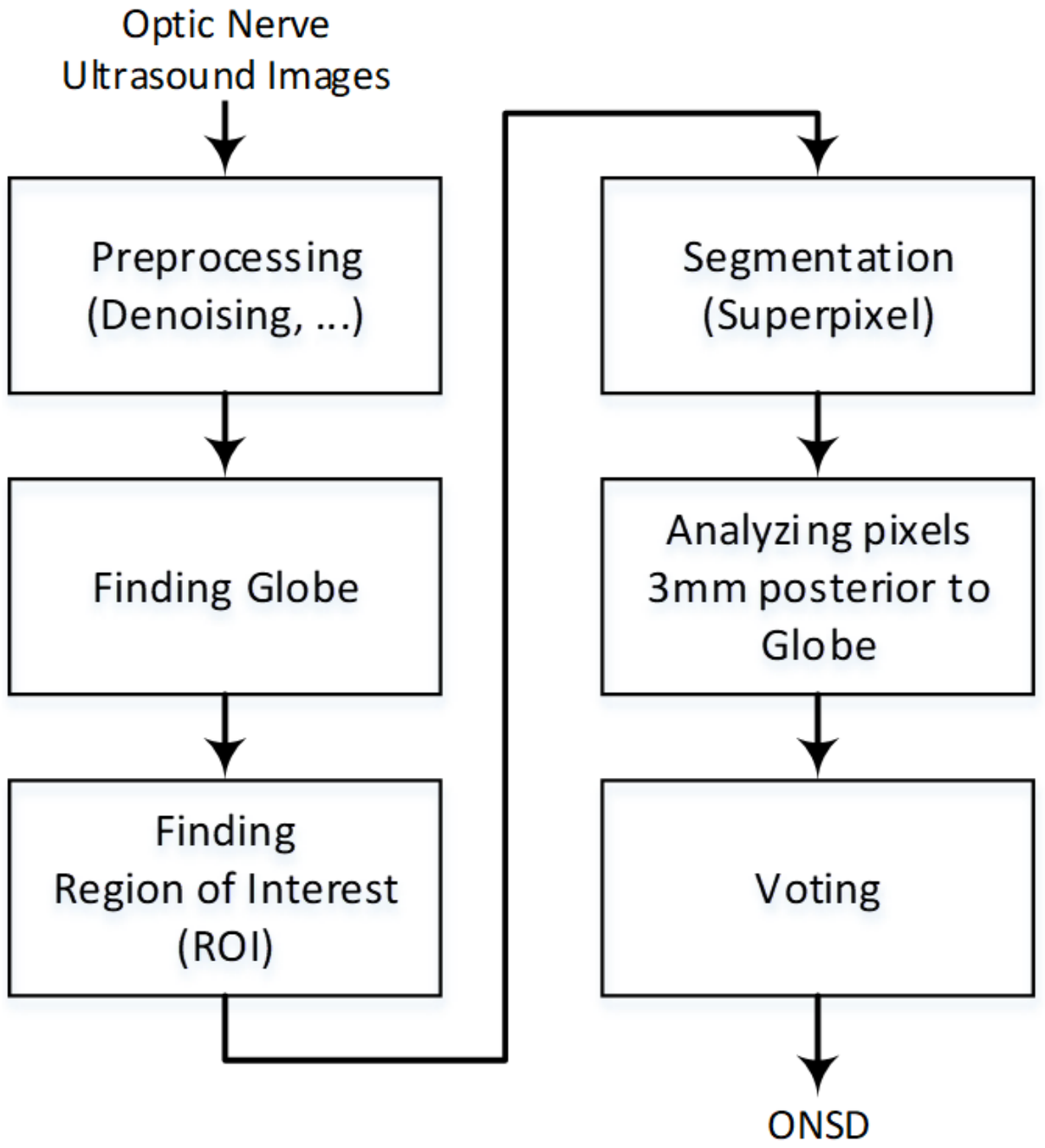

https://www.acep.org/sonoguide/smparts_ocular.html
https://bjo.bmj.com/content/bjophthalmol/86/10/1109.full.pdf

Globe Point

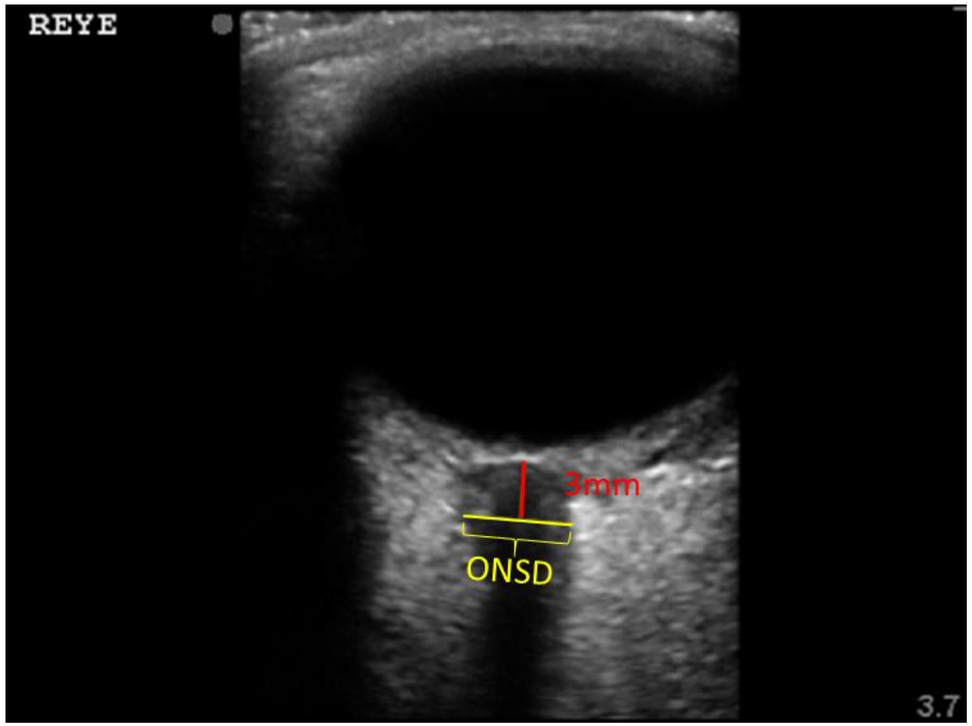

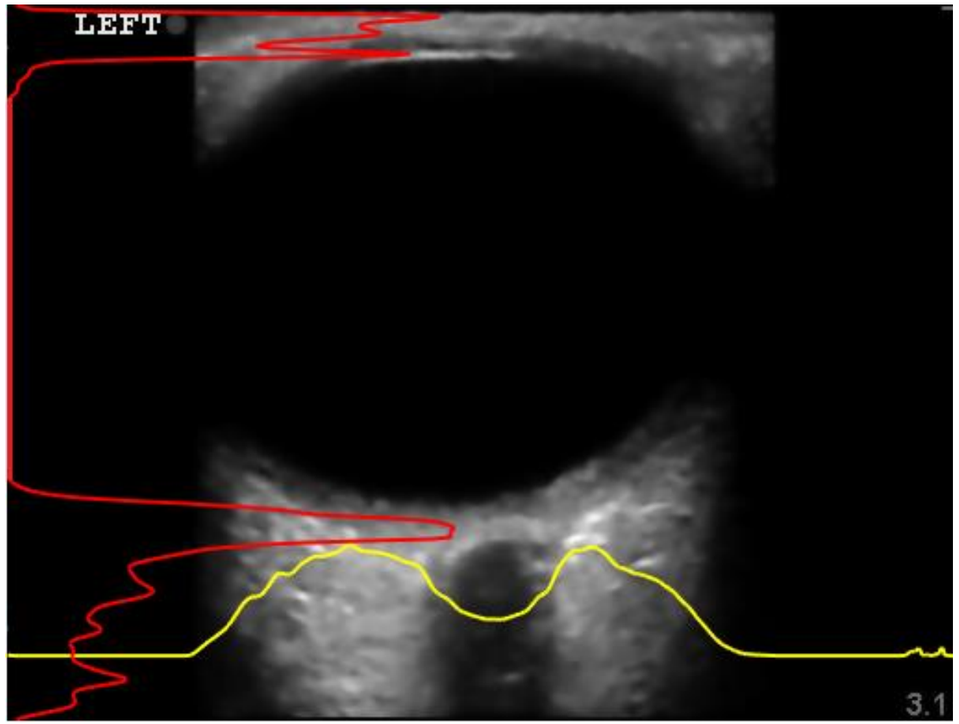

Vertical $v(n)$ and horizontal $h(m)$ line integrals for finding the globe point and the region of interest (ROI)

$$v(n) = \sum_{m=1}^{M} I_d(n,m) \quad for\ n = 1, \ldots, N$$

$$h(m) = \sum_{n=1}^{N} I_d(n,m) \quad for\ m = 1, \ldots, M$$

- Globe $\quad g = \underset{Max_1 \le i \le Max_2}{argmin} \; v(i)$

Super-pixel Analysis

Denoising

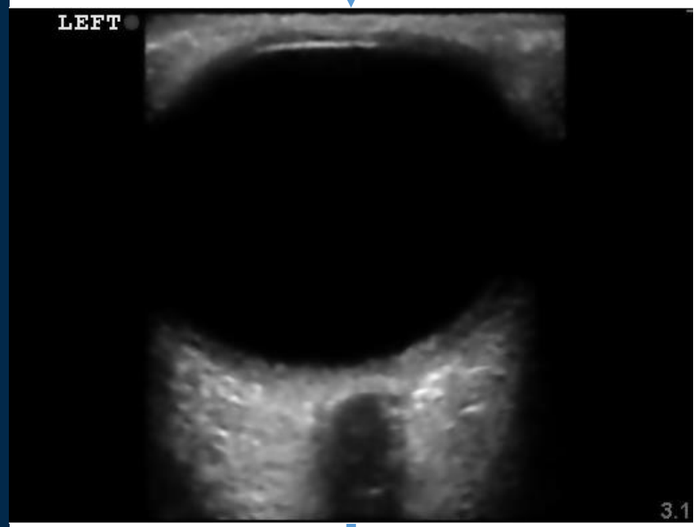

Cropping &
Superpixel Generation

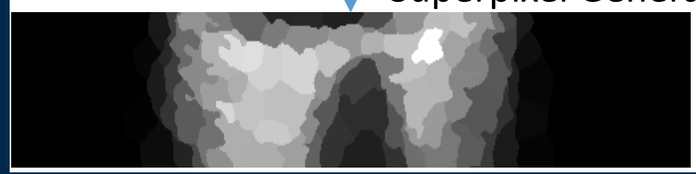

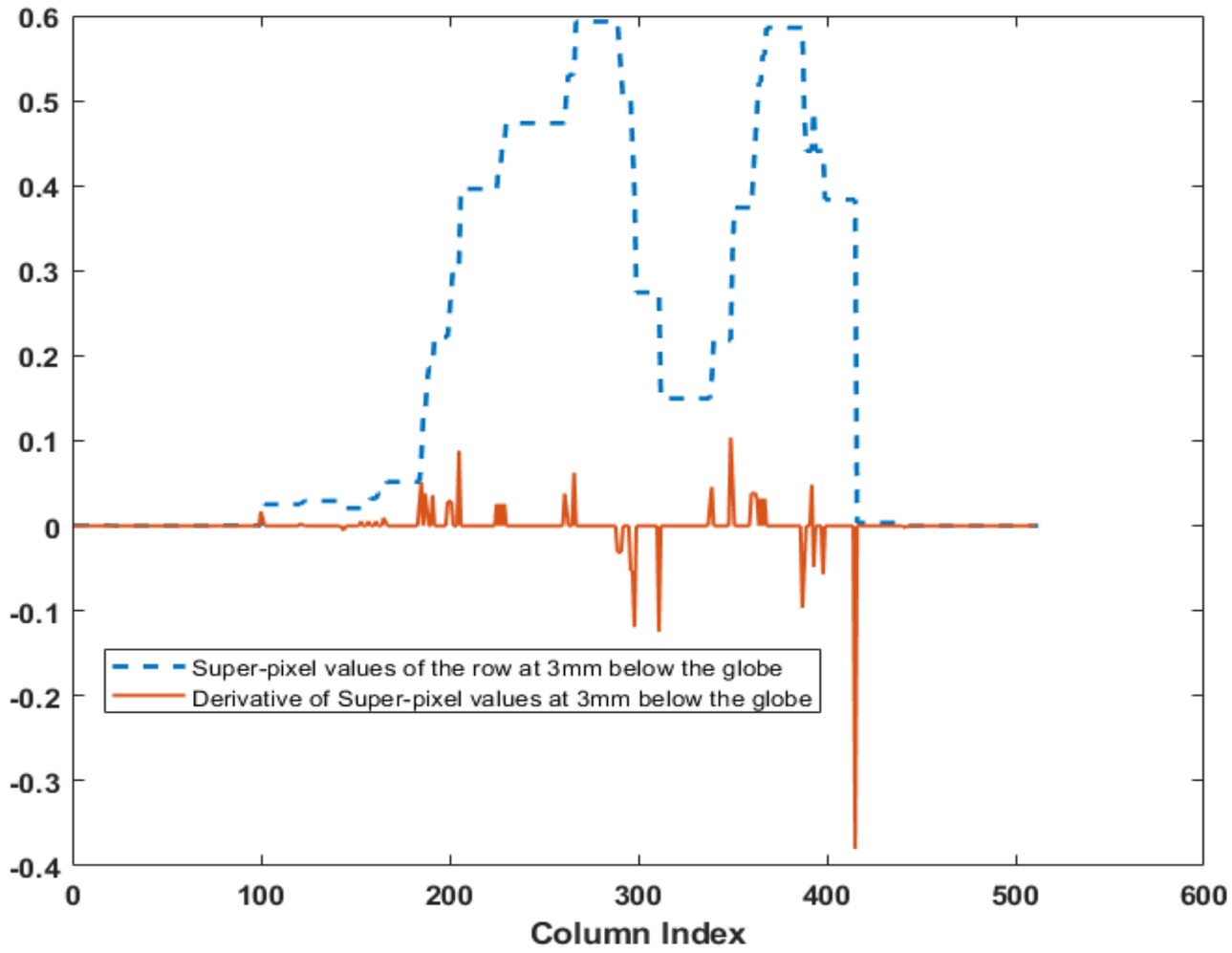

Superpixel values of the row 3 mm below the globe and also the derivatives of that row in one of the ultrasound images.

Results

- **Dataset:** 50 de-identified videos of 25 TBI patients from Michigan Medicine

- **Performance measures:**
  - ✓ Average error between the proposed method and the ground truth: $e = \frac{1}{n_u}\sum_{k=1}^{n_u}\left|1-\frac{ONSD_1(k)}{ONSD_2(k)}\right| \times 100$
  - ✓ Mean squared error: $MSE = \frac{1}{n_u}\|ONSD_1 - ONSD_2\|_2$
  - ✓ Intraclass correlation coefficient(ICC)
  - ✓ Student's t-test,

    Null hypothesis: the means of two measurements are not different.

	Alg. vs Avg. of Manual 1 and 2	Manual 1 vs Manual 2
e	5.52%	4.74%
MSE	0.0018	0.0016
ICC	0.70	0.80
p-value	0.45	0.26

Conclusion and Future Work

- ✓ The proposed method can measure the ONSD accurately.
- ✓ Strong correlation between the proposed method' s results and the ground truth.
- ✓ Future work: Running the method on more videos & calculating the correlation between the ONSD and the elevated ICP.

Appendix D:

Draft manuscript: Submitted for publication consideration in Military Medicine 2019 MHSRS Supplement. *"Rajajee, V, Soroushmehr, R, Williamson, C, Najarian, K, Gryak, J, Awad, A, Ward, K, and Tiba, M. H. Novel Algorithm for Automated Optic Nerve Sheath Diameter Measurement Using a Clustering Approach"*

Pages: 13
TEXT Words: 1977
Tables: 0
Figures: 4
Appendices: None
References: 25

Contact: Mohamad H. Tiba, MD, MS
Email: tibam@med.umich.edu
Guarantor: Mohamad H. Tiba, MD, MS

Novel Algorithm for Automated Optic Nerve Sheath Diameter Measurement Using a Clustering Approach

Automated Optic Nerve Sheath Diameter Measurement

Venkatakrishna Rajajee, MBBS[1,2,6]

Reza Soroushmehr, PhD[3,6]

Craig. A Williamson, MD, MS[1,2,6]

Kayvan Najarian, PhD[3,4,6]

Jonathan Gryak, PhD[3,6]

Abdelrahman Awad, MD[4,6]

Kevin. R Ward, LTC U.S. Army Reserve Medical Corps [4,5,6]

Mohamad H. Tiba, MD, MS[4,6]

[1]Department of Neurological Surgery, 1500 E. Medical Center Drive SPC 5338, Ann Arbor, MI 48109-5338

[2]Department of Neurology, 1500 E. Medical Center Drive, 1914 Taubman Center SPC 5316, Ann Arbor, MI 48109-5316

[3]Department of Computational Medicine and Bioinformatics, 100 Washtenaw Avenue, Ann Arbor, MI 48109-2218

[4]Department of Emergency Medicine, 2800 Plymouth Road, Ann Arbor, MI 48109-2800

[5]Department of Biomedical Engineering, 2200 Bonisteel, Blvd., Ann Arbor, MI 48109-2099

[6]Michigan Center for Integrative Research in Critical Care (MCIRCC), 2800 Plymouth Road, Ann Arbor, MI 48109-2800

Venkatakrishna Rajajee: venkatak@med.umich.edu

Reza Soroushmehr: ssoroush@med.umich.edu

Craig. A Williamson: craigaw@med.umich.edu

Kayvan Najarian: kayvan@med.umich.edu

Jonathan Gryak: gryakj@med.umich.edu

Abdelrahman Awad: abawad@med.umich.edu

Kevin. R Ward: keward@med.umich.edu

Mohamad H. Tiba: tibam@med.umich.edu

Keywords: Optic Nerve Sheath Diameter, Intracranial Pressure, Algorithm, Traumatic Brain injury**,** Clustering

Presentations: Presented as a poster at the 2019 Military Health System Research Symposium, Kissimmee, FL; MHSRS-19-01121).

Funding Sources: This study was supported by a grant from the Department of Defense (#W81XWH-18-1-0005).

Disclaimers: The views expressed in this paper are those of the authors and do not necessarily represent the official position or policy of the U.S. Government, the Department of Defense.

Acknowledgements: The authors would like to thank the Michigan Center for Integrative Research in Critical Care for their technical support.

Abstract:

Introduction: Using ultrasound to measure optic nerve sheath diameter (ONSD) has been shown to be a useful modality to detect elevated intracranial pressure. However, manual assessment of ONSD by a human operator is cumbersome and prone to human error. We aimed to develop and test an automated algorithm for ONSD measurement using ultrasound images and compare it to measurements performed by physicians.

Materials and Methods: Patients were recruited from the Neurological ICU. Ultrasound images of the optic nerve sheath from both eyes were obtained using an ultrasound unit with an ocular preset. Images were processed by two attending physicians to calculate ONSD manually. The images were processed as well using a novel computerized algorithm that automatically analyzes ultrasound images and calculates ONSD. Algorithm-measured ONSD was compared to manually-measured ONSD using multiple statistical measures.

Results: Forty-Four patients with an Average/Standard Deviation (SD) ICP of 14(9.7) mmHg were recruited and tested (with a range between 1 and 57 mmHg). A t-test showed no statistical difference between the ONSD from left and right eyes ($p>0.05$). Furthermore, a paired t-test showed no significant difference between the manual and algorithm measure ONSD with a mean difference(SD) of 0.012(0.046) cm ($p>0.05$) and percentage error of difference of 6.43% ($p=0.15$). Agreement between the two operators was highly correlated (ICC = 0.8, $p=0.26$). Bland-Altman analysis revealed Mean difference (SD) of 0.012 (0.046) ($p = 0.303$) and limits of agreement between -0.1 to 0.08. Receiver Operator Curve analysis yielded an AUC of 0.965 ($p<0.0001$) with high sensitivity and specificity.

Conclusions: The automated image-analysis algorithm calculates ONSD reliably and with high precision when compared to measurements obtained by expert physicians. The algorithm may have a role in computer-aided decision support systems in acute brain injury.

Introduction:

The ability to monitor and manage intracranial pressure (ICP) is critical for the effective management of patients with traumatic brain injury (TBI).[1] An ICP above 20mmHg associated with a threefold higher risk of a neurological deterioration in TBI.[2] The guidelines of the Brain Trauma Foundation recommend the use of invasive ICP monitoring in severe TBI, defined by a Glasgow Coma Scale (GCS) <9. [3] The use of ICP monitoring in severe TBI may be associated with a significant reduction in mortality in civilian centers.[4,5] Furthermore, several studies have also demonstrated that military personnel with combat -related TBI who receive early aggressive intervention, including timely decompressive surgery in the setting of intracranial hypertension, can in fact have good outcomes.[6-9] Current ICP monitoring modalities require invasive techniques that carry the risk of complications such as intracranial hemorrhage, dislocation, breakage of the fiber-optic cable and device-associated infection[10,11] Furthermore, the use of such techniques requires a high level of skill found only in specialized centers and thus significantly limit the ability to provide early precision interventions to victims of TBI.

Ultrasonographic measurement of the optic nerve sheath diameter (ONSD) is emerging as an effective non-invasive technique to assess ICP.[12,13] The optic nerve sheath (ONS) is a continuation of the brain's dura mater while the subarachnoid space around the optic nerve is continuous with the intracranial subarachnoid space. Characteristics of the ONS, as well as blood flow to the eye, are known to be affected by changes in ICP and cerebral blood flow (CBF), potentially allowing the eye to serve as a window into the brain.[12-14] Studies have shown that an increase in ICP results in distension of the retrobulbar ONS within seconds.[15] We have shown previously that measurement of ONSD using ocular sonography is an accurate, non-invasive technique for the detection of intracranial hypertension when performed by an experienced operator with high sensitivity and specificity.[14,16] However, manual calculation of ONSD is time-consuming, and subject to human errors leading to high variability in the measurement. The significant variation seen in the optimal ONSD threshold for identification of high

ICP across several studies greatly limits the practical application of this technique at the bedside.[12] Much of this variation in the optimal ONSD threshold is likely related to technique, with variation in the margins used to define the ONS on acquired ultrasound images resulting from different operators.

In this paper, we present the results of ONSD measurements obtained by developing a novel computer image-analysis algorithm using image processing techniques to automatically measure the optic nerve sheath diameter from ultrasound images. Such an algorithm is envisioned to standardize measurement of the ONSD, and to minimize operator-dependent variability. We hypothesize that algorithm-measured ONSD will be an effective technique to replace manually-measured ONSD.

Methods:

This research has been conducted under approval of the University of Michigan Institutional Review Board (IRB). Patients or their legally authorized representatives were consented for the study. Forty-Four patients were recruited and tested from the neurological intensive care unit. The average (SD) age was 49(16) years and weight was 85(26) kg. Twenty of the patients had sub-arachnoid hemorrhage or other spontaneous intracranial hemorrhage as their primary diagnosis, five patients had TBI, four had hydrocephalus, nine had brain tumors, and five had other neurological conditions requiring intensive care. Thirty-nine of the patients had an External Ventricular Drain and five had an intraparenchymal probe for the invasive measurement of ICP.

Measurement of Optic Nerve Sheath diameter

The sonographic measurements of ONSD were performed by a board certified neurointensivist with training to perform and obtain the ultrasound images. Sonographic images were obtained using an M-Turbo Edge ultrasound unit and an L25 linear 13-6 MHz array transducer probe (SonoSite Inc., Bothell, WA, USA). Axial still images and videos were obtained from each eye using the following procedures. The ultrasound probe was positioned on the eyelid to obtain an image where the entirety of

the globe as well as at least 2cm of the optic nerve sheath behind the globe are visible. Depth, and then gain were adjusted as necessary to obtain the optimal image (Figure 1-A) with confirmation that the ONS is clearly visible on both sides of the optic nerve and that the margins of the optic nerve sheath are clearly demarcated on both sides. Ten seconds of video were recorded. Next, a magnified image of the posterior globe and at least 2cm of the optic nerve were obtained **(**Figure 1-B). Using calipers, the ONSD was measured at 3mm into the Optic Nerve. Measurements were performed on both eyes. The manual assessment of ONSD was performed by two expert attending physicians. Both were blinded to the ICP values and each other's ONSD's values.

Automated ONSD Measurement

This automated process utilizes multiple image processing techniques, including denoising, region of interest detection by line integral calculation, and image segmentation by employing a clustering approach,[17] to separate out components of interest (Figure 2-A and B). Using B-mode ultrasound images obtained by the attending physician, the novel algorithm first de-noises images using a technique called image guided filtering [18] after which the region of interest (ROI) (Figure 2-C)[19] containing only the nerve sheath is found by analyzing the image integral. The algorithm then separates the ONS from both surrounding tissue and the optic nerve itself, allowing for the inner and outer ONSD to be quantitatively assessed. With a single optic nerve ultrasound sweep through the eye, the maximum diameter can be found through a combination of independent edge detection in both axial and lateral directions. After performing the pre-processing, images are segmented using a clustering approach that combines neighboring pixels based on their intensities. The results of the clustered images are then used to calculate the derivative at 3mm below the globe point. The globe point was also calculated based on the line integral analysis. The derivative values were used to find the edges and measure the ONSD. ONSD calculations were repeated on all images for each patient from which the median of the measurements was obtained. All of these steps were performed automatically.

Statistical Methodology

Descriptive statistics *are presented as average and standard deviation. Algorithm-measured ONSD* was compared to manually-measured ONSD by the two clinician experts. Interclass Correlation coefficient (ICC) was assessed for agreement between the two operators manually-assessed ONSD. Pearson correlation and the correlation coefficient were used to allow for visual inspection across a range of values of algorithm and manual ONSD. Percentage error difference between the readings of two operators as well as the algorithm and manual ONSD were calculated. Tukey mean-difference plot (Bland-Altman plot) was used to assess agreement between the two algorithm and manual ONSD. Limits of agreement were calculated with standard errors and 95% confidence intervals. Percentage of error between the results (operators and manual vs. algorithm), Receiver Operator Curve (ROC), and Area Under the Curve (AUC) were used to assess algorithm's predictive performance. Statistical analysis was performed using MATLAB 2018b and GraphPad Prism 8.

Results:

Manual and algorithm ONSD measurements were obtained from 88 ultrasound video images (44 from the left and 44 from the right eyes. Average(SD) ICP from all patients was 14(9.7) mmHg with a range between 1 and 57 mmHg. The average (SD) for manual ONSD from the left and right eyes was 0.64(0.07) cm and 0.62(0.067) cm, respectively. A t-test showed no statistical difference between the left and right eyes ($p>0.05$). Furthermore, average(SD) combined (left and right eyes) manual and algorithm ONSD was 0.63(0.067) and 0.64(0.055) cm respectively. A paired t-test showed no significant difference between the two measurements (manual and algorithm) with a mean difference(SD) of 0.012(0.046) mm ($p>0.5$) and percentage error of difference of 6.43% ($p=0.15$). In addition, the two measurements were highly correlated ($r=0.734$, $p<0.0001$) (Figure 3-A). Agreement between the two operators for the manual reading was highly correlated with an ICC of 0.8 ($p=0.26$) and a percentage

error of 4.74% (p=0.26). A Bland-Altman analysis revealed Mean difference (SD) 0.012 (0.046) (p = 0.303) and limits of agreement between -0.1 to 0.08 (Figure 3-B). ROC analysis yielded an AUC of 0.965 (p<0.0001) at an ONSD threshold of 0.56 mm with 0.86 and 1.0 sensitivity and specificity respectively (Figure 4).

Discussion:

Several recent studies have been conducted with promising results demonstrating the predictive value of sonographic assessed ONSD in comparison to invasive ICP measurement in the setting of brain injury.[12,13,20-22] Our previous studies comparing ONSD measurements to simultaneous invasive ICP measurements in a cohort of neurosurgical ICU patients with TBI have demonstrated high predictive power of ONSD and identified an ONSD cutoff of >0.51cm with high sensitivity and specificity, especially for the detection of ICP>25mmHg.[14] In addition, we have also demonstrated the feasibility of using ONSD to assess ICP in a resource-limited setting where invasive gold-standard monitoring was unavailable.[23] However, several studies have shown significant variation in the optimal ONSD threshold for the detection of high ICP (from 0.52 to 0.57cm),[12,13,21,24] which might limit the practical application of this technique at the bedside. Much of this variation in the optimal ONSD threshold is likely related to technique, with variation in the margins used to define the ONS on ultrasound images acquired by different operators. The ONS, visible as a linear, hypo-dense structure behind the eye can vary in its visualized dimension based on the angle and plane of insonation. Therefore, development of a computer image analysis algorithm might lead to standardization of measurement of the ONSD and minimize operator-dependent variability. We have used our data to develop an automated image analysis and an algorithm to quantify changes in ONSD. The algorithm utilizes multiple image processing techniques to separate out ONS from surrounding tissue and the optic nerve itself, allowing for the inner and outer ONSD to be quantitatively assessed.

A number of methods have been proposed for ultrasound image segmentation. Noble et al[25] have reviewed ultrasound image segmentation methods developed for applications such as left ventricle segmentation, breast cancer, prostate cancer, obstetrics and gynecology and vascular disease. They also reviewed state-of-the-art ultrasound segmentation techniques in terms of methodology. They refer to the techniques used for segmentation where they use different information such as image features (e.g. gray level distribution, intensity gradient, phase and texture), shape and temporal prior for those containing image sequences. In this study, we have utilized the methods described by Noble et al (such as the temporal information) to calculate ONSD. In addition, we have used traditional image processing techniques to calculate the diameter instead of using convolutional neural networks to reduce noise. Our results demonstrate that a computerized algorithm to process ultrasound images could be an appropriate methodology allowing for reliable assessment of ONSD removing the measurement error and uncertainty that comes from an operator's manual measurement. A robust methodology to non-invasively monitor and assess ICP would allow for early application by healthcare providers and allow for precision management of severe TBI patients, providing optimal and personalized cerebral health management.

This study has several limitations. First, the ONSD measurements were done only once on each patient without a follow-up measurement to track changes over time. In addition, patients' ICPs were within the allowed range as dictated by the management plan. Second, some of the images suffered from challenges such as low signal to noise ratio, low contrast, and blurry boundaries. This was overcome by using image denoising and median calculation of ONSD measurements. Lastly, data were collected from forty-four patients only, and may be underpowered to detect differences. Additional testing is warranted to further validate the technology.

Conclusions:

This fully automated technique is a reliable method to process ultrasound images and measure ONSD. It performs with high precision when compared to ONSD as measured by expert operators. This non-invasive assessment of ONSD may allow for a standardized prediction of ICP, and improve management and informed decision making during the early care of brain injury. More studies are warranted to allow for a validation of the technology at earlier stages of neurological injury and wider ranges of ICP.

References:

1. Chesnut R, Videtta W, Vespa P, Le Roux P, Participants in the International Multidisciplinary Consensus Conference on Multimodality M. Intracranial pressure monitoring: fundamental considerations and rationale for monitoring. Neurocrit Care 2014;21 Suppl 2:S64-84.

2. Juul N, Morris GF, Marshall SB, Marshall LF. Intracranial hypertension and cerebral perfusion pressure: influence on neurological deterioration and outcome in severe head injury. The Executive Committee of the International Selfotel Trial. J Neurosurg 2000;92:1-6.

3. Carney N, Totten AM, O'Reilly C, et al. Guidelines for the Management of Severe Traumatic Brain Injury, Fourth Edition. Neurosurgery 2017;80:6-15.

4. Agrawal D, Raghavendran K, Schaubel DE, Mishra MC, Rajajee V. A Propensity Score Analysis of the Impact of Invasive Intracranial Pressure Monitoring on Outcomes after Severe Traumatic Brain Injury. J Neurotrauma 2016;33:853-8.

5. Farahvar A, Gerber LM, Chiu YL, Carney N, Hartl R, Ghajar J. Increased mortality in patients with severe traumatic brain injury treated without intracranial pressure monitoring. J Neurosurg 2012;117:729-34.

6. Bell RS, Mossop CM, Dirks MS, et al. Early decompressive craniectomy for severe penetrating and closed head injury during wartime. Neurosurg Focus 2010;28:E1.

7. Bell RS, Vo AH, Neal CJ, et al. Military traumatic brain and spinal column injury: a 5-year study of the impact blast and other military grade weaponry on the central nervous system. J Trauma 2009;66:S104-11.
8. Ecker RD, Mulligan LP, Dirks M, et al. Outcomes of 33 patients from the wars in Iraq and Afghanistan undergoing bilateral or bicompartmental craniectomy. J Neurosurg 2011;115:124-9.
9. Weisbrod AB, Rodriguez C, Bell R, et al. Long-term outcomes of combat casualties sustaining penetrating traumatic brain injury. J Trauma Acute Care Surg 2012;73:1525-30.
10. Bekar A, Dogan S, Abas F, et al. Risk factors and complications of intracranial pressure monitoring with a fiberoptic device. J Clin Neurosci 2009;16:236-40.
11. Tavakoli S, Peitz G, Ares W, Hafeez S, Grandhi R. Complications of invasive intracranial pressure monitoring devices in neurocritical care. Neurosurg Focus 2017;43:E6.
12. Robba C, Santori G, Czosnyka M, et al. Optic nerve sheath diameter measured sonographically as non-invasive estimator of intracranial pressure: a systematic review and meta-analysis. Intensive Care Med 2018;44:1284-94.
13. Geeraerts T, Launey Y, Martin L, et al. Ultrasonography of the optic nerve sheath may be useful for detecting raised intracranial pressure after severe brain injury. Intensive Care Med 2007;33:1704-11.
14. Rajajee V, Vanaman M, Fletcher JJ, Jacobs TL. Optic nerve ultrasound for the detection of raised intracranial pressure. Neurocrit Care 2011;15:506-15.
15. Hansen HC, Helmke K. Validation of the optic nerve sheath response to changing cerebrospinal fluid pressure: ultrasound findings during intrathecal infusion tests. J Neurosurg 1997;87:34-40.
16. Rajajee V, Fletcher JJ, Rochlen LR, Jacobs TL. Comparison of accuracy of optic nerve ultrasound for the detection of intracranial hypertension in the setting of acutely fluctuating vs stable intracranial pressure: post-hoc analysis of data from a prospective, blinded single center study. Crit Care 2012;16:R79.

17. Achanta R, Shaji A, Smith K, Lucchi A, Fua P, Susstrunk S. SLIC superpixels compared to state-of-the-art superpixel methods. IEEE Trans Pattern Anal Mach Intell 2012;34:2274-82.

18. He K, Sun J, Tang X. Guided image filtering. IEEE Trans Pattern Anal Mach Intell 2013;35:1397-409.

19. Soroushmehr R, Rajajee V, Williamson C, et al. Automated Optic Nerve Sheath Diameter Measurement Using Super-pixel Analysis. Available at https://ieeexplore.ieee.org/abstract/document/8856449; accessed January 6, 2020.

20. Jimenez Restrepo JN, Leon OJ, Quevedo Florez LA. Ocular Ultrasonography: A Useful Instrument in Patients with Trauma Brain Injury in Emergency Service. Emerg Med Int 2019;2019:9215853.

21. Karakitsos D, Soldatos T, Gouliamos A, et al. Transorbital sonographic monitoring of optic nerve diameter in patients with severe brain injury. Transplant Proc 2006;38:3700-6.

22. Soldatos T, Karakitsos D, Chatzimichail K, Papathanasiou M, Gouliamos A, Karabinis A. Optic nerve sonography in the diagnostic evaluation of adult brain injury. Crit Care 2008;12:R67.

23. Rajajee V, Thyagarajan P, Rajagopalan RE. Optic nerve ultrasonography for detection of raised intracranial pressure when invasive monitoring is unavailable. Neurol India 2010;58:812-3.

24. Moretti R, Pizzi B, Cassini F, Vivaldi N. Reliability of optic nerve ultrasound for the evaluation of patients with spontaneous intracranial hemorrhage. Neurocrit Care 2009;11:406-10.

25. Noble JA, Boukerroui D. Ultrasound image segmentation: a survey. IEEE Trans Med Imaging 2006;25:987-1010.

Figure 1:

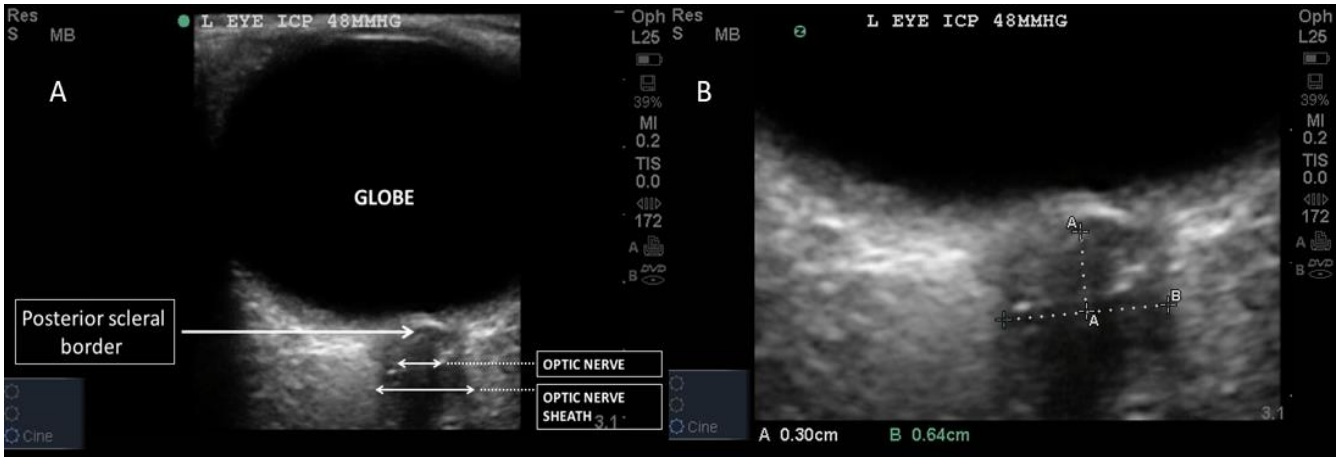

A) Ultrasound image of globe, optic nerve, and optic nerve sheath. B) Magnified image. Caliper A demarcates a point 3mm behind the posterior scleral border and Caliper B measures the optic nerve sheath diameter.

Figure 2:

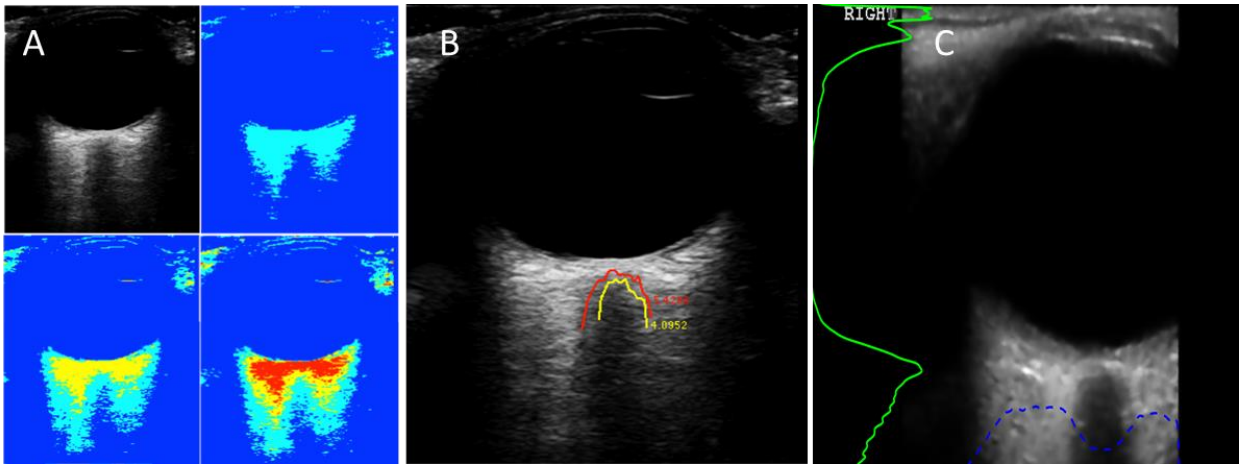

Multiple Threshold Image Segmentation of optic nerve ultrasound (ONUS) image. A) ONUS image separated by multiple thresholds until the ONS region of interest is isolated (ROI). B) Inner and outer diameter of the ONS found in the ROI. C) Vertical line integral (dashed blue line) and horizontal line integral (solid green line) for finding the globe point and the ROI.

Figure 3:

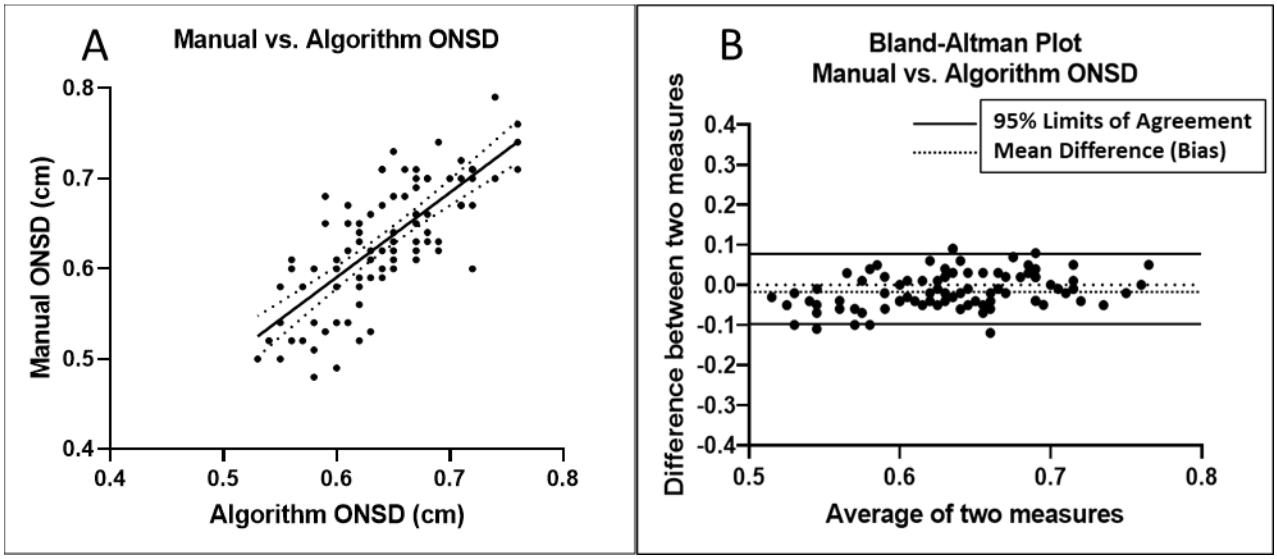

A) Regression of algorithm vs. manual ONSD measurements. B) Bland-Altman plot of algorithm vs. manual ONSD measurements. ONSD: Optic nerve sheath diameter.

Figure 4:

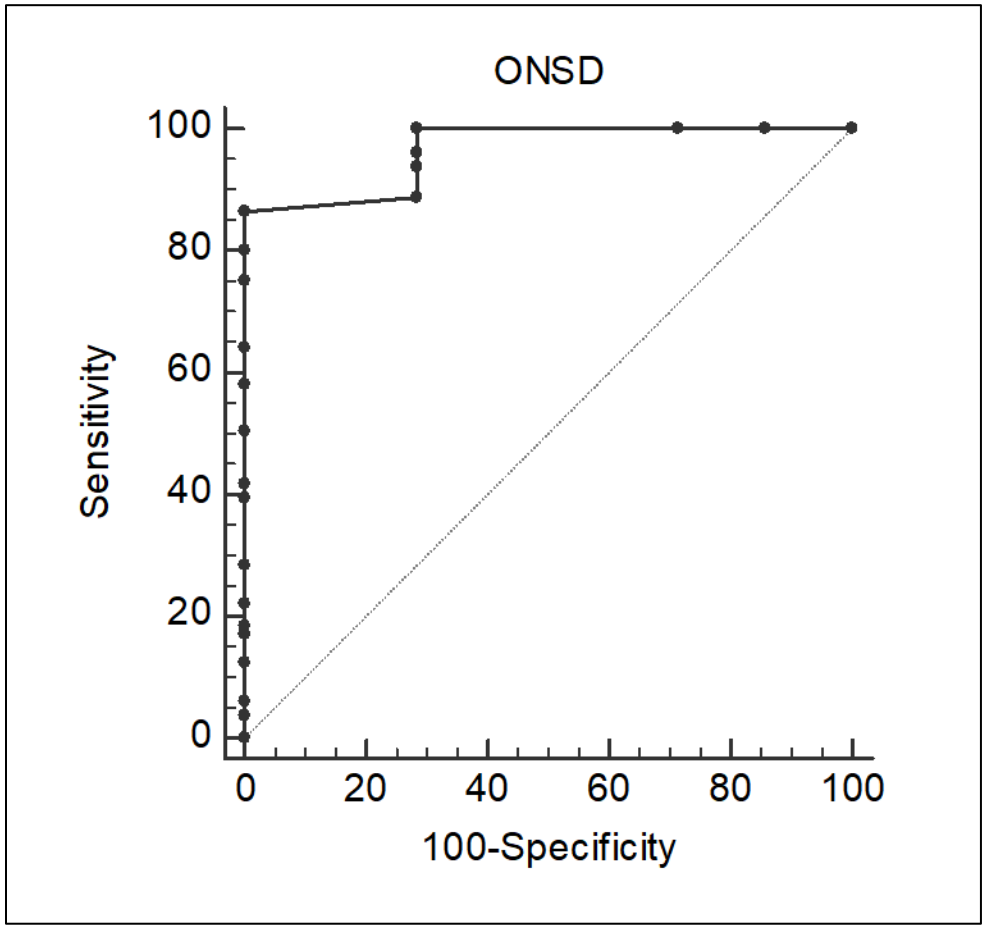

Receiver Operator Curve for the algorithm-measured optic nerve sheath diameter.

Appendix E:

Provisional patent application: *"Automated Optic Nerve Sheath Diameter Measurement" was filed on July 23, 2019, and assigned Serial No. 62/877,539.*

AUTOMATED OPTIC NERVE SHEATH DIAMETER MEASUREMENT

CROSS-REFERENCE TO RELATED APPLICATION

[0001] This application claims the benefit of U.S. provisional application entitled "Automated Optic Nerve Sheath Diameter Measurement," filed July 23, 2019, and assigned Serial No. 62/877,539, the entire disclosure of which is hereby expressly incorporated by reference.

STATEMENT REGARDING FEDERALLY SPONSORED RESEARCH OR DEVELOPMENT

[0002] This invention was made with government support under Contract No. W81XWH-18-1-0005 awarded by the United States Army Medical Research and Materiel Command (USAMRMC). The government has certain rights in the invention.

BACKGROUND OF THE DISCLOSURE

Field of the Disclosure

[0003] The disclosure relates generally to assessment of intracranial pressure based on automated measurement of optic nerve sheath diameter.

Brief Description of Related Technology

[0004] The optic nerve is a part of the central nervous system. The optic nerve is surrounded by cerebrospinal fluid and is encased in a sheath. The optic nerve sheath is an anatomical extension of the duramater, the outermost and most substantial meningeal layer of the central nervous system. The subarachnoid space around the optic nerve is continuous with the intracranial subarachnoid space, and is surrounded by cerebrospinal fluid (CSF).

[0005] Changes in CSF pressure can result from brain injury, tumor rupture, and other conditions. Changes in CSF pressure can, in turn, reflect changes in intracranial pressure (ICP). The degree of elevation and duration of elevated ICP are correlated with patient outcomes. Therefore, ICP monitoring can provide useful information for patients' management and treatment, and is widely used in the management of patients with severe traumatic brain injury (TBI).

[0006] However, ICP monitoring is an invasive monitoring procedure. ICP monitoring can thus cause complications, such as intracranial hemorrhage, dislocation, and infection. Moreover, direct measurement of ICP, especially for patients with minor brain injury, is an unrealistic and aggressive requirement.

[0007] Some clinical trials and research studies have attempted to replace the ICP monitoring with a non-invasive alternative measurement. It has been shown that the diameter of the optic nerve sheath changes rapidly with changes in CSF pressure. For instance, studies have shown that ventriculostomy measurements of intracranial pressure are correlated with ultrasound (US) optic nerve sheath diameter measurements. The optic nerve sheath diameter may thus be used as a non-invasive test for elevated ICP. Unfortunately, manual techniques for measuring optic nerve sheath diameter are often and typically tedious, time-consuming, and subject to human error.

SUMMARY OF THE DISCLOSURE

[0008] In accordance with one aspect of the disclosure, a method of determining a diameter of a sheath of an optic nerve includes obtaining, by a processor, scan data representative of the optic nerve sheath, analyzing, by the processor, the scan data to find a position of a globe-optic nerve interface point, segmenting, by the processor, the scan data, processing, by the processor, the segmented scan data at an offset from the position of the globe-optic nerve interface point to determine boundary positions of the optic nerve sheath, and calculating, by the processor, the diameter of the optic nerve sheath based on the determined boundary positions.

[0009] In accordance with another aspect of the disclosure, a system of determining a diameter of an optic nerve sheath includes a memory in which scan data input instructions, scan data analysis instructions, segmentation instructions, and boundary identification instructions are stored, and a processor in communication with the memory and configured to, upon execution of the scan data input instructions, obtain scan data representative of a two-dimensional slice through the optic nerve sheath and a globe from which the optic nerve extends, upon execution of the scan data analysis instructions, analyze the scan data to find an anterior-posterior position of a globe-optic nerve interface point, upon execution of the segmentation instructions, implement a segmentation procedure to generate a super-pixel representation of the scan data, and upon execution of the boundary identification instructions, process the super-pixel representation of the scan data at an offset from the anterior-posterior

position of the globe-optic nerve interface point to determine boundary positions of the optic nerve sheath, and calculate the diameter of the optic nerve sheath based on the determined boundary positions.

[0010] In accordance with yet another aspect of the disclosure, a computer readable storage medium having stored therein data representing instructions executable by a programmed processor for determining a diameter of an optic nerve sheath, the storage medium including instructions for obtaining scan data representative of a two-dimensional slice through the optic nerve sheath and a globe from which the optic nerve extends, analyzing the scan data to find a position of a globe-optic nerve interface point, implementing a segmentation procedure, the segmentation procedure being configured to generate a super-pixel representation of the scan data, processing the super-pixel representation of the scan data at an offset from the anterior-posterior position of the globe-optic nerve interface point to determine boundary positions of the optic nerve sheath, and calculating the diameter of the optic nerve sheath based on the determined boundary positions.

[0011] In connection with any one of the aforementioned aspects, the systems, storage media, and/or methods described herein may alternatively or additionally include or involve any combination of one or more of the following aspects or features. Processing the segmented scan data includes finding peaks in the segmented scan data at the offset, and determining a location of a minimum between the found peaks. Processing the segmented scan data includes processing the segmented scan data includes computing a derivative of the segmented scan data at the offset. Processing the segmented scan data includes determining a lateral position of the globe-optic nerve interface point at the offset based on a minimum between peaks in the segmented scan data, computing a derivative of the segmented scan data at the offset, and finding a pair of peaks in the derivative of the segmented scan data, each peak of the pair of peaks being disposed on a respective side of the lateral position. Finding the first and second peaks includes disregarding peaks in the derivative greater than a threshold. Finding the first and second peaks further includes, after disregarding the peaks greater than the threshold, finding a negative peak closest to the lateral position of the globe-optic nerve interface point, and finding a positive peak closest to the lateral position of the globe-optic nerve interface point. Analyzing the scan data includes computing a line integral of the scan data at each anterior-posterior position of the scan data, and finding a maximum of the line integral to determine the position of the globe-optic nerve interface point. The line integral is a first line integral, the

method further including computing a second line integral of the scan data at each lateral position of the scan data, and determining a subset of the scan data corresponding with a region of interest based on the first line integral and the second line integral. Segmenting the scan data is implemented on the determined subset of the scan data. The scan data includes a plurality of frames. The method further includes disregarding one or more frames of the plurality of frames based on whether the first and second line integrals present peaks indicative of the globe and the optic nerve such that analyzing the scan data, segmenting the scan data, processing the segmented scan data, and calculating the diameter are repeated for the scan data of each remaining frame of the plurality of frames. The scan data includes two-dimensional slice data, the two-dimensional slice data being representative of a slice through the globe and the optic nerve. Processing the segmented scan data includes selecting a line of the scan data located about 3 millimeters in a posterior direction from the globe-optic nerve interface point as a subset of the segmented scan data at the offset to be processed. Obtaining the scan data includes capturing ultrasound scan data, cropping the ultrasound data, and removing noise from the cropped ultrasound scan data to generate the scan data. Removing the noise includes implementing a filtering procedure configured to preserve edges in the cropped ultrasound scan data. The scan data includes a plurality of frames. Analyzing the scan data, segmenting the scan data, processing the segmented scan data, and calculating the diameter are repeated for the scan data of each frame of the plurality of frames, and the method further includes compiling the calculated diameters of the optic nerve sheath for the plurality of frames to determine a value for the diameter of the optic nerve sheath. A method of determining an assessment of intracranial pressure including the method as described herein, and further including determining an intracranial pressure level based on the value for the diameter and based on a database correlating diameter values with corresponding levels of intracranial pressure. The segmentation procedure includes a k-means clustering procedure. The execution of the segmentation instructions further configures the processor to discard super-pixels below a threshold size. The execution of the boundary identification instructions further configures the processor to determine a lateral position of the globe-optic nerve interface point at the offset based on a minimum between peaks in the super-pixel representation of the scan data, compute a derivative of the super-pixel representation of the scan data at the offset, and find a pair of peaks in the derivative of the super-pixel representation of the scan data, each peak of the pair of peaks being disposed on a respective side of the lateral position. Processing the super-pixel representation of the scan data includes determining a lateral position of the

globe-optic nerve interface point at the offset based on a minimum between peaks in the super-pixel representation of the scan data, computing a derivative of the super-pixel representation of the scan data at the offset, and finding a pair of peaks in the derivative of the super-pixel representation of the scan data, each peak of the pair of peaks being disposed on a respective side of the lateral position.

BRIEF DESCRIPTION OF THE DRAWING FIGURES

[0012] For a more complete understanding of the disclosure, reference should be made to the following detailed description and accompanying drawing figures, in which like reference numerals identify like elements in the figures.

[0013] Figure 1 is a flow diagram of a method of determining optic nerve sheath diameter in accordance with one example.

[0014] Figure 2 is a rendered image of ultrasound scan data of a two-dimensional, sagittal slice of a globe and optic nerve that may be used by the method of Figure 1 to determine the optic nerve sheath diameter in accordance with one example.

[0015] Figure 3 depicts plots of two line integrals superimposed on ultrasound scan data from which the line integrals are computed in the method of Figure 1 in accordance with one example.

[0016] Figure 4 is a rendered image of ultrasound scan data (e.g., raw ultrasound scan data) before implementation of a filtering procedure of the method of Figure 1 in accordance with one example.

[0017] Figure 5 is a rendered image of the ultrasound scan data of Figure 4 after implementation of a filtering procedure of the method of Figure 1 in accordance with one example.

[0018] Figure 6 is a rendered image of super-pixels generated from the filtered ultrasound scan data of Figure 5 via implementation of a segmentation procedure of the method of Figure 1 in accordance with one example.

[0019] Figure 7 depicts plots of (1) intensity levels of a line (e.g., row) of super-pixels generated via implementation of a segmentation procedure of the method of Figure 1 in

accordance with one example, and (2) values of the derivative of the intensity levels as computed in the method of Figure 1 in accordance with one example.

[0020] Figure 8 is a block diagram of a system of determining optic nerve sheath diameter in accordance with one example.

[0021] The embodiments of the disclosed systems and methods may assume various forms. Specific embodiments are illustrated in the drawing and hereafter described with the understanding that the disclosure is intended to be illustrative. The disclosure is not intended to limit the invention to the specific embodiments described and illustrated herein.

DETAILED DESCRIPTION OF THE DISCLOSURE

[0022] Methods and systems of automated measurement of optic nerve sheath diameter are described. Methods and systems for assessing intracranial pressure based on the calculated diameter are also described. The disclosed methods and systems measure the sheath diameter via analysis of scan data, such as ultrasound scan data. The analysis may include image segmentation and other image processing. In some cases, the image segmentation procedure includes or involves super-pixel analysis. The automated nature of the disclosed methods and systems avoids the errors of the manual measurement techniques. The disclosed methods and systems may also be useful in supporting further study of ICP and other monitoring.

[0023] The image segmentation and/or other aspects of the disclosed methods and systems address a number of challenges arising from the use of scan data, such as ultrasound scan data, to measure the sheath diameter. For instance, the ultrasound scan data may have a low signal to noise ratio (SNR), low contrast, and/or blurry boundaries. In some cases, filtering and/or other preprocessing steps are used to remove noise while maintaining edges and other boundaries. Additionally or alternatively, restricting the image segmentation to a region of interest and/or otherwise cropping the scan data may be used to address the challenges arising from the nature of the ultrasound scan data.

[0024] A number of different segmentation procedures may be used to segment the ultrasound scan data. Suitable segmentation procedures include those used on ultrasound scan data for applications involving left ventricle analysis, cancer screening, obstetrics and gynecology, and vascular disease. The segmentation procedures may use a wide variety of information,

including, for instance, various image features (e.g., gray level distribution, intensity gradient, phase and texture), shape information, and temporal information (e.g., for those containing image sequences). The image segmentation procedures implemented by the disclosed methods and systems may avoid relying on complex processing techniques (e.g., convolutional neural networks), due to, for instance, the recognition that the consecutive images in the ultrasound video sequence are correlated. Notwithstanding the correlated nature of the images, those and other segmentation techniques may nonetheless be used by the disclosed methods and systems in some cases.

[0025] The disclosed methods and systems may use and process temporal information to determine the sheath diameter from image frames throughout an ultrasound video sequence. The diameters calculated for each image frame may then be compiled to arrive at a final value via voting and/or other statistical computation(s).

[0026] Although described in connection with scan data captured as a two-dimensional ultrasound video, the disclosed methods and systems may be applied to a wide variety of scan data. Other types of ultrasound scan data may be used, including, for instance, three-dimensional ultrasound scan data. Other types of imaging modalities may also be used to capture the scan data, including, for instance, magnetic resonance imaging. The formatting and other characteristics of the scan data may also vary. The characteristics of the scan data may also result in a modification of one or more aspects of the disclosed methods and systems, including, for instance, image de-noising or other procedure step in the image processing, or an act in the disclosed method.

[0027] Figure 1 depicts a method 100 of determining (e.g., measuring) a diameter of a sheath of an optic nerve. The method 100 may be implemented by a processor, such as an image processor. The processor may or may not be part of an imaging system, such as an ultrasound imaging system. In some cases, the method 100 is implemented by a processor configured via execution of instructions stored on a computer-readable storage medium.

[0028] The method 100 includes an act 102 in which scan data is obtained. The scan data is representative of the optic nerve, including the optic nerve sheath, and a globe of the eye from which the optic nerve extends. In some cases, the scan data is or includes two-dimensional slice data. The slice data is representative of a slice through the optic nerve and the globe. The slice may be oriented as a sagittal slice. Alternative or additional types of scan data may be obtained. For instance, the scan data may be or include three-dimensional scan data.

[0029] The scan data may be or include ultrasound scan data. In such cases, obtaining the scan data may include capturing ultrasound scan data in an act 102. The raw data generated by an ultrasound imaging system may then be processed (e.g., pre-processed). For example, the pre-processing may include cropping the raw ultrasound data in an act 104 and/or removing noise from the ultrasound data in an act 106. An example of raw ultrasound data representative of the globe and optic nerve is shown in Figure 4.

[0030] Cropping may be implemented via Digital Imaging and Communications in Medicine (DICOM) attributes (e.g., metadata) that specify, for instance, the location of the entire scan containing the nerve sheath and the retinal detachment. In some cases, the cropping may be result in scan data limited to depicting the globe and a portion of the optic nerve. An example of a cropped frame of scan data is shown in Figure 2, in which the diameter of the optic nerve sheath is labeled ONSD at a position offset from the interface with the globe. A variety of other cropping techniques may be used. DICOM metadata may alternatively or additionally be relied upon to provide information regarding the resolution of image, such as how many pixels correspond with a millimeter (mm).

[0031] De-noising and/or other resolution enhancement of the ultrasound data in the act 106 of Figure 1 may be achieved via implementation of one or more filtering procedures. The filtering may be configured to preserve edges in the cropped ultrasound scan data, such as the edges of the globe and the optic nerve sheath. In some cases, image guided filtering is used to filter the scan data while preserving edges. In image guided filtering, the filtering input image and guidance image are shown as p and I respectively. The images are divided to overlapped windows with radius of r and following coefficients are computed in each window:

$$a_k = \frac{cov_k(I,P)}{var_k(I)+\varepsilon}$$

$$b_k = \bar{p}_k - a_k \bar{I}_k$$

where k is the window index, I_k and p_k are average of intensities in k^{th} window in noisy and guidance images, respectively. Also ε is a regularization parameter that determines the edge-preserving property of the filter. The filtered pixel q_i is the average of $a_k I_i + b_k$ in all the windows that cover q_i. The cov and var functions compute the covariance and variance, respectively. Figure 5 shows the raw ultrasound data of Figure 4 after de-noising.

[0032] Alternative or additional types of filtering procedures may be implemented to de-noise the scan data while preserving edges. For example, a Savitzky-Golay filter as described in

Chinrungrueng et al. “Fast edge-preserving noise reduction for ultrasound images” IEEE Transactions on Nuclear Science, 48(3), pp. 849-854 (2001), may be used.

[0033] Fewer, additional, or alternative pre-processing steps may be implemented in connection with obtaining the scan data. For instance, cropping the ultrasound data at this stage of the method 100 may not be necessary in some cases. For example, cropping may be effectively implemented later in the method 100 in connection with selection of a subset of the scan data, as described further below.

[0034] In an act 108, the scan data is analyzed to find a position of a globe-optic nerve interface point. The act 108 may be directed to finding the position of the interface point in the anterior-posterior dimension or direction. The analysis may be directed to selecting subsets of the scan data. The subsets may correspond with a subset of the frames and/or with a cropped portion of each frame.

[0035] In the example of Figure 1, the analysis of the scan data includes computing line integrals of the scan data in an act 110. An anterior-posterior (AP) line integral may involve summing the scan data at each anterior-posterior position of the scan data. An example of the AP line integral is depicted in Figure 2 as signal 300. In that example, the AP line integral is a vertical signal v that has a minimum 302 within the globe and maxima 304, 306 at either edge of the globe. In an act 112, the maximum 306 of the AP line integral may be used to determine the AP position, or vertical pixel, of the point at which the globe and the optic nerve meet, i.e., the globe-optic nerve interface point.

[0036] Another line integral may also be computed in the act 110 at each lateral position of the scan data. The lateral line integral is depicted in Figure 2 as signal 308, a horizontal signal h having a minimum 310 at the optic nerve and two peaks 312, 314 that establish a region of interest encompassing the optic sheath. The lateral line integral may be used to determine the lateral position, or horizontal pixel, of the globe-optic nerve interface point.

[0037] The integrals may be calculated via a summation of pixel values of the image array in each column and each row separately. If the denoised image is an N×M image shown as I_d, then the line integrals are computed as the following one-dimensional signals.

$$v(n) = \sum_{m=1}^{M} I_d(n,m) \quad for\ n = 1, \ldots, N$$

$$h(m) = \sum_{n=1}^{N} I_d(n,m) \quad for\ m = 1, \ldots, M$$

[0038] An example of the v signal is depicted as the signal 308 of Figure 3. The v signal is a result of the vertical line, or column, integrals, and has two main peaks 312, 314, corresponding to the brighter regions and a local minimum 310 between the peaks 312, 314 corresponding to the dark region inside the sheaths. The peaks 312, 314 may be used to identify or define the region of interest, as described below. For instance, if the minimum of the v signal is the g^{th} element of the signal, then the value of the v signal corresponds to the column at which the globe is located.

$$g = \underset{Max_1 \le i \le Max_2}{argmin} \; v(i)$$

[0039] An example of the h signal is depicted as the signal 300 of Figure 3. The h signal is a result of the horizontal line, or row, integrals, and is used to identify the globe-optic nerve interface point.

[0040] In an act 114, the AP and lateral line integrals may also be used to determine a subset of the scan data corresponding with a region of interest. The region of interest may only include a portion of the optic nerve, but the region of interest may vary. The scan data may thus be further cropped based on the line integrals to a region of interest. The region of interest may, for example, correspond with only relevant portions of the globe and optic nerve. Further image processing, such as image segmentation, may then be implemented on the subset of the scan data.

[0041] One or both of the line integrals may be used to focus, filter, or reduce the scan data down to a subset in alternative or additional ways. For example, the line integrals may be used to select which images should be further processed and relied upon to measure the optic nerve sheath diameter. In some ultrasound examples, the scan data includes a plurality of frames of the ultrasound video. In such cases, the analysis may include an act 116 in which one or more frames are discarded or otherwise disregarded based on whether the line integrals indicate that the frame has suitably captured the globe and optic nerve. For example, the act 116 may include analyzing each frame to determine whether the line integrals present peaks indicative of the globe and the optic nerve. For each such qualifying frame, the remaining acts of the method 100 may then be repeated as described below.

[0042] The method 100 includes an act 118 in which the scan data is segmented. In the example of Figure 1, the segmentation may occur after finding the interface point and defining the region of interest (ROI) subset of the scan data. The segmentation may generate super-

pixels of the scan data. For example, a super-pixel segmentation procedure, such as simple linear iterative clustering (SLIC) may be used in an act 120 to segment the scan data to super-pixels. The SLIC segmentation procedure includes a k-means clustering procedure implemented in which the image is partitioned into homogenous regions based on the k-means clustering technique. In that technique, the scan data of the image is first partitioned to non-overlapped blocks/tiles, and the center of each tile is used as an initial parameter for clustering. After that, the center of each tile is refined and also its shape is modified in an iterative process using the Lloyd algorithm. The modified shape is the super-pixel.

[0043] As part of the SLIC procedure or otherwise, the super-pixels may then be analyzed in an act 122 in terms of area, in which super-pixels below a threshold size are excluded from the results or otherwise discarded. Alternative or additional image segmentation procedures may be implemented. For example, a random walks segmentation procedure may be implemented in an act 124.

[0044] Figure 6 depicts the ultrasound data of Figures 4 and 5 in the region of interest after implementation of SLIC segmentation.

[0045] Returning to Figure 1, in an act 126, the segmented scan data (e.g., the super-pixel data) is processed to determine positions of boundaries of the optic nerve sheath. The processing is implemented at an offset from the position of the globe-optic nerve interface point. The offset is in the posterior direction, away from the interface point. In some cases, the offset is about 3 mm, but other offset amounts may be used.

[0046] The processing of the segmented scan data may include an act 128 in which a line of the scan data is selected. The selection may include determining how many pixels correspond with the 3 mm (or other) offset amount. The selection then determines a subset of the segmented scan data to be processed. For example, a single row of pixels may be selected. Alternatively, multiple rows of pixels are selected.

[0047] The processing of the segmented scan data may include finding, in an act 130, a number of peaks in the segmented scan data selected in the act 128. For example, the positions (e.g., lateral positions) of a pair of peaks in the row at the offset (e.g., the 3mm row) may be located. The row at the offset may be determined based on the size of each pixel, which can be extracted from DICOM metadata. An example of the segmented scan data at the offset is depicted in a plot 700 of Figure 7. The processing may include analysis of the peaks

and derivative of this row of super-pixel data. A first intensity peak 700 is located at about column index 280 and a second intensity peak is located at about column index 370. Each column index may correspond with a pixel number in the lateral direction.

[0048] The lateral location of a minimum between the found peaks may then be found or otherwise determined in an act 132 (Figure 1). The minimum may correspond with the lateral location or position of the globe-optic nerve interface point. In the example of Figure 7, a minimum 706 between the pair of peaks 702, 704 is located at about column index 320. The lateral position of the globe-optic nerve interface point may be based on the minimum between peaks in the segmented scan data in alternative or additional ways. For example, the minimum location or position may be alternatively or additionally determined by finding a midpoint between the pair of peaks 702, 704.

[0049] Processing the segmented scan data may include an act 134 in which a derivative of the segmented scan data at the offset is computed. The derivative may be calculated by subtracting each intensity value from the previous one. Figure 7 depicts a plot of an example of the computed derivative.

[0050] A pair of peaks in the derivative may then be found in an act 136. Each peak is disposed on a respective side of the lateral position of the minimum 706, i.e., the globe-optic nerve interface point.

[0051] Finding the peaks in the derivative may be subject to one or more rules, conditions, or other guidelines. For instance, a peak in the derivative may be disqualified if the magnitude of the derivative exceeds a predetermined threshold. Alternatively or additionally, peaks below a floor may be disregarded as noise. Finding the peaks may thus be configured to find the first significant peaks reached from the minimum. Other conditions or guidelines may be applied or considered. For example, the distance between the globe-optic nerve interface point and the peak should fall within a predetermined range.

[0052] Whether the derivative is positive or negative may also be used to select the peaks. For example, the first significant positive peak closest to, and after (i.e., to the right of), the globe-optic nerve interface point, and the first significant negative peak closest to, and before (i.e. to the left of), the globe-optic nerve interface point, may be selected. In the example of Figure 7, first significant positive and negative peaks 708, 710 in the derivative curve are at about column indices 330 and 290, respectively.

[0053] The diameter of the optic nerve sheath is then calculated in an act 138 based on the determined positions of the boundaries. For example, in connection with the data depicted in Figure 7, the diameter is calculated as the distance corresponding to the difference between the column indices 290 and 330.

[0054] In some cases, an image of the scan data and/or segmented scan data from which the diameter is measured is generated in an act 140. The act 140 may, for example, include rendering an image on a display. The image may be rendered or otherwise generated at other times during implementation of the method 100. For instance, the image may be rendered before the processing of the act 126 to provide an operator an opportunity to discard the scan data of a frame, thereby removing some of the scan data from the measurement.

[0055] The method 100 may include a decision block 142 to determine whether a last frame has been processed. For example, the last frame may be final frame in an ultrasound video or other sequence of images. If not, control passes to a block 144 in which the next frame of scan data is selected. In the example of Figure 1, some or all of the pre-processing and analysis of the act 108 is then implemented. For example, the frames may be separately cropped, pre-qualified, and/or otherwise pre-processed in preparation for segmentation. Computation and/or analysis of the line integrals to determine whether the scan data for the frame is suitable may also be performed for the next frame. In other cases, control may return to alater step in the method 100, such as implementation of the segmentation procedure. Either way, in cases in which the scan data includes a plurality of frames, the above-described analysis, segmentation, and processing may be repeated to measure the sheath diameter for each frame.

[0056] Once the last frame has been processed, control passes to an act 146 in which the diameter measurements for all of the frames are compiled to determine a value, e.g., a final value for the ultrasound video. In some cases, the compilation involves a voting procedure. For example, a median value may be determined. Other voting procedures or other techniques for the determination may be used. For example, one or more statistical procedures may be used to filter the measurements before finding the median or otherwise implementing a voting procedure.

[0057] In the example of Figure 1, the final measurement value for the sheath diameter is used in an act 148 to determine an assessment of a corresponding intracranial pressure (ICP) level. In some cases, the corresponding ICP level is estimated via a look-up table or other database correlating sheath diameters and ICP levels. The ICP level may be estimated from such

correlation data via interpolation. Alternatively or additionally, the ICP level may be computed as a function of the sheath diameter, the function being or including a polynomial expression fit to the data.

[0058] The method 100 may include one or more additional acts. In one example, one or more acts are directed to providing the measurement value as an output. Alternatively or additionally, the method 100 may be repeated, e.g., daily, hourly or otherwise, to see if the sheath diameter is increasing or changing. Such repetition is not problematic because the method 100 is non-invasive, not painful, and otherwise not undesirable or troubling for the patient.

[0059] Figure 8 depicts a system 800 of determining a diameter of an optic nerve sheath and/or ICP level based on the sheath diameter. The system 800 may be used to implement the methods described above, and/or a different method. The system 800 may also be used to determine the sheath diameter and/or ICP level via execution of one or more sets of instructions, as described below.

[0060] The system 800 may be or include an imaging system. In the example of Figure 8, the system 800 includes an ultrasound imaging system having a transmit beamformer 802, a receive beamformer 804, and a transducer 806. Additional, fewer, or alternative imaging system components may be provided. For instance, the system 800 may not include the front-end components of the imaging system. Thus, in some cases, the system 800 is a medical diagnostic ultrasound system. In other cases, the system 800 is a computer or workstation.

[0061] The transducer 806 is an array of elements. For example, the elements are piezoelectric or capacitive membrane elements. The array is configured as a one-dimensional array, a two-dimensional array, a 1.5D array, a 1.25D array, a 1.75D array, an annular array, a multidimensional array, a wobbler array, combinations thereof, or any other now known or later developed array. The transducer elements transduce between acoustic and electric energies. The transducer 806 connects with the transmit beamformer 802 and the receive beamformer 804 through a transmit/receive switch, but separate or other connections may be used in other cases.

[0062] The transmit and receive beamformers 802, 804 are configured for scanning with the transducer 14. The transmit beamformer 802, using the transducer 806, transmits one or more

beams to scan a region. Various scan formats may be used. The receive beamformer 804 samples the receive beams at different depths.

[0063] In some cases, the transmit beamformer 802 is or includes a processor, delay, filter, waveform generator, memory, phase rotator, digital-to-analog converter, amplifier, combinations thereof or any other now known or later developed transmit beamformer components. Using filtering, delays, phase rotation, digital-to-analog conversion and amplification, the desired transmit waveform is generated. Other waveform generators may be used, such as switching pulsers or waveform memories.

[0064] The transmit beamformer 802 may be configured as a plurality of channels for generating electrical signals of a transmit waveform for each element of a transmit aperture on the transducer 806. The waveforms may be unipolar, bipolar, stepped, sinusoidal or other waveforms of a desired center frequency or frequency band with one, multiple or fractional number of cycles. The waveforms may have relative delay and/or phasing and amplitude for focusing the acoustic energy. The transmit beamformer 802 may include a controller for altering an aperture (e.g. the number of active elements), an apodization profile (e.g., type or center of mass) across the plurality of channels, a delay profile across the plurality of channels, a phase profile across the plurality of channels, center frequency, frequency band, waveform shape, number of cycles and combinations thereof. A transmit beam focus is generated based on these beamforming parameters.

[0065] The receive beamformer 804 is or includes a preamplifier, filter, phase rotator, delay, summer, base band filter, processor, buffers, memory, combinations thereof or other now known or later developed receive beamformer components. The receive beamformer 804 is configured into a plurality of channels for receiving electrical signals representing echoes or acoustic energy impinging on the transducer 806. A channel from each of the elements of the receive aperture within the transducer 804 connects to an amplifier and/or delay. An analog-to-digital converter digitizes the amplified echo signal. The digital radio frequency received data is demodulated to a base band frequency. Any receive delays, such as dynamic receive delays, and/or phase rotations are then applied by the amplifier and/or delay. A digital or analog summer combines data from different channels of the receive aperture to form one or a plurality of receive beams. The summer is a single summer or cascaded summer. In one embodiment, the beamform summer is operable to sum in-phase and quadrature channel data in a complex manner such that phase information is maintained for the formed beam. Alternatively, the

beamform summer sums data amplitudes or intensities without maintaining the phase information.

[0066] The receive beamformer 804 is operable to form receive beams in response to the transmit beams. For example, the receive beamformer 804 receives one, two, or more (e.g., 30, 40, or 50) receive beams in response to each transmit beam. The receive beams are collinear, parallel and offset or nonparallel with the corresponding transmit beams. The receive beamformer 804 outputs spatial samples representing different spatial locations of a scanned region. Once the channel data is beamformed or otherwise combined to represent spatial locations along the scan lines, the data is converted from the channel domain to the image data domain. The phase rotators, delays, and/or summers may be repeated for parallel receive beamformation. One or more of the parallel receive beamformers may share parts of channels, such as sharing initial amplification.

[0067] In the example of Figure 8, the system 800 includes a computing system 808 having a processor 810, a memory 812, and a display 814. The computing system 808 may be integrated with the ultrasound imaging system to any desired extent. The processor 810 is in communication with the memory 812 for execution of instructions stored in the memory 812. In this example, scan data input instructions, scan data analysis instructions, segmentation instructions, and boundary identification instructions are stored in the memory 812. Additional, fewer, or alternative instructions are provided. For instance, the instructions may be integrated with one another to any desired extent.

[0068] The execution of the instructions stored in the memory 812 may cause the processor 810 to implement one or more acts of the above-described methods. For instance, upon execution of the scan data input instructions, the processor 810 is configured to obtain scan data representative of a two-dimensional slice through the optic nerve sheath and a globe from which the optic nerve extends. Upon execution of the scan data analysis instructions, the processor 810 is configured to analyze the scan data to find an anterior-posterior position of a globe-optic nerve interface point. Upon execution of the segmentation instructions, the processor 810 is configured to implement a segmentation procedure to generate a super-pixel representation of the scan data. Upon execution of the boundary identification instructions, the processor 810 is configured to process the super-pixel representation of the scan data at an offset from the anterior-posterior position of the globe-optic nerve interface point to determine boundary positions of the optic nerve sheath, and calculate the diameter of the optic nerve

sheath based on the determined boundary positions. The configuration of the processor 810 via these instructions may vary as described above. For instance, the segmentation procedure implemented by the processor 810 may include a k-means clustering procedure and/or another segmentation procedure. The execution of the segmentation instructions may further configure the processor 810 to discard super-pixels below a threshold size. The execution of the boundary identification instructions further configures the processor 810 to (i) determine a lateral position of the globe-optic nerve interface point at the offset based on a minimum between peaks in the super-pixel representation of the scan data, (ii) compute a derivative of the super-pixel representation of the scan data at the offset, and (iii) find a pair of peaks in the derivative of the super-pixel representation of the scan data, each peak of the pair of peaks being disposed on a respective side of the lateral position.

[0069] The processor 810 may include one or more processors or processing units. In some cases, the processor 810 is or includes a digital signal processor, a general processor, an application specific integrated circuit, a field programmable gate array, a control processor, digital circuitry, analog circuitry, a graphics processing unit, combinations thereof or other now known or later developed device for implementing calculations, algorithms, programming or other functions. The processor 810 may or may not be configured to execute instructions provided in the memory 812, or a different memory, for directed to controlling the imaging system and/or rendering of the captured ultrasound scan data.

[0070] The memory 812 may include one or more memories. In some cases, the memory 812 is or includes video random access memory, random access memory, removable media (e.g. diskette or compact disc), a hard drive, a database, or other memory device for storing instructions, scan data, and/or other data. The memory 812 may be operable to store signals responsive to multiple transmissions along a substantially same scan line. The memory 812 is operable to store ultrasound data in various formats.

[0071] The display 814 is or includes a CRT, LCD, plasma, projector, monitor, printer, touch screen, or other now known or later developed display device. The display 814 receives RGB or other color data and outputs an image. The image may be a gray scale or color image. The image represents the region of the patient scanned by the transducer 806 and other components of the imaging system.

[0072] The instructions for implementing the processes, methods and/or techniques discussed above are provided on computer-readable storage media or memories, such as a cache, buffer,

RAM, removable media, hard drive or other computer readable storage media. In one embodiment, the instructions are for volumetric quantification. Computer readable storage media include various types of volatile and nonvolatile storage media. The functions, acts or tasks illustrated in the figures or described herein are executed in response to one or more sets of instructions stored in or on computer readable storage media. The functions, acts or tasks are independent of the particular type of instructions set, storage media, processor or processing strategy and may be performed by software, hardware, integrated circuits, firmware, micro code and the like, operating alone or in combination. Likewise, processing strategies may include multiprocessing, multitasking, parallel processing and the like. In one embodiment, the instructions are stored on a removable media device for reading by local or remote systems. In other embodiments, the instructions are stored in a remote location for transfer through a computer network or over telephone lines. In yet other embodiments, the instructions are stored within a given computer, CPU, GPU or system.

[0073] Experimental Results. An example of the disclosed method was applied to 50 de-identified videos of 25 traumatic injured patients. Ultrasound images of both eyes were captured for each patient. The results of the disclosed method were compared with ground truth measurements, which were measurements from two experts. The correlation between two experts' measurements was also calculated. It should be noted that the individuals performing the manual measurements were blinded to each other's measurements as well as the algorithm measurement. Four types of comparisons were implemented. In the first one, the average error between the proposed method and the ground truth was calculated using the equation below.

$$e = \frac{1}{n_u}\sum_{k=1}^{n_u}\left|1 - \frac{ONSD_1(k)}{ONSD_2(k)}\right| \times 100$$

[0074] In Equation (5), n_u is the number of ultrasound images. Also, $ONSD_1$ and $ONSD_2$ are the ONSD measurements from two sources. For instance, for comparing the results of the proposed method with the ground truth, $ONSD_1$ and $ONSD_2$ are the algorithm results and the average of two experts' measurements respectively. Moreover, for comparing two experts' measurement, $ONSD_1$ and $ONSD_2$ are the measurements from each expert. The average percentage of error between the results of the algorithm and the average manual measurements was 5.52%. This error was 4.74% between two experts' measurements. The difference between these two errors show that the disclosed methods and systems can calculate the ONSD accurately. In the second comparison, the mean square error (MSE) was

calculated using the equation below, where $\|.\|_2$ is the norm-2.

$$MSE = \frac{1}{n_u}\|ONSD_1 - ONSD_2\|_2$$

[0075] The MSE between the algorithm results and the average of two experts' measurements was 0.0018, while the MSE between two experts' measurement was 0.0016. In the third comparison, intraclass correlation coefficient (ICC) was calculated, which shows the similarity between two quantitative measurements. The ICC between the algorithm results and the average of two experts' measurements was 0.70, while the ICC between two experts' measurement was 0.80. In the last comparison, the student t-test was performed, which is a statistical test to test the null hypothesis that the means of two measurements are not different. Using the confidence interval of 95%, the p-value of the t-test between the algorithm results and the average of two experts' measurements was 0.45, while this value for the t-test between the two experts' measurements was 0.26. These p-values show that the t-test doesn't reject the null hypothesis. All of the four aforementioned comparisons indicate strong correlation between the proposed method' s results and the ground truth.

[0076] The methods and systems described above may be used to calculate additional or alternative parameters or characteristics regarding the optic nerve sheath. For instance, the area inside the optic nerve sheath for each frame (i.e., two-dimensional slice) may be calculated. The area may be bounded laterally by the optic nerve sheath, and from the globe-optic nerve interface point to the 3 mm depth (or another depth) in the anterior-posterior dimension. The area may accordingly have a semi-circular shape, as shown by the lines superimposed on the image of Figure 2. The area may then be used to estimate the ICP level. The correlation between the area and the ICP level may be stored in a look-up table or other database, as described above.

[0077] Described above are methods and systems for automatically and non-invasively measuring optic nerve sheath diameter from scan data, such as ultrasound imaging data. As a non-invasive procedure, the measurement techniques of the disclosed methods and systems reduce the costs associated with efforts to use sheath diameter as a predictor of ICP increase. The automated nature of the measurement techniques of the disclosed methods and systems avoid the time consuming and error prone aspects of manual measurement techniques. In some cases, the disclosed methods and systems implement image processing in which the optic nerve sheath diameter is measured automatically by removing noise from the image scans, detecting a region of interest using a line integral method, and analyzing super-pixels

generated via image segmentation. Results of tests of the disclosed method did not differ substantially from manual measurements conducted by two experts. The average percentage of error between the disclosed method and the experts' measurements did not substantially differ from the error between the respective measurements of the two experts.

[0078] Even though intracranial-pressure monitoring is a standard care for severe traumatic injured patients, using such invasive devices might be associated with worsening of survival and there might be complications following the placement of ICP sensors. Therefore, the non-invasive monitoring provided by the disclosed methods and systems can prevent secondary complications. It has been shown that there is a correlation between the ICP elevation and the optic nerve sheath diameter. The disclosed methods and systems calculate this diameter using image processing techniques. In one example, images are first denoised, and a region of interest is identified using a line-integral method. A super-pixel segmentation method is then applied to the subset of scan data in the region of interest. After that, the row or line of segmented scan data at 3mm below the globe is used to measure the diameter of the nerve sheath. The diameter may be measured by computing the derivative of that row and finding the peaks in the derivative.

[0079] The present disclosure has been described with reference to specific examples that are intended to be illustrative only and not to be limiting of the disclosure. Changes, additions and/or deletions may be made to the examples without departing from the spirit and scope of the disclosure.

[0080] The foregoing description is given for clearness of understanding only, and no unnecessary limitations should be understood therefrom.

What is Claimed is:

1. A method of determining a diameter of a sheath of an optic nerve, the method comprising:

obtaining, by a processor, scan data representative of the optic nerve sheath;

analyzing, by the processor, the scan data to find a position of a globe-optic nerve interface point;

segmenting, by the processor, the scan data;

processing, by the processor, the segmented scan data at an offset from the position of the globe-optic nerve interface point to determine boundary positions of the optic nerve sheath; and

calculating, by the processor, the diameter of the optic nerve sheath based on the determined boundary positions.

2. The method of claim 1, wherein processing the segmented scan data comprises:

finding peaks in the segmented scan data at the offset; and

determining a location of a minimum between the found peaks.

3. The method of claim 1, wherein processing the segmented scan data comprises processing the segmented scan data comprises computing a derivative of the segmented scan data at the offset.

4. The method of claim 1, wherein processing the segmented scan data comprises:

determining a lateral position of the globe-optic nerve interface point at the offset based on a minimum between peaks in the segmented scan data;

computing a derivative of the segmented scan data at the offset; and

finding a pair of peaks in the derivative of the segmented scan data, each peak of the pair of peaks being disposed on a respective side of the lateral position.

5. The method of claim 4, wherein finding the first and second peaks comprises disregarding peaks in the derivative greater than a threshold.

6. The method of claim 4, wherein finding the first and second peaks further comprises, after disregarding the peaks greater than the threshold:

finding a negative peak closest to the lateral position of the globe-optic nerve interface

point; and

finding a positive peak closest to the lateral position of the globe-optic nerve interface point.

7. The method of claim 1, wherein analyzing the scan data comprises:

computing a line integral of the scan data at each anterior-posterior position of the scan data; and

finding a maximum of the line integral to determine the position of the globe-optic nerve interface point.

8. The method of claim 7, wherein the line integral is a first line integral, the method further comprising:

computing a second line integral of the scan data at each lateral position of the scan data; and

determining a subset of the scan data corresponding with a region of interest based on the first line integral and the second line integral;

wherein segmenting the scan data is implemented on the determined subset of the scan data.

9. The method of claim 8, wherein:

the scan data comprises a plurality of frames; and

the method further comprises disregarding one or more frames of the plurality of frames based on whether the first and second line integrals present peaks indicative of the globe and the optic nerve such that analyzing the scan data, segmenting the scan data, processing the segmented scan data, and calculating the diameter are repeated for the scan data of each remaining frame of the plurality of frames.

10. The method of claim 1, wherein the scan data comprises two-dimensional slice data, the two-dimensional slice data being representative of a slice through the globe and the optic nerve.

11. The method of claim 1, wherein processing the segmented scan data comprises selecting a line of the scan data located about 3 millimeters in a posterior direction from the globe-optic nerve interface point as a subset of the segmented scan data at the offset to be processed.

12. The method of claim 1, wherein obtaining the scan data comprises:

capturing ultrasound scan data;

cropping the ultrasound data; and

removing noise from the cropped ultrasound scan data to generate the scan data;

wherein removing the noise comprises implementing a filtering procedure configured to preserve edges in the cropped ultrasound scan data.

13. The method of claim 1, wherein:

the scan data comprises a plurality of frames;

analyzing the scan data, segmenting the scan data, processing the segmented scan data, and calculating the diameter are repeated for the scan data of each frame of the plurality of frames; and

the method further comprises compiling the calculated diameters of the optic nerve sheath for the plurality of frames to determine a value for the diameter of the optic nerve sheath.

14. A method of determining an assessment of intracranial pressure comprising the method of claim 13, and further comprising determining an intracranial pressure level based on the value for the diameter and based on a database correlating diameter values with corresponding levels of intracranial pressure.

15. A system of determining a diameter of an optic nerve sheath, the system comprising:

a memory in which scan data input instructions, scan data analysis instructions, segmentation instructions, and boundary identification instructions are stored; and

a processor in communication with the memory and configured to –

upon execution of the scan data input instructions, obtain scan data representative of a two-dimensional slice through the optic nerve sheath and a globe from which the optic nerve extends;

upon execution of the scan data analysis instructions, analyze the scan data to find an anterior-posterior position of a globe-optic nerve interface point;

upon execution of the segmentation instructions, implement a segmentation procedure to generate a super-pixel representation of the scan data; and

upon execution of the boundary identification instructions, process the super-pixel representation of the scan data at an offset from the anterior-posterior position of the

globe-optic nerve interface point to determine boundary positions of the optic nerve sheath, and calculate the diameter of the optic nerve sheath based on the determined boundary positions.

16. The system of claim 15, wherein the segmentation procedure comprises a k-means clustering procedure.

17. The system of claim 15, wherein the execution of the segmentation instructions further configures the processor to discard super-pixels below a threshold size.

18. The system of claim 15, wherein the execution of the boundary identification instructions further configures the processor to -

determine a lateral position of the globe-optic nerve interface point at the offset based on a minimum between peaks in the super-pixel representation of the scan data;

compute a derivative of the super-pixel representation of the scan data at the offset; and

find a pair of peaks in the derivative of the super-pixel representation of the scan data, each peak of the pair of peaks being disposed on a respective side of the lateral position.

19. A computer readable storage medium having stored therein data representing instructions executable by a programmed processor for determining a diameter of an optic nerve sheath, the storage medium comprising instructions for:

obtaining scan data representative of a two-dimensional slice through the optic nerve sheath and a globe from which the optic nerve extends;

analyzing the scan data to find a position of a globe-optic nerve interface point;

implementing a segmentation procedure, the segmentation procedure being configured to generate a super-pixel representation of the scan data;

processing the super-pixel representation of the scan data at an offset from the anterior-posterior position of the globe-optic nerve interface point to determine boundary positions of the optic nerve sheath; and

calculating the diameter of the optic nerve sheath based on the determined boundary positions.

20. The computer readable storage medium of claim 19, wherein processing the super-pixel representation of the scan data comprises:

determining a lateral position of the globe-optic nerve interface point at the offset based on a minimum between peaks in the super-pixel representation of the scan data;

computing a derivative of the super-pixel representation of the scan data at the offset; and

finding a pair of peaks in the derivative of the super-pixel representation of the scan data, each peak of the pair of peaks being disposed on a respective side of the lateral position.

ABSTRACT OF THE DISCLOSURE

A method of determining a diameter of a sheath of an optic nerve includes obtaining, by a processor, scan data representative of the optic nerve sheath, analyzing, by the processor, the scan data to find a position of a globe-optic nerve interface point, segmenting, by the processor, the scan data, processing, by the processor, the segmented scan data at an offset from the position of the globe-optic nerve interface point to determine boundary positions of the optic nerve sheath, and calculating, by the processor, the diameter of the optic nerve sheath based on the determined boundary positions.

Appendix F:

PI Curriculum Vitae

Mohamad Hakam Tiba
Research Assistant Professor
North Campus Reseach Complex
2800 Plymouth Road, 026-323N, Ann Arbor, MI 48109
Phone: (734) 764-6702
Fax: (734) 763-9389
Email: tibam@med.umich.edu

Education and Training

Education

09/1985-09/1991	MD, Medicine, Damascus University, Damascus, Syrian Arab Republic
10/2013-04/2015	MS, Clinical Research Design and Statistical Analysis, University Of Michigan, Ann Arbor, MI

PostDoctoral Training

10/1991-08/1992	Internship, Intern in General Medicine, Ministry of Health Hospitals and Alshifa Hospital, Damascus, Syrian Arab Republic

Academic, Administrative, Clinical, Research and Military Appointments

Academic Appointments

07/2012-08/2016	Research Investigator in Emergency Medicine - Adult, University of Michigan - Ann Arbor, Ann Arbor, Michigan
09/2016-present	Research Assistant Professor in Emergency Medicine - Adult, University of Michigan - Ann Arbor, Ann Arbor, Michigan

Administrative Appointments

06/1994-09/1994	Observership and research assistant, Receiving Hospital, Wayne State University, Detroit, MI
01/1995-05/1995	Observership, Good Samaritan Hospital, Dayton, OH
02/1996-04/1998	Volunteer Research Assistant, Tufts University, Boston, MA
06/1998-05/2000	Senior Quality Control and Production Chemist, Owl Separation System, Portsmouth, New Hampshire
06/2000-05/2010	Life/Phys Science Research Associate, Virginia Commonwealth University, Richmond, Virginia
05/2010-06/2012	Laboratory and Research Manager, Virginia Commonwealth University, Richmond, Virginia

Research Interests

- Development of large animals models to study critical care illness and injury
- Development of non-invasive technologies to evaluate intravenous volume status in critically ill patients using bioimpedance
- Development of non-invasive technologies to evaluate cerebrovascular autoregulation using ocular bioimpedance
- Development of non-invasive spectroscopic technologies to monitor tissue oxygenation using Resonance Raman Spectroscopy (RRS)
- Development of resuscitation Fluids, hemoglobin and non-hemoglobin oxygen carriers
- Development of closed-loop feedback CPR devices
- Development of hemorrhage control materials and devices

Grants

Current Grants

Device to Aid in Arterial Microanastomosis Baxter Healthcare Corporation- 19-PAF08048
Co-I with Effort (Principal Investigator: Adeyiza Momoh)
11/2019-11/2020. $156,952 ($156,952)

ART-123: Recombinant Human Thrombomodulin Alpha in Prolonged Porcine Cardiac Arrest Asahi Kasei Pharma America Cor- 19-PAF03836
Co-I with Effort (Principal Investigator: Colin F Greineder)
10/2019-06/2020. $35,988 ($35,988)

AWD012537-MOD001: Michigan Resuscitation Innovation and Science Enterprise (M-RISE) American Heart Association
Co-I without Effort (Principal Investigator: Robert Neumar and Thomas Sanderson)
07/2019-06/2023. $645,245

STAT: Systolic Target Assessment Tool Massey Family Foundation
Co-I with Effort (Principal Investigator: David Hackenson)
07/2019-06/2020. $113,710 ($113,710)

DM160299: Gastroesophageal Resuscitative Occlusion of the Aorta (GROA) Dept. of the Army -- USAMRAA- 16-PAF08148
Co-I with Effort (Principal Investigator: Ward, Kevin Ralph)
02/2018-01/2021. $2,995,616

DM160294: Development and Testing of New Noninvasive Monitoring Tools for Prolonged Field Care Goal-Directed Therapy Dept. of the Army -- USAMRAA
Co-I with Effort (Principal Investigator: Kevin Ward)
01/2018-12/2020. $2,999,754 ($969,599)

DM160225: Novel Noninvasive Methods of Intracranial Pressure and Cerebrovascular Autoregulation Assessment: Seeing the Brain through the Eyes Dept. of the Army -- USAMRAA- 17-PAF00214
Tiba, Mohamad Hakam, PI
01/2018-12/2020. $1,481,538

5 R01 HL133129-04: ECPR After Prolonged Cardiac Arrest: Targeting Mechanisms of the No-Reflow NIH-DHHS-US- 16-PAF07624
Co-I with Effort (Principal Investigator: Neumar, Robert;Bartlett, Robert Hawes)
07/2017-06/2022. $3,894,128

Submitted Grants

Continuous, non-invasive hemodynamic compensation monitoring and assessment for trauma Army-DoD-US- 20-PAF02751
Co-I with Effort (Principal Investigator: Oldham, Kenn Richard)
09/2020-09/2022. $1,880,380

PRECISE ARDS: PRogram to Enhance PreCISion of thE Acute Respiratory Distress Syndrome NIH-DHHS-US- 20-PAF00297
Co-I with Effort (Principal Investigator: Stringer, Kathleen A;Standiford, Theodore J)
07/2020-06/2025. $11,779,823

Non-Invasive Monitoring of Hemodynamic Compensatory Mechanisms in Simulated Hypovolemic Conditions 20-PRE00049
Co-I without Effort (Principal Investigator: Oldham, Kenn Richard)
07/2020-06/2023. $750,000

Pharmacologic Allosteric Hemoglobin Modification for Enhanced Delivery of Oxygen and Nitric Oxide to Preserve Vital Organ Function in Acute Hemorrhagic Shock SubK-Army-DoD-US through a consortium with Illexcor Therapeutics, LLC- 19-PAF07273
Tiba, Mohamad Hakam, PI
01/2020-12/2021. $594,703

Past Grants

Swine-Sepsis and ARDS MICHR
Co-I with Effort (Principal Investigator: Robert Dickson and Kathleen Stringer)
09/2018-08/2019. $100,000 ($100,000)

Intracranial Pressure Monitor Enhancement for Cerebral Hemodynamic Monitoring The Massey Family Foundation
Co-I with Effort (Principal Investigator: Kenn Oldham)
07/2018-06/2019. $104,433 ($104,433)

Real-Time, Non-Invasive Brain Metabolism The Massey Family Foundation
Co-I with Effort (Principal Investigator: Oliver D. Kripfgans)
07/2018-06/2019. $143,666 ($143,666)

Novel Noninvasive Method of Cerebrovascular Blood Volume Assessment Using Brain Bioimpedance The Massey Family foundation
Tiba, MH and Ward, KR, Co-PI
07/2017-09/2018. $130,565 ($130,565)

Systolic Target Assessment Tool (STAT) for TBI Management The Massey Family Foundation
Co-I (Principal Investigator: Hackenson)
07/2017-09/2018. $73,975 ($73,975)

Redox POC Platform for Evaluation and Treatment of Sepsis, Septic Shock, and Multiple Organ Dysfunction
Michigan Translational Research and Commercialization Program
Co-I with Effort (Principal Investigator: Rodney C. Daniels)
02/2016-01/2017. $155,435 ($155,435)

15-PAF06146: Comparison of Respiratory Induced Limb Bioimpedance Changes With Inferior Vena Cava Diameter Changes to Assess Intravascular Volume Status in Patients Undergoing Hemodialysis Renal Research Institute, LLC
Co-I with Effort (Principal Investigator: Michael Heung)
06/2015-12/2016. $42,830 ($42,830)

G016123: Novel Noninvasive Methods of Intracranial Pressure Assessment: Seeing the Brain Through the Eyes
Massey Family Foundation
Co-I with Effort (Principal Investigator: Krishna Rajajee and Kevin Ward)
02/2015-02/2016. $106,262 ($106,262)

Comparison of Respiratory Induced Limb Bioimpedance Changes with Inferior Vena Cava Diameter Changes to Assess Intravascular Volume Status Baxter Healthcare Corporation- 15-PAF03360
Tiba, Mohamad Hakam;Ward, Kevin Ralph, PI
01/2015-06/2015. $150,476

N017668: Dynamic Respiratory Impedance Volume Evaluation (DRIVE) Michigan Translation and Commercialization (MTRAC) for Life Sciences Program
Mohamad Hakam Tiba, PI
02/2014-01/2015. $92,958 ($92,958)

14-PAF05256: Multi-laboratory Study of Epinephrine in Experimental Cardiac Arrest St. Michaels Hospital
Robert Neumar Mohamad Hakam Tiba, Co-PI
11/2013-12/2015. $10,000

ART-123 (recombinant human thrombomodulin alpha) in porcine cardiac arrest Zoll Foundation- 19-PAF01707
Co-I without Effort (Principal Investigator: Colin F Greineder)
11/2019. ($47,773)

Honors and Awards

Regional

2010	Mentorship Award, Goldwater Scholarship committee. For mentorship of Elizabeth Proffitt, a Goldwater Scholar
2016	Outstanding Poster Award. Massey Regional TBI Conference

Institutional

2014	Spoor Memorial Scholarship Award
2015	First place in the poster competition award. The Eighth Annual Symposium, A. Alfred Taubman Medical Research Institute.

Memberships in Professional Societies

2012-present	Member, The Shock Society
2013-present	Member, American Association for the Advancement of Science
2013-present	Member, Society for Academic Emergency Medicine
2013-present	Member, Society of Critical Care Medicine
2014-present	Member, American Heart Association

Editorial Positions, Boards, and Peer-Review Service

Study Sections

National

2015-present	Peer review panel of the 2015 Combat Casualty Care Research Program (CCCRP) for the Department of Defense U.S. Army Medical Research and Materiel Command (MRMC).
2018-present	Autonomous and Unmanned Medical Capability (AUMC-1) peer review panel of the 2017 Defense Medical Research and Development Program (DMRDP) Joint Program Committee-1 (JPC-1) for the Department of Defense Congressionally Directed Medical Research Programs (CDMRP).
2019	FY18 Combat Casualty Care Research Program's Prolonged Field Care and En Route Care (PFC-ERC) panel (Ad Hoc)

Journal Reviewer

2016-present	American Journal of Emergency Medicine (Ad Hoc)

Teaching

Clinical Fellow

10/2018-10/2020	Yub Raj Sedhai, MD, Spectrum system, Grand Rapids, MI

Graduate Student

06/2013-12/2015	Barry Belmont, MS, Biomedical Engineering, University of Michigan
10/2014-04/2015	Brandon Cummings, MS, The Undergraduate Research Opportunity Program (UROP). University of Michigan
02/2019-06/2019	Ross Kendall, MS, The University of Michigan, Capstone Program

Medical Student

06/2015-08/2015	Spencer Thompson, BS, Summer Biomedical Research Proposal. University of Michigan
06/2015-08/2015	Shawn Kache, BS, Summer Biomedical Research Proposal. University of Michigan
08/2015-11/2015	Isaac Ezra Perry, BS, Edward Via College of Osteopathic Medicine
06/2017-08/2017	Alexander Khouri, BS, Summer Biomedical Research Proposal, University of Michigan.

Undergraduate Student

01/2006-01/2010	Elizabeth K. Proffitt, Virginia Commonwealth University

10/2013-05/2014	Eman Hejab, The Undergraduate Research Opportunity Program (UROP). University of Michigan
10/2015-04/2016	Justine Garfinkel, The Undergraduate Research Opportunity Program (UROP). University of Michigan
10/2015-04/2016	Mambwe C. Lupiya, The Undergraduate Research Opportunity Program (UROP). University of Michigan
05/2016-08/2016	John Soukar, University of Michigan
07/2016-05/2017	Stephen Dowker, University of Michigan
10/2016-04/2017	Stephanie Francalancia, The Undergraduate Research Opportunity Program (UROP). University of Michigan
10/2017-04/2018	Benjamin Koehler, The Undergraduate Research Opportunity Program (UROP). University of Michigan
10/2017-04/2018	Alysha Loraff, The Undergraduate Research Opportunity Program (UROP). University of Michigan
10/2017-04/2018	Varisha Essani, The Undergraduate Research Opportunity Program (UROP). University of Michigan
10/2017-04/2018	Tessa Magsoudi, The Undergraduate Research Opportunity Program (UROP). University of Michigan
09/2018-04/2019	Katherine Davis, Undergraduate Research Opportunity Program (UROP)
09/2018-04/2019	Claire Roberge, Undergraduate Research Opportunity Program (UROP)

Visiting Scholars

09/2015-08/2016	Jae Hyuk Lee, MD, Seoul National University Bundang Hospital, South Korea

Teaching Activity

Institutional

08/2013	Surgery concentration. Surgical techniques training session for University Laboratory Animal Medicine (ULAM) veterinary residents
08/2014	Surgery concentration. Surgical techniques training session for University Laboratory Animal Medicine (ULAM) veterinary residents
08/2016	Surgery concentration. Surgical techniques training session for University Laboratory Animal Medicine (ULAM) veterinary residents
08/2018-09/2018	Surgery concentration. Surgical techniques training session for University Laboratory Animal Medicine (ULAM) veterinary residents
08/2019-09/2019	Surgery concentration. Surgical techniques training session for University Laboratory Animal Medicine (ULAM) veterinary residents

Committee and Administrative Services

Committee Services

National

2014-2015	Task force to evaluate animal research publications' compliance with ARRIVE reporting standards. Shock Society, Member

Institutional

2013-present	Institutional Animal Care and Use Committee (IACUC), Member
2014-2016	Large Animals Working Group, Member
2015-2016	IACUC Subcommittee for eRAM Online Protocol Changes and Updates, Member
2015	IACUC Subcommittee for Standard Operating Procedures (SOP) Approval, Member
2016-2017	IACUC Task Force for Review of PI Managed Space Request Application, Member
2017-present	Animal Care and Use Faculty Advisory Committee. ACU-FAC, Chair
2018-present	Strategic Advisory Committee to the UM Animal Care and Use Program (ACUP)., Member

2020-present	LARCC Subcommittee, Organizing Subcommittee for the Laboratory Animal Research Coordinator Certification Program

Administrative Services

Volunteer

2015-present	Judge, The Undergraduate Research Opportunity Program (UROP), University of Michigan, Ann Arbor, The Undergraduate Research Opportunity Program's Annual Research Spring Symposium
2019	Volunteer, Ann Arbor Running Co., Gallup Park, Gallup Gallop 5K run

Visiting Professorships and Extramural Invited Presentations

Extramural Invited Presentations

1. Mohamad H. Tiba, H. Mowafi, G. Gawor, R. W. Barbee, R. Ivatury, K. R. Ward. Preliminary Studies of a New Impedance Based Measure to Noninvasively Determine Central Venous Pressure, Advanced Technologies Applications in Combat Casualty Care, August 2003, St. Pete Beach, Florida. (Poster Presentation)
2. Mohamad H. Tiba, T. A. Timmons, R. W. Barbee, R. R. Ivatury, B. D. Spiess, P. S. Reynolds, and K. R. Ward. Bispectral Index Monitoring of Intubated Trauma Patients Indicates Inadequate Sedation, Advanced Technologies Applications in Combat Casualty Care, August 2004, St. Pete Beach, Florida. (Poster Presentation)
3. Mohamad H. Tiba, Kate Proffitt; R. Wayne Barbee, Gerard Draucker, Rao R. Ivatury, Kevin R. Ward. Noninvasive Bioimpedance Base for Central Venous Pressure Measurement, Advanced Technologies Applications in Combat Casualty Care, August 2005, Pete Beach Florida. (Poster Presentation)
4. Mohamad H. Tiba, G. T Draucker, R. W. Barbee, J. Terner, I. P. Torres Filho, K. R. Ward. Performance of Tissue Hemoglobin Oxygen Saturation as Measured by Resonance Raman Spectroscopy and Near Infrared Spectroscopy Compared to Mixed Venous Hemoglobin Oxygen Saturation and Systemic Lactate Levels During Hemorrhage, 36th Annual Conference on Shock, June 2013, San Diego, California. (Poster Presentation)
5. Mohamad H. Tiba, G. T. Draucker, B. M. McCracken, K. R. Ward. Controlling Pelvic Hemorrhage using a Novel Pressure Garment, 37th Annual Conference on Shock, June 2014, Charlotte, North Carolina. (Poster Presentation)
6. Mohamad H. Tiba, G. T. Draucker, B. M. McCracken, H. B. Alam, J. L. Eliason, K. R. Ward. Testing of a novel Pelvic Hemostasis Belt to Control Lethal Pelvic Arterial Hemorrhage, American Heart Association. Resuscitation Science Symposium, November 2014, Chicago, Illinois. (Poster Presentation)
7. Mohamad H. Tiba, Barry Belmont, Nik Theyyunni, Robert Huang, David F. Barton, Amanda J. Pennington, Gerard T. Draucker, Albert J. Shih, Kevin R. Ward. Coparison of Respiratory Induced Inferior Vena Cava Diameter Changes With Limb Bioimpedance Changes to Assess Intravascular Volume Status, 38th Annual Conference on Shock, June 2015, Denver Colorado. (Poster Presentation)
8. Evaluation of Intravascular Volume Status Using Dynamic Respiratory Induced Bioimpedance of the Limb, Society for Academic emergency Medicine, May 2016, New Orleans, LA. (Oral Presentation)
9. Mohamad H. Tiba, Barry Belmont, Michael Heung, Nik Theyyunni, Robert Huang, Christopher D. Fung, Amanda J. Pennington, Kevin R. Ward: Comparison of Respiratory Induced Inferior Vena Cava Diameter Changes with Limb Bioimpedance Changes In dialysis and mechanically ventilated patients, Thirty-Ninth Annual Conference on Shock, June 2016, Austin, Texas. (Poster Presaentation)
10. Mohamad H. Tiba, Amanda Pennington, Kyle Gunnerson, Kevin R. Ward. Monitoring of Tissue Microvasculature Oxygenation using Resonance Raman Spectroscopy, Thirty-Ninth Annual Conference on Shock, June 2016, austin, Texas. (Poster Presentation)
11. Mohamad. Tiba, Michael Heung, Nik Theyyunni, Barry Belmont, Robert Huang, Ross Kessler, Christopher Fung, Amanda Pennington, Brandon Cummings, Kevin Ward: Development of a Novel Non-Invasive Technologies to Evaluate Intravascular Volume Status Using Bioimpedance, The 2016 Military Health System Research Symposium (MHSRS), August 2016, Orlando, Florida. (Poster Presentation)
12. Mohamad H. Tiba, Robert Barbee, James Terner, Ivo. Torres Filho, Kevin Ward: Measurement of tissue hemoglobin oxygen saturation using Resonance Raman Spectroscopy in a large animal model of hemorrhage, The 2016 Military Health System Research Symposium (MHSRS), August 2016, Orlando, Florida. (Poster Presentation)

13. Mohamad H. Tiba, Brendan McCracken, Gerard Draucker, Hasan Alam, Jonathan Eliason, Kevin Ward: Use of a Novel Pelvic Hemostasis Belt to Control Lethal Arterial Hemorrhage, The 2016 Military Health System Research Symposium (MHSRS), August 2016, Orlando, Florida. (Poster Presntation)
14. Mohamad Hakam Tiba; Brendan McCracken; Sardar Ansari; Venkatakrishna Rajajee; Kevin Ward. Novel Noninvasive Method of Cerebrovascular Autoregulation Assessment: Seeing the Brain through the Eyes., Fortieth Annual Conference on Shock., June 2017, Fort Lauderdale, Florida. (Poster Presentation)
15. Novel Noninvasive Method of Cerebrovascular Autoregulation Assessment, Military Health System Research Symposium (MHSRS), August 2017, Kissimmee, Florida (Oral Presentation)
16. A Novel Large Animal Model of Sepsis, Forty-First Annual Conference on Shock., June 2018, Scottsdale, Arizona. (Poster Presentation)
17. Monitoring Traumatic Brain Injury Patients using Transocular Brain Impedance (TBI)., Military Health System Research Symposium (MHSRS), August 2018, Orlando, Florida. (Poster Presentation)
18. Use of Resuscitative Balloon Occlusion of the Aorta in a Swine Model of Prolonged Cardiac Arrest., American Heart Association. Resuscitation Symposium. (Poster Presentation), November 2018, Chicago, IL
19. Cytokines and Bacterial DNA Coincide with Sepsis Pathogenesis and Progression, Shock Society 42nd Meeting on Shock (Poster Presentation), June 2019, Coronado, California
20. Novel Monitoring Modality of Traumatic Brain Injury Patients using Transocular Brain Impedance (TOBI), Military Health System Research Symposium (MHSRS), August 2019, Kissimmee, Florida
21. Automated Optic Nerve Sheath Diameter Measurement, Military Health System Research Symposium (MHSRS), August 2019, Kissimmee, Florida

Other

1. DRIVE Performance and update, Baxter Healthcare, March 2015, Chicago, Illinois
2. Mohamad H. Tiba, Barry Belmont, Spencer Thompson, Michael Heung, Nik Theyyunni, Robert Huang, Christofer Fung, Amanda Pennington, Gerard Draucker, Kevin R. Ward. Development of a Novel Non-Invasive Technologies to Evaluate Intravascular Volume Status Using Bioimpedance, Eighth Annual Symposium, A. Alfred Taubman Medical Research institute. University of Michigan., October 2015, Ann Arbor, Michigan. (Poster Presentation)
3. Mohamad H. Tiba, Shawn Kache, Brandon Cummings, Amanda Pennington, Kyle Gunnerson, Kevin R. Ward. Monitoring of Tissue Microvasculature Oxygenation using Resonance Raman Spectroscopy, Eighth Annual Symposium, A. Alfred Taubman Medical Research institute. University of Michigan., October 2015, Ann Arbor, Michigan. (Poster Presentation)
4. Mohamad H. Tiba. Sample Size and Power Analysis: What Do We Need to Know, Institutional Animal Care and Use committee (IACUC). A presentation as part of the training protocol for IACUC members, February 2016, Ann Arbor, MI
5. Mohamad H. Tiba, MD, MS; Nik Theyyunni, MD; Barry Belmont, PhD; Michael Heung, MD, MS; Robert Huang, MD; Christopher Fung, MD; Amanda Pennington, MS; Brandon Cummings; Gerard Draucker, EMT; Kevin R. Ward, MD. Comparison of Respiratory Induced Inferior Vena Cava Diameter Changes with Limb Impedance Changes in Hemodialysis Patients., First Annual William G. Barsan Emergency Medicine Research Forum. (Poster Presentation), April 2016, Ann Arbor, Michigan
6. Mohamad H. Tiba, MD; Amanda Pennington, MS; Gerard Draucker, EMT; Brandon Cummings; Kyle Gunnerson, MD; Kevin R. Ward, MD. Monitoring of Tissue Microvasculature Oxygenation using Resonance Raman Spectroscopy, First Annual William G. Barsan Emergency Medicine Research Forum. (Poster Presentation), April 2016, Ann Arbor, Michigan
7. Mohamad H. Tiba, MD; Gerard T. Draucker, EMT-P; Brendan M. McCracken, BS; Hasan B. Alam, MD; Jonathan L. Eliason, MD; Kevin R. Ward, MD. Controlling Pelvic Hemorrhage Using a Novel Pressure Garment, First Annual William G. Barsan Emergency Medicine Research Forum. (Poster Presentation), April 2016, Ann ARbor, Michigan
8. Novel Noninvasive Method of Cerebrovascular Autoregulation Assessment: Seeing the Brain through the Eyes, University of Michigan / Massey Foundation, October 2016, Ann Arbor, MI. (Oral Presentation)
9. Mohamad H. Tiba, MD, MS; Brendan McCracken, BS; Sardar Ansari, PhD; Ashwin Belle, PhD; Kevin Ward, MD. Novel Noninvasive Method of Cerebrovascular Autoregulation Assessment: Seeing the Brain through the Eyes, Second Annual William G. Barsan Emergency Medicine Research Forum. (Poster Presentation), April 2017, Ann Arbor, Michigan
10. Noninvasive Assessment of Cerebrovascular Blood Volume and Autoregulation Using Bioimpedance, Massey Foundation Second TBI Summit. (Oral Presentation), October 2017, Ann ARbor, Michigan

11. Monitoring Traumatic Brain Injury Patients using Transocular Brain Impedance (TBI). Grand Challenge Experience., The Massey Foundation TBI Grand Challenge, March 2018, Ann Arbor, Michigan
12. Trans-Ocular Brain Impedance: Novel Non-invasive Monitoring of the TBI Patient, 2018 Massey TBI Regional Conference. Oral Presentation), October 2018, Ann Arbor, MI

Seminars

1. Tissue Hemoglobin Oxygen Saturation in the critically ill, as Measured by Resonance Raman Spectroscopy, University Laboratory Animals Medicine (ULAM) Fall Seminar Series, November 2013, Ann Arbor, Michigan
2. Emergency Department Tour and Description of Two Non-Invasive Monitoring Modalities, University of Michigan. The Undergraduate Research Opportunity Program (UROP) Seminar Series, December 2015, Ann Arbor, Michigan
3. Bolus Versus Continuous Epinephrine Infusion In a Large animal model of Cardiac Arrest: A Multicenter Trial, MCIRCC/OSCAR CONFERENCE, March 2016, Ann Arbor, MI
4. Large Animal Model of Sepsis, University Laboratory Animals Medicine (ULAM) Fall Seminar Series, November 2017, Ann Arbor, Michigan
5. Laboratory Animal Research Coordinator Certificate (LARCC), University of Michigan / Animal Care and Use Office, September 2019, Ann Arbor, Michigan

Patents

Granted

06/2019 EVALUATING CARDIOVASCULAR HEALTH USING INTRAVASCULAR VOLUME, 20150031966, 10314532, Co-inventor, Submitted on 07/2014

Application in Process

Automated Optic Nerve Sheath Diameter Measurement, Co-inventor, Submitted on 07 /2019

Ocular Impedance-Based System for Brain Health Monitoring, Co-inventor, Submitted on 05/2017

Disclosures

04/2019 Transocular Electroencephalogram Awareness Monitor (TEAM), 2019-092, Co-inventor, Submitted on 04/2019

Device for Control of Non-Compressible Abdominal Hemorrhage, 2020-129, Co-inventor, Submitted on 10/2019

Bibliography

Peer-Reviewed Journals and Publications

1. Torres LN, Torres Filho IP, Barbee RW, Tiba MH, Ward KR, Pittman RN: Systemic responses to prolonged hemorrhagic hypotension Am. J. Physiol. Heart Circ. Physiol. 286(5 55-5): H1811-H1820, 2004. PM14726303
2. Smith L, Tiba MH, Goldberg ME, Barbee RW: Chronic implantation of transit-time flow probes on the ascending aorta of rodents Lab. Anim. 38(4): 362-370, 2004. PM15479550
3. Torres LN, Torres Filho IP, Barbee RW, Tiba MH, Ward KR, Pittman RN: Continuous peripheral resistance measurement during hemorrhagic hypotension Am. J. Physiol. Heart Circ. Physiol. 287(5 56-5): H2341-H2345, 2004. PM15256369
4. Ward KR, Torres Filho I, Barbee RW, Torres L, Tiba MH, Reynolds PS, Pittman RN, Ivatury RR, Terner J: Resonance Raman spectroscopy: A new technology for tissue oxygenation monitoring Crit. Care Med. 34 (3): 792-799, 2006. PM16521273
5. Ward KR, Tiba MH, Barbee RW, Ivatury RR, Arrowood JA, Spiess BD, Hummel R: A new noninvasive method to determine central venous pressure Resuscitation 70(2): 238-246, 2006. PM16820258
6. Ward KR, Barbee RW, Reynolds PS, Filho IP, Tiba MH, Torres L, Pittman RN, Terner J: Oxygenation monitoring of tissue vasculature by resonance Raman spectroscopy Anal. Chem. 79(4): 1514-1518, 2007. PM17297949

7. Evans MC, Diegelmann RF, Barbee RW, Tiba MH, Edwards E, Sreedhar S, Ward KR: Protein synthesis inhibition as a potential strategy for metabolic down-regulation Resuscitation 73(2): 296-303, 2007. PM17250947
8. Ward KR, Tiba MH, Holbert WH, Blocher CR, Draucker GT, Proffitt EK, Bowlin GL, Ivatury RR, Diegelmann RF: Comparison of a new hemostatic agent to current combat hemostatic agents in a swine model of lethal extremity arterial hemorrhage J Trauma 63(2): 276-283, 2007. PM17693824
9. Ward KR, Tiba MH, Draucker GT, Proffitt EK, Barbee RW, Gunnerson KJ, Reynolds PS, Spiess BD: A novel noninvasive impedance-based technique for central venous pressure measurement Shock 33(3): 269-273, 2010. PM19487978
10. Ward KR, Tiba MH, Ryan KL, Filho IP, Rickards CA, Witten T, Soller BR, Ludwig DA, Convertino VA: Oxygen transport characterization of a human model of progressive hemorrhage Resuscitation 81(8): 987-993, 2010. PM20418009
11. Leong B, Reynolds PS, Tiba MH, Holbert WH, Draucker GT, Medina JA, Barbee RW, White NJ, Ward KR: Effects of a combination hemoglobin based oxygen carrier-hypertonic saline solution on oxygen transport in the treatment of traumatic shock Resuscitation 82(7): 937-943, 2011. PM21497981
12. Tiba MH, Draucker GT, Barbee RW, Terner J, Filho IT, Romfh P, Vakhshoori D, Ward KR: Tissue oxygenation monitoring using resonance Raman spectroscopy during hemorrhage J Trauma Acute Care Surg 76(2): 402-408, 2014. PM24378619
13. Tiba MH, Draucker GT, McCracken BM, Alam HB, Eliason JL, Ward KR: Use of pelvic hemostasis belt to control lethal pelvic arterial hemorrhage in a swine model. The journal of trauma and acute care surgery 78(3): 524-9, 2015. PM25710422
14. Tiba MH, Belmont B, Theyyunni N, Heung M, Huang RD, Fung, CM, Pennington AJ, Cummings BC, Draucker GT, Shih AJ, Ward KR: Dynamic Limb Bioimpedance and Inferior Vena Cava Ultrasound in Patients Undergoing Hemodialysis ASAIO J 62(4): 463-9, 2016. PM26919184
15. Tiba MH, Belmont B, Heung M, Theyyunni N, Huang RD, Fung CM, Pennington AJ, Cummings BC, Draucker GT, Shih AJ, Ward KR: Dynamic limb bioimpedance and inferior vena cava ultrasound in patients undergoing hemodialysis ASAIO Journal 62(4): 463-469, 2016. PM26919184
16. Tiba MH, McCracken BM, Ansari S, Belle A, Cummings BC, Rajajee V, Patil PG, Alam HB, Ward KR: Novel Noninvasive Method of Cerebrovascular Blood Volume Assessment Using Brain Bioimpedance. J Neurotrauma 34(22): 3089-3096, 2017. PM28657491
17. Daniels RC, Jun H, Tiba H, McCracken B, Herrera-Fierro P, Collinson M, Ward KR: Whole Blood Redox Potential Correlates With Progressive Accumulation of Oxygen Debt and Acts as A Marker of Resuscitation in A Swine Hemorrhagic Shock Model. Shock 49(3): 345-351, 2018. PM28658006 /PMC5745311
18. Belmont B, Kessler R, Theyyunni N, Fung C, Huang R, Cover M, Ward KR, Shih AJ, Tiba M: Continuous Inferior Vena Cava Diameter Tracking through an Iterative Kanade-Lucas-Tomasi-Based Algorithm. Ultrasound Med Biol 44(12): 2793-2801, 2018. PM30213669
19. Coute RA, Shields TA, Cranford JA, Ansari S, Abir M, Tiba MH, Dunne R, O'Neil B, Swor R, Neumar RW, SaveMiHeart Consortium and the CARES Surveillance Group.: Intrastate Variation in Treatment and Outcomes of Out-of-Hospital Cardiac Arrest. Prehosp Emerg Care 22(6): 743-752, 2018. PM29624088
20. Sando IC, Plott JS, McCracken BM, Tiba MH, Ward KR, Kozlow JH, Cederna PS, Momoh AO: Simplifying Arterial Coupling in Microsurgery-A Preclinical Assessment of an Everter Device to Aid with Arterial Anastomosis. J Reconstr Microsurg: 2018. PM29452442
21. Tiba MH, McCracken BM, Cummings BC, Colmenero CI, Rygalski CJ, Hsu CH, Sanderson TH, Nallamothu BK, Neumar RW, Ward KR: Use of resuscitative balloon occlusion of the aorta in a swine model of prolonged cardiac arrest. Resuscitation 140: 106-112, 2019. PM31121206

Other Media

Other

1. Sumeyra Demir, Nazanin Mirshahi, M. Hakam Tiba, Gerard Draucker, Kevin Ward, Rosalyn Hobson and K. Najarian.: Image Processing and Machine Learning for Diagnostic Analysis of Microcirculation., Conference Paper. 2009 ICME International Conference on Complex Medical Engineering, IEEE, 2009.
2. Sardar Ansari ; Kayvan Najarian ; Kevin Ward ; Mohamad Hakam Tiba.: Extraction of Respiratory Rate from Impedance Signal Measured on Arm: A Portable Respiratory Rate Measurement Device.

   , Conference Paper. 2009 IEEE International Conference on Bioinformatics and Biomedicine, IEEE, 2009.

3. Reza Soroushmehr; Krishna Rajajee; Craig Williamson; Jonathan Gryak; Kayvan Najarian; Kevin Ward; Mohamad H. Tiba.: Automated Optic Nerve Sheath Diameter Measurement Using Super-pixel Analysis.

   , Conference Paper. 2019 41st Annual International Conference of the IEEE Engineering in Medicine and Biology Society (EMBC), IEEE, 2019.

Abstracts

1. Ward KR, Barbee RW, Tiba, MH, Arrowood J, Ivatury RR, Lyders E, Spiess BP.: A Noninvasive Method of Determining Central Venous Pressure, 25th Annual Conference on Shock, Big Sky, Montana, Shock, 17, Supplement 1, 15, 2002.
2. Carr M, Kenawy E, Layman G, Wnek G, Ward KR, Barbee W, Tiba MH.: Development of The BioHemostat- A Treatment Modality for High Pressure Bleeding Based on Super Absorbent Polymers, 25 th Annual Conference on Shock, Big Sky, Shock, 17, Supplement 1, 54, 2002.
3. Barbee RW, Ward KR, Terner J, Torres I, Tiba MH, Torres L, Ivatury R, Spiess B, Pittman R.: Noninvasive Tissue Oxygenation Monitoring Using Resonance Raman Spectroscopy (RRS), 25th Annual Conference on Shock, Big Sky, Montana, Shock, 17, Supplement 1, 58, 2002.
4. Barbee RW, Ward KR, Terner J, Torres IP, Torres L, Pittman R, Ivatury R, Tiba MH.: Preliminary Studies Using Near Ultraviolet Excitation Fluorescence Spectroscopy to Monitor Tissue Dysoxia During Hemorrhage, 26th Annual Conference on Shock, Phoenix, Arizona, Shock, 19, Supplement 1, 26, 2003.
5. Ward K, Tiba M. H, Barbee W, Timmons T, Spiess B, Ivatury R.: Bispectral Index Monitoring of Intubated Paralyzed Trauma Patient Indicates Inadequate Sedation., Critical Care Medicine, 33, Supplement, A45, 2005.
6. Ward K, Tiba M. H, Proffitt K, Draucker J, Ivatury R, Barbee R, Spiess B, Arrowood J.: Noninvasive Central Venous Pressure Monitoring, Critical Care Medicine, 33, Supplement, A54, 2005.
7. Ward K, Tiba MH, Draucker G, Reynolds P, Torres R, Barbee RW, Ivatury RR.: Performance of Noninvasive Tissue Oxygenation Indicators in Detecting Shock Due to Hemorrhage, Critical Care Medicine, 33, Supplement, A23, 2005.
8. Ward K, Torres I, Barbee W, Torres L, Tiba M. H, Reynolds P, Pittman R, Ivatury R, Terner J.: Resonance Raman Spectroscopy for Noninvasive Tissue Oxygenation Monitoring, Critical Care Medicine, 33, Supplement, A35, 2005.
9. Ward K, Tiba M. H, Holbert W, Blocher C, Draucker G, Proffitt E, Bowlin G, Ivatury R, Diegelmann R.: Comparison of New Hemostatic Agent to Current Combat Hemostatic Agents in a Swine Model of Lethal Extremity Arterial Hemorrhage, Society for Academic Emergency Medicine (SAEM) Annual Meeting, Chicago, Illinois, Academic Emergency Medicine, 14, Supplement, pS61, 2007.
10. Ward K, Tiba M. H, Draucker G, Proffitt K, Gawor G, Barbee R.: Noninvasive Measurement of Central Venous Pressure, Society for Academic Emergency Medicine (SAEM) Annual Meeting, Chicago, Illinois, Academic Emergency Medicine, 14, Supplement, pS182, 2007.
11. Mohamad H. Tiba, Kathy Ryan, Ivo Torres Filho, Carloine Rickards, Tarynn M Witten, Babs Soller, Victor Convertino, Kevin R. Ward: Oxygen Transport Characterization of a Human Model of Hemorrhage , American Heart Association Resuscitation Science Symposium, New Orleans, Louisiana, Circulation, 118, S_1447, 2008.
12. Ward K, Tiba M. H, Draucker G, Barbee R, Proffitt E, Gunnerson K: Noninvasive Central Venous Pressure Measurements in Mechanically Ventilated Patients, Society for Academic Emergency Medicine (SAEM) Annual Meeting, Washington, DC, Academic Emergency Medicine, 15, Supplement 1, S32, 2008.
13. Ward K, Tiba M. H, Medina J, Holbert W, Draucker J, Reynolds P, Blocher C, Barbee R.: Oxygen Debt and its Relationship to Lactate, Hemoglobin Levels, and Hemorrhage Volume in Hemorrhagic Shock and Resuscitation, Society for Academic Emergency Medicine (SAEM) Annual Meeting, Washington, DC, Academic Emergency Medicine, 15, Supplement 1, S32, 2008.
14. Kevin R. Ward, Mohamad H. Tiba, Gerald T. Draucker, Kyle Gunnerson, Robert W. Barbee, Penny S. Reynolds, Bruce Spiess, Rao R. Ivatury: Noninvasive Measurement of Central Venous Pressure, American Heart Association Resuscitation Science Symposium, Orlando, Florida, Circulation, 120, S1460, 2009.
15. Benjamin Leong, Nathan White, Mohamad H. Tiba, William Holbert, Gerard T. Draucker, Juliana Medina, Mary A Peberdy, Joseph P Ornato, Kevin R. Ward: Oxygen Transport in Post Cardiac Arrest Syndrome with Goal Directed Hemodynamic Optimization, American Heart Association Resuscitation Science Symposium, Orlando, Florida, Circulation, 120, S1469, 2009.

16. Benjamin Leong, Mohamad H. Tiba, Gerard T. Draucker, Juliana Medina, William Holbert, Robert W. Barbee, Penny S. Reynolds, Kevin R. Ward: The Importance of Measuring Oxygen Debt in Hemorrhagic Shock., American Heart Association Resuscitation Science Symposium, Orlando, Florida, Circulation, 120, S1465-S1466, 2009.
17. Leong B, Tiba M. H, Holbert W, Draucker G, Medina J, Barbee R, Reynolds P, Ward K.: Low Volume Resuscitation and Repayment of Oxygen Debt from Traumatic Shock, Society for Academic EmergencyMedicine (SAEM) Annual Meeting, New Orleans, Louisiana, Academic Emergency Medicine, 16, Suppl 1, S9, 2009.
18. Leong B, Tiba M. H, Holbert W, Draucker G, Medina J, Barbee R, Reynolds P, Ward K.: Low Volume Resuscitation and Repayment of Oxygen Debt from Traumatic Shock, Society for Academic EmergencyMedicine (SAEM) Annual Meeting, New Orleans, Louisiana, Academic Emergency Medicine, 16, Suppl 1, S9, 2009.
19. Robert W. Barbee, Penny S. Reynolds, Nathan White, Mohamad H. Tiba, Kevin R. Ward: Oxygen Debt Repayment Predicts Survival in a Swine Model of Trauma Shock, 33rd Annual Conference on Shock, Portland, Oregon, Shock, Supplement 1, 2010.
20. Penny S. Reynolds, Robert W. Barbee, Nathan White, Mohamad H. Tiba, Kevin R. Ward: Sequential Lactate Predicts 3-Hr Survival is a Swine Model of Traumatic Shock, 33rd Annual Conference on Shock, Portland, Oregon, Shock, Supplement 1, 2010.
21. Penny S. Reynolds, Robert W. Barbee, Nathan J. White, Mohammed H. Tiba, Kevin R. Ward: Physiological Response Space: Mapping Resuscitation Response in a Swine Model of Traumatic Shock , American Heart Association. Resuscitation Science Symposium, Los Angeles, California, Circulation, 122, Suppl 3, 2010.
22. Musana AK, Ward KR, Draucker GT, Tiba MH, Stravitz RT, Bajaj JS, Sanyal AJ: Hyperbilirubinemia Drives Microcirculatory Dysfunction, Tissue Hypoxia and Development of SIRS in Cirrhotic Subjects, The 61st Annual Meeting of the American Association for the Study of Liver Disease., Boston, MA, Hepatology, 890A, 2010.
23. Penny S. Reynolds, Robert W. Barbee, Mohamad H. Tiba, Kevin R. Ward: Visualization of Lactate-Perfusion Relationships During Hemorrhage and Resuscitation Using Artificial Neural Networks, 34th Annual Conference on Shock, Norfolk, Virginia, Shock, Supplement 1, 2011.
24. Bhogal A.K. Musana, K.R. Ward, M.H. Tiba, G.T. Draucker, V. Mishra, A. Sanyal: Microcirculatory Dysfunction and Tissue Hypoxia Drive Mortality in Patients with Cirrhosis, The 63rd Annual Meeting of the American Association for the Study of Liver Disease., Boston, Massachusetts, Hepatology, 931A, 2012.
25. Kevin R. Ward, Mohamad H. Tiba, Gerard T. Draucker: Comparison of Tissue Hemoglobin Oxygen Desaturation Using Resonance Raman Spectroscopy Versus Near Infrared Spectroscopy, 36th Annual Conference on Shock, San Diego, California, Shock, 39, Supplement 2, 64, 2013.
26. Mohamad H. Tiba, GGerard T. Draucker, Robert W. Barbee, James Terner, Ivo P. Torres Filho, Kevin R. Ward: Performance of Tissue Hemoglobin Oxygen Saturation as Measured by Resonance Raman Spectroscopy and Near Infrared Spectroscopy Compared to Mixed Venous Hemoglobin Oxygen Saturation and Systemic Lactate Levels During Hemorrhage, 36th Annual conference on Shock, San Diego, California, Shock, 39, Supplement 2, 56, 2013.
27. Mohamad H. Tiba, Gerard T. Draucker, Brendan M. McCracken, Kevin R. Ward.: Controlling Pelvic Hemorrhage Using a Novel Pressure Garment., 37th Annual Conference on Shock, Charlotte, North Carolina, Shock, 2014.
28. Mohamad H. Tiba, Gerard T Draucker,Brendan M. McCracken, Hasan B. Alam, Jonathan L. Eliason, Kevin R. Ward: Testing of a Novel Pelvic Hemostasis Belt to Control Lethal Pelvic Arterial Hemorrhage, American Heart Association. Resuscitation Science Symposium, Chicago, Illinois, Circulation, 130, A177, 2014.
29. Marwan R. Al-hajeili, Faris Elkhider, Mohamad H. Tiba: Cost-Effectiveness for Extended RAS/RAF Testing in Metastatic Colorectal Cancer, 2015 ASCO Annual Meeting, Chicago, Illinois, Journal of Clinical Oncology, 33, 5s, 3572, 2015.
30. Mohamad H Tiba, Barry Belmont, Nik Theyyunni, Robert Huang, David F. Barton, Amanda J. Pennington, Gerard T. Draucker, Albert J. Shih, Kevin R. Ward: Comparison of Respiratory Induced Inferior Vena Cava Diameter Changes with Limb Bioimpedance Changes to Assess Intravascular Volume Status, 38th Annual Conference on Shock, Denver, Colorado, Shock, 43, Supplement 1, 116, 2015.

31. Sardar Ansari, Daniel Slavin, Mohamad H. Tiba, Harm Derksen, Kenn Oldham, Kevin Ward and Kayvan Najarian: A Novel Portable Polyvinylidene Fluoride Based Sensor for Detection of Hemorrhage, American Heart Association. Resuscitation Science Symposium, Orlando, Florida, Circulation, 132, Suppl 3, 2015.
32. Steve Lin, Li Ka Shing, Matthew L Sundermann, Paul Dorian, Sarah Fink, Henry Halperin, Alex Kiss, Allison C Koller, Brendan M McCracken, Laurie J Morrison, Robert W Neumar, James T Niemann, Andrew Ramadeen, David D Salcido, Mohamad H Tiba, Scott T Youngquist, Menekam Zviman, James J Menegazzi.: Epinephrine In Cardiac Arrest: A Randomized, Multicenter, Doubleblinded, PlaceboControlled Experimental Trial, American Heart Association. Resuscitation Science Symposium, Orlando, Florida, Circulation, 132, Suppl 3, 2015.
33. Ryan A Coute, Theresa A Shields, James A Cranford, Sardar Ansari, M. Hakam Tiba and Robert W Neumar: Intrastate Variation in Treatment and Outcome Measures for Out-of-Hospital Cardiac Arrest, American Heart Association. Resuscitation Science Symposium, New Orleans, LA, Circulation, 134, Suppl 1, 2016.
34. Ryan A Coute, Nicole L Werner, Alvaro Rojas-Pena, Stephanie Rakestraw, Fares Alghanem, M. Hakam Tiba, Robert H Bartlett and Robert W Neumar: Intravascular Coagulation During Prolonged Cardiac Arrest, American Heart Association. Resuscitation Science Symposium, New Orleans, Circulation, 134, Suppl 1, 2016.
35. Mohamad Hakam Tiba, Barry Belmont, Michael Heung, Nik Theyyunni, Robert D. Huang, Christopher M. Fung, and Kevin R. Ward: Evaluation of Intravascular Volume Status Using Dynamic Respiratory Induced Bioimpedance of the Limb, Society of Academic Emergency Medicine Annual Meeting, New Orleans, LA, Academic Emergency Medicine, Volume 23, Supplement S1, S18-S19, 2016.
36. Christopher Fung, Robert Huang, Mohamad H. Tiba, Barry Belmont, Amanda J. Pennington, Brandon C. Cummings, Gerard T. Draucker, Kevin R. Ward, and Nik Theyyunni: Measurement of Carotid Artery Flow Time Via Point-of-Care Ultrasound in Hemodialysis Patients, Society of Academic Emergency Medicine Annual Meeting, New Orleans, LA, Academic Emergency Medicine, 23, S1, A170, 2016.
37. Mohamad H. Tiba, Barry Belmont, Michael Heung, Nik Theyyunni, Robert Huang, Christopher D. Fung, Amanda J. Pennington, Kevin R. Ward: Comparison of Respiratory Induced Inferior Vena Cava Diameter Changes with Limb Bioimpedance Changes In dialysis and mechanically ventilated patients, Thirty-Ninth Annual Conference on Shock, Austin, Texas, Shock, 45, Supplement 1, 125-126, 2016.
38. Rodney C. Daniels, Hyesun Jun, Mohamad H. Tiba, Pilar Herrera-Fierro, Kevin Ward MD: Evaluating Whole Blood vs. Plasma Redox Measures in Healthy Humans and in Swine Hemorrhagic Shock Model, Thirty-Ninth Annual Conference on Shock, Austin, Texas, Shock, 45, Supplement 1, 91, 2016.
39. Mohamad H. Tiba, Amanda Pennington, Kyle Gunnerson, Kevin R. Ward: Monitoring of Tissue Microvasculature Oxygenation using Resonance Raman Spectroscopy, Thirty-Ninth Annual Conference on Shock, Austin, Texas, Shock, 45, Supplement 1, 118, 2016.
40. Sardar Ansari, Mohamad Hakam Tiba, Kenn Oldham, Kevin R Ward and Kayvan Najarian: Noninvasive Peripheral Vascular Resistance Measured by a Polyvinylidene Fluoride Sensor Identifies Patterns of Oxygen Debt Repayment During Resuscitation After Hemorrhage, american Heart Assocition. Resuscitation Science Symposium, New Orleans, LA, Circulation, 134, Suppl 1, 2016.
41. Sando IC, Plott JS, McCracken BM, Tiba MH, Ward KR, Kozlow JH, Cederna PS, Momoh AO.: A Preclinical Assessment of an Everter Device to Aid with Arterial Anastomosis, American Society for Reconstructive Microsurgery Annual Meeting, Waikoloa, HI., 2017.
42. Amanda Pennington; Mohamad H. Tiba; Kevin R. Ward.: Novel Monitoring of Tissue Microvasculature Oxygenation Using Resonance Raman Spectroscopy, Forthieth Annual Conference on Shock, Fort Lauderdale, Florida, Shock, 47, Supplement 1, 115, 2017.
43. Mohamad Hakam Tiba; Brendan McCracken; Sardar Ansari; Venkatakrishna Rajajee; Kevin Ward.: Novel Noninvasive Method of Cerebrovascular Autoregulation Assessment: Seeing the Brain through the Eyes, Forthieth Annual Conference on Shock, Fort Lauderdale, Florida, Shock, 47, Supplement 1, 62, 2017.
44. Brendan M McCracken, Mohamad H Tiba, Brandon C Cummings, Carmen I Colmenero, Alvaro Rojas-Pena, Pavel Hala, Matias Caceres, Cindy H Hsu, Aaron Prater, Jensyn J VanZalen, Kevin R Ward, Robert H Bartlett, and Robert W Neumar: Examination of the Effects of Extracorporeal Cardiopulmonary Resuscitation on Sublingual Microcirculation in a Swine Model of Cardiac Arrest., American Heart Association. Resuscitation Symposium (ReSS), Chicago, IL, Circulation, 138, Suppl_2, 2018.
45. Pavel Hala, Matias Caceres, Aaron Prater, Josh Jung, Jensyn Van Zalen, Brendan M McCracken, Mohamad H Tiba, Cindy H Hsu, Stephen Harvey, Alyssa Enciso, Jake Pitcher, Brandon C Cummings, Robert H Bartlett, Alvaro Rojas-Pena, and Robert W Neumar: Goal-Directed CPR is Less Effective with an Increased Interval from Cardiac Arrest Onset to Initiation of Chest Compressions., American Heart Association. Resuscitation Symposium (ReSS), Circulation, 138, Suppl_2, 2018.

46. Pavel Hala, Matias Caceres, Aaron Prater, Jensyn Van Zalen, Joshua Jung, Brendan M McCracken, Mohamad H Tiba, Cindy H Hsu, Jake Pitcher, Stephen Harvey, Katia Shpilband, Brandon C Cummings, Robert H Bartlett, Alvaro Rojas-Pena, and Robert W Neumar: Impact of No-Flow Time on the Coagulopathy of Prolonged Cardiac Arrest, American Heart Association. Resuscitation Symposium (ReSS), Chicago, IL, Circulation, 138, Suppl_2, 2018.
47. Mohamad H Tiba, Brendan M McCracken, Brandon C Cummings, Carmen I Colmenero, Chandler J Rygalski, Cindy H Hsu, Thomas H Sanderson, Brahmajee K Nallamothu, Robert W Neumar, and Kevin R Ward: Use of Resuscitative Balloon Occlusion of the Aorta in a Swine Model of Prolonged Cardiac Arrest., American Heart Association. Resuscitation Symposium (ReSS), Chicago, IL, Circulation, 138, Suppl_2, 2018.
48. Brandon Cummings, BS, Brendan McCracken, BS, Chandler Rygalski, BS, Ashwin Belle, PhD, Kevin Ward, MD, M. Hakam Tiba, MD, MS.: A Signal Processing Approach for the Calculation of a Bioimpedance Index in the Assessment of Cerebrovascular Autoregulatory Status., Military Health System Research Symposium (MHSRS), Kissimmee, Florida, 2018.
49. M. Hakam Tiba, MD, MS, Krishna Rajajee, MD, Craig Williamson, MD, Ashwin Belle, PhD, Sardar Ansari, PhD, Brandon Cummings, BS, Brendan McCracken, BS, Amanda Pennington, MS, Kevin Ward, MD.: Monitoring Traumatic Brain Injury Patients using Transocular Brain Impedance (TBI)., Military Health System Research Symposium (MHSRS), Kissimmee, Florida, 2018.
50. Brandon Cummings; Hakam Tiba; Ashwin Belle; Brendan McCracken; Sardar Ansari; Krishna Rajajee; Kevin Ward: A Novel Method of Cerebrovascular Autoregulation Assessment Using Bioimpedance, SHOCK, Scottsdale Arizona, SHOCK, 49, Supplement 1, 73, 2018.
51. Jae Hyuk Lee; M. Hakam Tiba; Brendan McCracken; Brian Carlson; Kevin Ward: Basal oxygen delivery-consumption status and its impact on injury response in experimental traumatic hemorrhagic shock, SHOCK, Scottsdale, Arizona, SHOCK, 49, Supplement 1, 87, 2018.
52. Hakam Tiba; Brendan McCracken; Brandon Cummings; Kathleen Stringer; Robert Dickson; Jean Nemzek; Rodney Daniels; Alvaro Rojas-Pena; Scott VanEpps; Christopher Fung; Timothy Cornell; Kevin Ward: Novel Porcine Large Animal Model of Sepsis: A Pilot Study, SHOCK, Scottsdale Arizona, SHOCK, 49, Supplement 1, 68-69, 2018.
53. Rodney C. Daniels; Yan Rou Yap; Hakam Tiba; Brendan McCracken; Brandon Cummings; Kevin R. Ward; Kathleen A. Stringer: WHOLE BLOOD REDOX POTENTIAL CORRELATES WITH CHANGES IN METABOLITE CONCENTRATIONS ATTRIBUTABLE TO PATHWAYS INVOLVED IN OXIDATIVE STRESS IN A SWINE MODEL OF HEMORRHAGIC SHOCK, Shock Society 41nd Meeting on Shock, Scottsdale, Arizona, SHOCK, 49, Supplement 1, 53, 2018.
54. Amanda Pennington; Hakam Tiba; Brandon Cummings; Kyle Gunnerson; Kevin Ward: Novel monitoring of tissue microvasculature oxygenation using resonance Raman spectroscopy, Shock Society 41st Meeting on Shock, Scottsdale, Arizona, SHOCK, 49, Supplement 1, 53, 2018.
55. Brendan McCracken; Hakam Tiba; Brandon Cummings; Cindy Hsu; Alvaro Rojas-Pena; Pavel Hala; Matias Caceres; Kevin Ward; Robert Neumar: Reverse Translation of Goal Directed Cardiopulmonary Resuscitation in a Swine Model of Cardiac Arrest, Shock Society 41st Meeting on Shock, Scottsdale, Arizona, SHOCK, 49, Supplement 1, 52-53, 2018.
56. Cover M, Tiba MH, Cummings B, Pennington A, Huang R, Kessler R, Theyyunni N: Comparison of Algorithm-Assisted to Manually Obtained Left Ventricular Outflow Tract Velocity Time Integral, Society of Academic Emergency Medicine Annual Meeting, Indianapolis, Indiana, Academic Emergency Medicine, 25, S1, S59-S60, 2018.
57. S.M.Reza Soroushmehr, Krishna Rajajee, Craig Williamson, Jonathan Gryak, Kayvan Najarian, Kevin Ward, Mohamad H. Tiba: Automated Optic Nerve Sheath Diameter Measurement Using Super-Pixel Analysis, 41st Annual International Conference of the IEEE, Berlin, Germany, Engineering in Medicine & Biology Society (EMBC), 2019.
58. R. P. Dickson, H. Tiba, B. McCracken, B. Cummings, T. Flott, R. Sharma, J. Nemzek, M. W. Sjoding, T. J. Standiford, K. A. Stringer, S. Fan, K. Ward; University of Michigan, Ann Arbor, MI, United States.: Filling the Translational Gap in ARDS with a Clinically-Relevant, HighFidelity Swine Model, American Thoracic Society, Dallas, Texas, Am J Respir Crit Care Med, 199, A1141, 2019.
59. 12- Brendan M. McCracken, Mohamad H. Tiba, Brandon C. Cummings, Carmen I. Colmenero, Danielle Leander, Anne M. Weitzel, Thomas Flott, Ruchi Sharma, Rodney Daniels, Jean Nemzek, Kevin R. Ward, Stringer A. Stringer and Robert P. Dickson.: Bridging The Translational Gap in ARDS Research with an Innovative, Clinically relevant, High-Fidelity Swine Model., Shock Society 42nd Meeting on Shock, Coronado, California, Shock, 51, Supplement 1-6S, 46, 2019.

60. Mohamad H. Tiba, Brendan M. McCracken, Robert P. Dickson, Jean A. Nemzek, Brandon C. Cummings, Carmen I. Colmenero, Danielle Leander, Anne M. Weitzel, Rodney C. Daniels, Scott VanEpps, Kathleen A. Stringer and Kevin R. Ward.: Temporal Changes in Blood Concentration of Inflammatory Cytokines and Bacterial DNA Coincide with Sepsis Pathogenesis and Progression., Shock Society 42nd Meeting on Shock, Coronado, California, Shock, 51, Supplement 1-6S, 144-145, 2019.